CHAPTER ONE

1.1 Introduction

The international literature uses the term 'Bushveld' as the ultramafic to mafic rocks of the largest layered complex located in South Africa. According to SACS (1980), the Bushveld Complex includes the ultramafic to mafic layered rocks, the granophyres and granites, and the ultramafic to mafic sills. For the purpose of this research, the term 'Bushveld Complex' shall be used to include the ultramafic to mafic rocks, the granites and the granophyres as well as the felsic volcanic rocks of the Rooiberg Group.

The Bushveld Complex is comprised of suites of rocks that exhibit a wide and varied assemblage of both extrusive and intrusive rocks (Willemse, 1964; Wager and Brown, 1968; Truswell, 1977; Eriksson et al., 1995). Truswell (1977) summarized that three phases are recognized in these suites of rocks; the volcanic phase (Rooiberg Felsites), the layered mafic intrusive phase and the granitic phase. The roof of the layered mafic rocks (Rustenburg Layered Suite) of the Bushveld Complex is constructed by the extrusive Rooiberg Felsites (Willemse, 1969; Truswell, 1977), which are considered to be part of the Bushveld Complex (Hatton and Schweitzer, 1995). After the emplacement of the mafic portion of the Bushveld Complex, the granophyric and granitic rocks, called the Rashoop Granophyre and Lebowa Granite

Suites respectively were intruded onto the Rooiberg Felsites and Rustenburg Layered Suite.

Multiple injections of magma into a cratonic setting resulted in the emplacement of the world's largest layered mafic intrusion (Wager and Brown, 1968; Eales and Cawthorn, 1996; Cawthorn and Walraven, 1998) that hosts the world's largest reserves of platinum-group elements (PGE), chromium and vanadium. The repeated injections may be responsible for the intricate mineralogical and chemical variations. The multiple injection theory was proved by isotopic and chemical evidence, specifically breaks in the initial strontium isotopic ratios (Hamilton, 1977; Kruger and

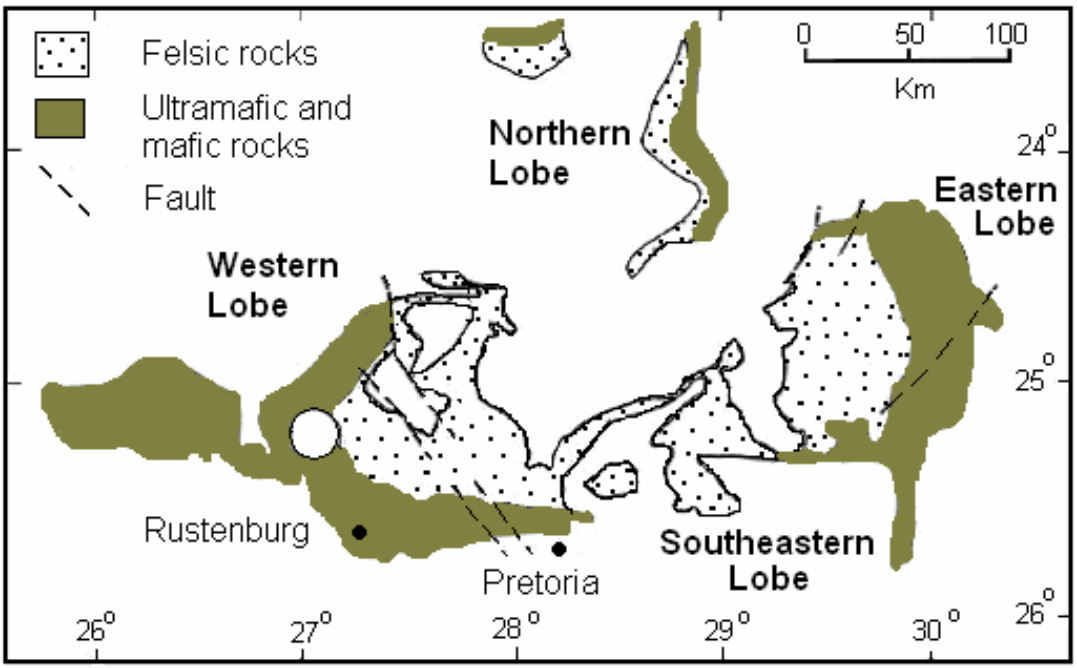

Fig. 1.1 Simplified geological map of the ultramafic and mafic rocks of the Bushveld Complex, including the associated felsic suites of rocks; Rooiberg Group, Lebowa Granite Suite, as well as the Rashoop Granophyre.

Marsh, 1982; Sharpe, 1985; Eales et al., 1993; Kruger, 1994). The ultramafic to mafic phase of the Bushveld Complex (Fig. 1.1) is spread over an area of 65 000 km^2 (SACS, 1980; Eriksson et al., 1995, Eales and Cawthorn, 1996) and can reach a maximum thickness of 9 km (SACS, 1980).

Although the mafic rocks in the Bushveld Complex are 2060 million years old (Walraven et al., 1990), they are still remarkably undeformed and unmetamorphosed (Eales and Cawthorn, 1996).

The mafic rocks of the Bushveld Complex outcrop as four of five lobes. The southern, sometimes called the Bethal lobe is not exposed at surface because it is concealed by younger sedimentary covers. Of the four exposed lobes, the 200 km-long western and eastern lobes are crescent-shaped and dip toward each other so as to form a bowl-shaped structure. The lobes mentioned above are considered to be connected at depth (Cawthorn et al. 1998, Webb et al., 2004). The layering and chemical compositions of the Critical and Main Zones as well as in the Upper Zone are similar in the western and eastern lobes.

1.2 Rustenburg Layered Suite

The mafic Rustenburg Layered Suite which is contained in the five lobes already discussed and is divided into five zones. The average thicknesses of these zones are shown in brackets; Marginal, Lower (820 m), Critical (1300 m), Main (3400 m) and

the Upper Zones (1700 m). The zones in the Bushveld Complex have lithologies that change with height.

The Marginal Zone of the Rustenburg Layered Suite is represented by norites. Above the Marginal Zone lies the Lower Zone which is comprised of high temperature rocks such as peridotites and pyroxenites as well as harzburgites. The lower part of the Critical Zone is dominated by pyroxenites. The upper Critical Zone contains anorthosites and norites and also contains the Merensky Reef. Substantial chromitite layers mark the boundary that separates that lower and upper Critical Zone and Merensky Reef. Overlying the Critical Zone is the Main Zone which is mostly composed of a uniform sequence of gabbros with some anorthosites and rare pyroxenites. The iron-rich, and gabbroic Upper Zone grades into olivine diorites. The Upper Zone also contains anorthosites and vanadium-bearing magnetitite layers.

1.3 Merensky Unit

The Merensky Unit, studied in detail by Wagner (1929), is one of the distinctive repetitive or cyclic units in the upper Critical Zone of Rustenburg Layered Suite. The Merensky Unit is the thinner of the two topmost cyclic units, the other being the Bastard Unit. According to Irvine et al. (1983), a cyclic unit results from a significant addition of undifferentiated magma. The sulphide- and PGE-bearing Merensky Unit is generally composed of a basal chromitite, occasional pegmatitic pyroxenite,

pyroxenite, norite, and finally an anorthosite layer that marks the top of the cyclic unit. Up to three chromitite layers can develop in the Merensky Unit.

Viljoen (1999) studied and described the facies (or reef types) of the western Bushveld and concluded that there are four subfacies that are grouped according to the regional variations of the nature of the Merensky Reef. His findings are based in part on geophysical data. According to Viljoen (1999), the four subfacies are a narrow, pegmatitic, highly potholed, and wide non-pegmatitic reef. The mineralization also varies in the respective subfacies.

Davey (1992) conducted a study on the Rooikoppies farm 297 QJ where part of the Lonplats' Mines (area of interest for this research) lies. His study concentrated on three reef types; Rustenburg Platinum Mine reef type (currently known as the Brakspruit reef type) which is pegmatitic, and the Marikana and the Westplats reef types which are wide and non-pegmatitic. Davey (1992) found that the thickness of the Merensky pyroxenite in the reef types on the Rooikoppies farm increases from the west to the east. He noted that the thin pyroxenite is bounded below by a single and only chromitite layer and additional chromitite layers develop as the thickness of the pyroxenite increases. Where the pyroxenite is underlain by a pegmatitic pyroxenite, a third additional chromitite layer occurs. Davey (1992) also noted that the variation in location of the PGE mineralization is dependent on the reef types.

Subsequent work indicates that the Merensky Unit across all Lonplats' Mines is actually represented by four reef types, according to the geologists at Lonplats; Thin (narrow), Brakspruit (pegmatitic), Marikana and Westplats (wide non-pegmatitic) reef types. All these reef types carry unique and distinguishing features. The reef types vary laterally in thickness, lithology and mineralization along the strike length of the Lonplats' lease area. The thickness of the Merensky pyroxenite in the Westplats reef type at Lonplats' Mines can reach just over 11 m. The Merensky pyroxenite in the other three reef types develops to a maximum of just over 2 m.

Vermaak (1976) and Kruger and Marsh (1985) described the Merensky Reef as that portion of the Merensky pyroxenite that is economic with appreciable quantities of PGE. The stratiform Merensky economic horizon which can be traced throughout most of the strike of the Bushveld Complex (Lee, 1996), can reach a thickness of approximately a meter. A pronounced concentration of PGE and base metal sulphides that occur as interstitial phases in the cumulate mafic rocks in the Merensky Unit occurs toward the top of the Merensky pyroxenite, making up the prominent marker Merensky Reef (Brynard et al., 1976). Lee (1996) has described the Merensky pyroxenite as feldspathic and texturally inhomogeneous as well as pegmatitic.

1.4 Previous models

The Bushveld Complex and its associated mineral deposits have been studied by many workers over the past century and many reports on investigations about its

geochemistry, petrogenesis, mineralogy and mining activities have been published. Information gathered about the Bushveld Complex has also had pronounced influence in the development of various concepts such as the origin of sulphide and PGE mineralization elsewhere in the world. Many theories about the manner in which PGE and sulphides deposited in the Merensky Reef have been formulated and tested. Through research and study, these postulates have been modified and challenged. There are two principal schools of thought on how the base metal sulphides as well as PGE mineralization in the Merensky Unit formed; the hydrothermal magmatic models (epigenetic) and orthomagmatic models (syngenetic).

1.4.1 Epigenetic Models

Because of the pegmatitic nature of part of the Merensky Reef, theories have been used to attribute the mineralization of the reef to hydrothermal processes. Jackson (1961) assumed that the chromitite layers that occur above the pegmatitic pyroxenites were responsible for mineralization as they assumed the role of impermeable barriers against hydrothermal solutions formed during the crystallization of the magma. Hydrothermal fluids were thought to be active beneath a barrier of impermeable rock Lauder, 1970). Lauder (1970) argued that if the Merensky Reef was a vein that did not form a primary layer, then it would be plausible that the concentration of sulphides and PGE as well as the pegmatitic nature of the reef formed hydrothermally, during the consolidation of the Bushveld Complex.

Vermaak (1976), Boudreau et al. (1986) and Boudreau and Meurer (1999), among others, formulated an alternative hydrothermal hypothesis suggesting that the mineralization in the Merensky Reef was a result of a chlorine-rich intercumulus fluid ascending through a crystal pile. Boudreau et al. (1986) argued that these chlorine-rich hydrothermal fluids, exsolved from the solidifying cumulate sequence, and acted as scavengers and carriers of the platinum-group elements and rare earth elements. Boudreau et al. (1986) based their arguments on the preferentially chlorine-rich minerals of apatite, amphiboles and phlogopite in the Bushveld Complex. Boudreau and Meurer (1999) also argued that the chlorine-rich fluids were mobilized to reach the crystal-magma interface and re-dissolved to produce an immiscible sulphide that is rich in platinum-group elements.

1.4.2 Syngenetic Models

Theories of magma addition and magma mixing have been considered as genetic contributors to the Merensky Unit and its platiniferous sulphide mineralization. The compositions of the sulphide assemblages have also been used to show their magmatic affinity; in order to substantiate the magmatic models proposed for the mineralization thereof. Pressure and temperature changes in magma chambers have also been used to explain the origin of sulphides in mafic complexes. The manner in which pressure and temperature changes affects sulphide immiscibility is discussed in later chapters.

Hamilton (1977) proposed that the step-like increase of initial strontium isotopic ratios ($^{87}Sr/^{86}Sr$) in the Merensky Unit is due to magma influx and also proposed that the new magma influx occurred at a level about 3 m above the basal chromitite layer of the Merensky Unit. Kruger and Marsh (1982) also proposed, using strontium isotopic ratios, that the new influx of basic magma was added at the base of the Merensky Unit. Cameron (1982) suggested that the Merensky Reef registered a sudden event that changed the chemistry of the system and trigged the precipitation of sulphides and PGE in the magma chamber. Campbell et al. (1983) and Kruger and Marsh (1985), among others proposed that the new influx of magma mixed with the resident magma already in the magma chamber by turbulent convection.

Irvine (1977) suggested that the mineralization especially of chromite in the Bushveld Complex is a derivative of the mixing of magmas. The mixing process led to the formation and separation of a hybrid magma with dense immiscible sulphide droplets, which scavenged nickel, copper and platinum group elements with remarkable efficiency (Campbell et al., 1983, Naldrett, 1989). Naldrett and von Gruenewaldt (1989) and Naldrett (1989) as well as Li et al. (2001a) also proposed that the sulphide and PGE mineralization is a result of mixing of differentiated residual and replenishing parental magmas. Once the immiscible sulphides separated, they concentrated PGE because of high partition coefficients (D) and high silicate to sulphide ratios (R-factor), and settled to the floor of the magma chamber. The sulphide mineralization in the rocks below the Merensky Reef can be attributed to the sinking of this sulphide liquid into the incompletely solidified footwall (Lee, 1996;

Cawthorn, 1999). Although the magma mixing theory has been accepted for a length of time, Cawthorn (2002) demonstrated that mixing of magmas does not produce immiscible sulphide liquids, whilst work by Seabrook et al. (2005) also argued that magma mixing did not occur in the Merensky Unit (and Bastard Unit).

Li et al. (2001b) proposed that liquids generated by partial mantle melting are rich in PGE, Ni and Cu if the molten sulphides are dissolved completely, but such partial melts are unlikely to produce sulphide saturation upon ascent through the crust. Sulphide saturation in magma can therefore be achieved by fractional crystallization (Li et al., 2001b) and crustal contamination (Irvine, 1975; Ripley and Alawi, 1988; Maier et al., 2000; Li et al., 2001b). Li et al. (2001b) argue that during fractional crystallization and contamination, temperature and FeO contents are decreased thereby causing sulphide saturation. Contamination by a crustal source may result in sulphide saturation irrespective of the presence or absence of sulphur in the contaminant (Li et al., 2001b).

Other methods of PGE collection suggested by workers such as Hiemstra (1985) and Merkle (1992), who proposed that PGE existed as discreet phases which formed directly from the magma. Tredoux et al. (1995) suggested that PGE occur as 50 -100 atom size particles that self-nucleated in the magma. Many researchers have agreed, Tredoux et al. (1995) included, that the PGE in some form were scavenged by the immiscible sulphide globules or chromite sinking to the floor of the chamber.

1.5 Objectives of the project

Theories about the origin of the Merensky Unit and the Merensky Reef have been the pivot of many investigations in the Bushveld Complex. As a result, workers have developed postulates that are based on findings about sulphide assemblages that were thought to carry magmatic immiscible sulphide liquid signatures, and on the existence of chlorine-rich fluids in the mineralized succession of the Merensky Unit. The postulates are principally rooted in orthomagmatic and hydrothermal origins. This project seeks to investigate and contribute to this debate. Thus an investigation on the bulk composition of sulphides, trace elements (mainly Ni, Cu and S in the sulphides) in the project samples is vital to the main object of this project and this will assist in answering the question of the origin of sulphides in the Merensky Unit.

The Merensky Unit at Lonplats' Mines is essentially characterized by four reef types that all contain sulphide assemblages to some degree. The geochemistry and distribution of these sulphides might vary depending on reef types. The investigation of the distribution and change, if any, in geochemistry of the sulphides is also the focus of this project.

Research on the characteristics of the chromitite layers in the four reef types may help detect change in geochemistry. The chromite mineral chemistry may provide information on the correlation of chromitite layers in one reef type to another at

Lonplats' Mines. This may help explain the variation of the thicknesses of the different reef types.

Profiles for initial strontium isotopic ratios ($^{87}Sr/^{86}Sr$) in the narrow and thick Merensky Unit in various places in the Bushveld Complex have been produced by several workers. Another object of this research is also to establish a profile of the R_o in the very thick reef type from the Merensky Unit at Lonplats' Mines. This resultant profile will aid in identifying the level of new magma influx that is proposed to have resulted in the Merensky Unit. The comparison of this resultant profile with other initial strontium isotope profiles from narrow and thick Merensky Unit is also important in this research project.

No deposit is exactly identical to another. Thus the aim of this research attempts to provide reasons for the differences between the Merensky Unit at Lonplats' Properties and other deposits. Vertical and lateral variations of the Merensky Unit have been looked at in a variable range of reef types over a wide area in the Western Bushveld Complex. However, not many scientific workers have put emphasis on the Merensky Unit at Lonplats' Mines. Thus all the observations resulting from this project will also help in the understanding of processes that influenced the evolution of the Merensky Unit as a whole and will also contribute to the scientific observations in the Bushveld Complex.

CHAPTER TWO

DIFFERENT REEF TYPES ON LONPLATS' MINES

2.1 Introduction

The Lonmin Platinum Division (Lonplats' Mines) east of the Rustenburg Platinum Mine is situated 70 km northwest of Johannesburg. For the purpose of simplicity, the Lonmin Platinum Division will be referred to as Lonplats. Lonplats is divided into Karee, Western and Eastern Platinum Mines (Fig. 2.1).

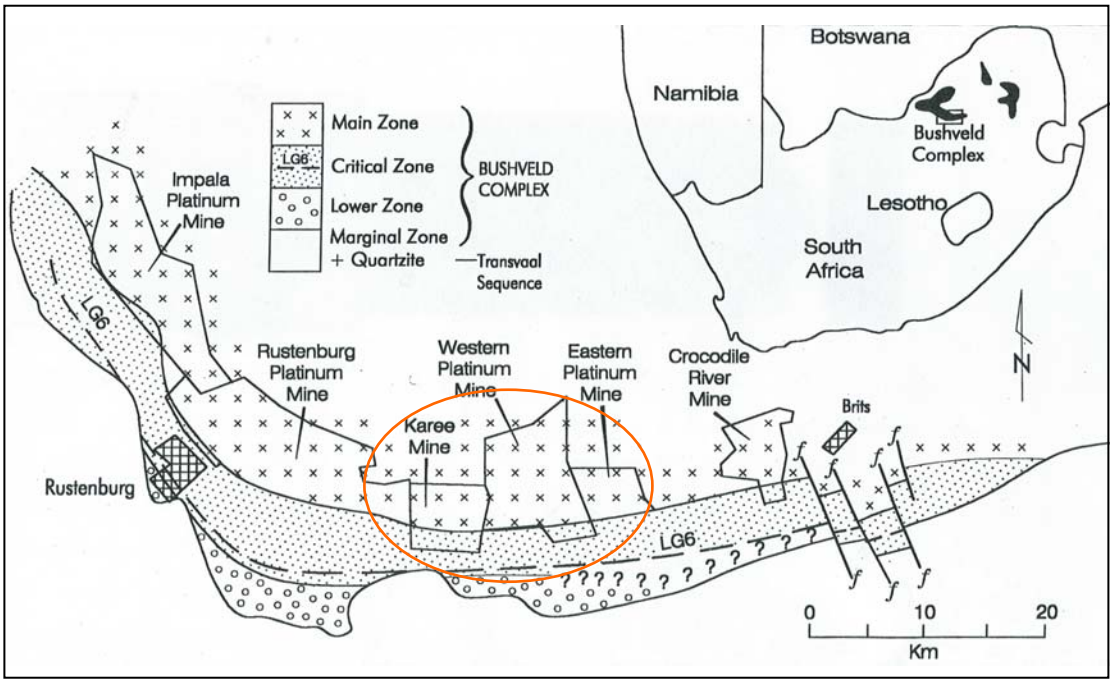

Fig. 2.1 A simplified geological map showing the lithology of south of Pilanesberg Complex in the western lobe of the Bushveld Complex. The locations of Lonplats' Mines are shown on the map by an ellipse.

Material from Karee and Eastern Platinum Mines, which are two out of fourteen producing platinum-group metals mines in the western limb of the Bushveld Complex, are used for this research project.

2.2 Rock nomenclature

The terminology used in this study is listed below.

Anorthosite

A leucocratic plutonic rock principally composed (more than 90%) of cumulus plagioclase minerals often with minor amounts of pyroxene.

Mottled anorthosite

A poikilitic anorthosite with orthopyroxene and/or clinopyroxene as oikocrysts. This results in a mottled texture. Plagioclase is the only cumulus phase in this rock.

Spotted anorthosite

An anorthosite with sporadic or discreet crystals of cumulus orthopyroxene.

Pyroxenite

A rock primarily composed of more than 80% orthopyroxene with minor amounts of plagioclase, clinopyroxene, biotite and olivine.

Pegmatitic pyroxenite

A very coarse-grained rock which principally consists of one or more pyroxene minerals (clinopyroxene < orthopyroxene) and minor plagioclase.

Chromitite

An ultramafic rock which essentially consists of chromite minerals as the only cumulus phase. Minor plagioclase, orthopyroxene and clinopyroxene are also present.

Norite

A plutonic rock with cumulus plagioclase and orthopyroxene as major minerals.

2.3 The Merensky Unit

The lithology of the Merensky Unit at Lonplats' Mines is described by a consistent basal chromitite layer, an occasional pegmatitic pyroxenite, pyroxenite, a very thin norite and finally a mottled anorthosite that marks the top of the unit. The norite that overlies the Merensky pyroxenite is may either be sparsely developed or absent. In this regard, an anorthosite often overlies the Merensky pyroxenite, instead of a norite. On the Lonplats' lease area, the Merensky pyroxenite, which becomes feldspathic with increase in height, may become pegmatitic close to the base. This basal

Merensky pegmatitic pyroxenite only occurs in the west of the lease area and is poorly developed to the east of the lease area. Also, the number of chromitite layers varies from reef type to reef type and a maximum number of three. The chromitite layers range in thickness from 1 mm to 2.5 cm. the chromitite layer that overlies the Merensky anorthosite is often not present but occurs on the east of Lonplats' lease area. The order of the lithology at Lonplats' Mines is not necessarily the same as that described by Kruger and Marsh (1985) for the western Bushveld Complex. Kruger and Marsh (1985) described the lithology of the Merensky unit as having a cyclicity that is marked by a basal chromitite layer, a pyroxenite, norite and anorthosite which marks the top of the cyclic unit and is terminated by a basal chromitite layer of the following cyclic unit (Bastard Unit).

Lateral variations of the Merensky Cyclic Unit are present along the strike length of the Lonplats' lease area. Thickness, lithology and mineralization in the Merensky Unit vary from place to place at Lonplats' Mines and this variation is represented in different reef types called Thin, Brakspruit, Marikana and Westplats reef types. This is according to the geologists at Lonplats' Mines. One distinguishing feature of the different reef types representing the Merensky Unit is the varying thickness of the Merensky pyroxenite. The Merensky pyroxenite in the different reef types ranges in thickness from 0.7 m to 11m from the west to the east at Lonplats' Mines (Fig. 2.2). Another variation is the vertical change in lithology in the reef types.

2.4 Reef types

Terminology and characteristics of reef types are based on compilations by geologists at Lonplats' Mines.

According to the Collins Dictionary of Geology, the term facies refers to an "assemblage or association of minerals, rocks or fossil features reflecting the environment and conditions of the origin of the rocks". This term; facies, also refers to the "appearance and peculiarities that distinguish a rock unit from the associated or adjacent rock units". Although the four reef types have distinguishing features that qualify them to be termed facies, for the purpose of simplicity, these will be referred to as reef types. In the case of this research project, the term 'reef type' refers to a vertical profile through the Merensky Unit and the Bastard Unit as well as through adjacent units.

The Thin, Brakspruit, Marikana reef types occur in the west on the Lonplats' lease area at Karee Mine and Westplats reef type is situated in the far east on the Lonplats' lease area at Eastern Platinum Mine. These four reef types have lateral variations in thickness, lithology and mineralization. The thickness of the reef types that are of concern to this study is based principally on the thickness of the Merensky pyroxenite. For the purpose of this research, a reef type is considered as a narrow reef type if the thickness of the Merensky pyroxenite is less than 2 m and considered thick reef type if the thickness of the Merensky pyroxenite is more than 2 m.

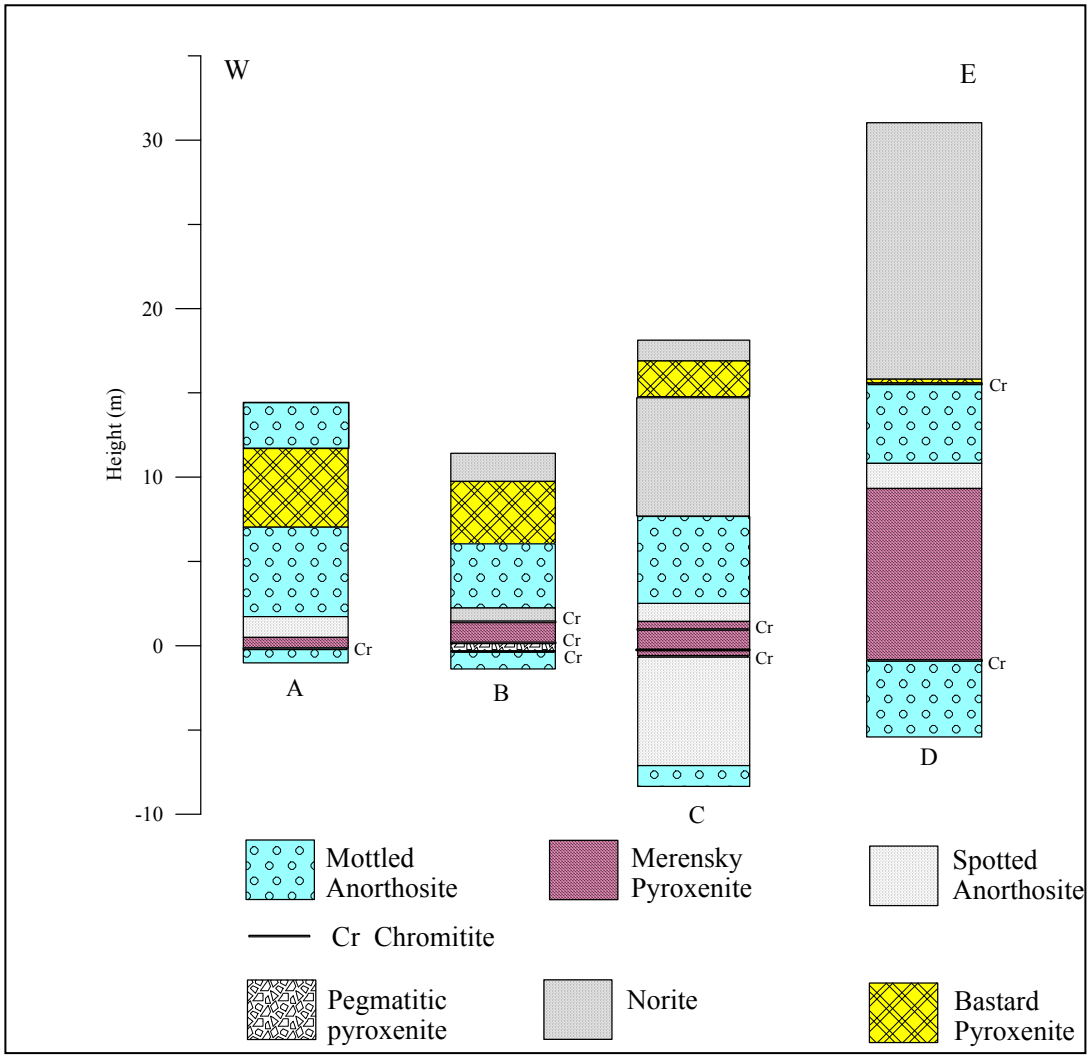

Fig. 2.2 Lithology of the four reef types at Lonplats' Mines. Borehole numbers are shown in brackets. A: Thin (ZS 07), B: Brakspruit (R 37), C: Marikana (ML 44) and D: Westplats (TN 70, TN 71) reef types. Height in meters is shown using the base of the lowest chromitite layer below the Merensky pyroxenite as datum.

With the variable thickness demonstrated in the reef types, differences occur; where the Merensky pyroxenite is thinnest, a single chromitite layer occurs at the base of the pyroxenite. A second and sometimes a third chromitite layer, is developed as the thickness of the pyroxenite increases. A third chromitite layer usually occurs where

the Merensky pyroxenite is underlain by a pegmatitic pyroxenite. The mineralization of PGE and base metal sulphides is characteristic of each reef type at Lonplats' Mines. Descriptions of the reef types are based on the borehole cores selected for detailed study.

2.4.1 Thin reef type

The Thin reef type has the thinnest (0.7 m) Merensky pyroxenite (Fig. 2.2 A), hence its name. The Merensky pyroxenite in this reef type is bounded below by a single 2.5 cm thick chromitite layer and has a mottled anorthosite as its footwall. The Merensky pyroxenite is overlain by spotted anorthosite which is 1.35 m thick. A gradational contact separates the latter spotted anorthosite from the overlying 6.4 m thick mottled anorthosite. The Thin reef type has the thickest (5 m) Bastard pyroxenite with respect to the other three reef types. A sharp contact separates the Bastard pyroxenite and the underlying mottled anorthosite. The mineralization in the Thin reef type is concentrated close to the chromitite layer (Davey, 1992).

2.4.2 Brakspruit reef type

The Brakspruit (Fig. 2.2 B), formerly known as the RPM (Rustenburg Platinum Mine) facies (Vermaak, 1976), is a narrow reef type that is a type example frequently referred to in publications. The Brakspruit reef type is the only reef type at Lonplats characterized by a pegmatitic pyroxenite (46 cm thick) that is basal to the 1.48 m

thick Merensky pyroxenite. Unlike other reef types, the Merensky pyroxenite in the Brakspruit reef type grades into a norite which is 84 cm thick. The norite in turn grades into a 4.3 m thick mottled anorthosite. The top of the Merensky Unit in this reef type is marked by a Bastard pyroxenite that is 4 m in thickness and is overlain by a norite. The Brakspruit reef type also contains three chromitite layers (maximum thickness is 9 mm) confined within the Merensky pyroxenite and its basal pegmatitic pyroxenite. Mineralization occurs in the Merensky pyroxenite and pegmatitic pyroxenite and the highest grade is close the chromitite layer that is at the base of the Merensky pyroxenite.

2.4.3 Marikana reef type

The Marikana reef type (Fig 2.2 C) is a transition between the Brakspruit and the Westplats reef types. It is a wide or thick non-pegmatitic reef type and has a 2.4 thick Merensky pyroxenite. The footwall and the hanging wall, of the Merensky pyroxenite are anorthositic. The immediate hanging wall of the Merensky pyroxenite is a spotted anorthosite with a thickness of 1.2 m. Above the spotted anorthosite is a 5.9 m thick mottled anorthosite. A norite with a thickness of 7.8 m occurs above the mottled anorthosite and below the Bastard pyroxenite. The Bastard pyroxenite is 2.4 m thick in the Marikana reef type. The Marikana reef type contains three chromitite layers that are confined to the Merensky pyroxenite, with one 7 mm thick chromitite layer marking the base of the pyroxenite and a 3 mm thick chromitite layer that occurs at 1.9 m for the basal layer. Continuous mineralization occurs from the chromitite layer

at the base of the Merensky pyroxenite to the chromitite layer that occurs toward the top of the Merensky pyroxenite.

2.4.4 Westplats reef type

The Westplats reef type (Fig 2.2 D), situated in the far east on the Lonplats' lease area, is also classified as a thick reef type because it contains the Merensky pyroxenite which reaches a thickness of 11 m. The Merensky pyroxenite has anorthosite as both its footwall and hanging wall. A spotted anorthosite (1.7 m thick) overlies the Merensky pyroxenite and grades into a 5 m mottled anorthosite. The Merensky pyroxenite has as its base a chromitite layer. The upper chromitite layer is not well developed. The Westplats reef type contains the thinnest (46 cm) Bastard pyroxenite which, unlike other sections, has a basal chromitite layer. The Bastard pyroxenite is overlain by a norite. Mineralization in the Westplats reef type occurs in the top 1 m of the Merensky pyroxenite and some around the chromitite layer that occurs at the base of the pyroxenite.

2.5 Mineralization

Although Lonplats' Mines are principally producing platinum-group minerals, the interest of this research project lies also in the base-metal sulphides. The sulphide mineralization in the Merensky Unit is generally restricted to a specific stratigraphic interval. However, very small amounts of mineralization occur in the hanging wall

norite. Sulphide mineralization at Lonplats' Mines is generally high grade in the top one meter of the Merensky pyroxenite (top loaded mineralization). The sulphide mineralization also occurs in the proximity of the chromitite layers of the different reef types.

The Merensky pyroxenite contains a limited amount of sulphide minerals and this assemblage is typically pyrrhotite, pentlandite, chalcopyrite and pyrite, in decreasing order of abundance. The sulphide mineralization in the different reef types occur in varied mode of fashion. Chapter 4 makes a detailed discussion about the different modes of occurrence of the sulphides within the mafic cumulate rocks of the Merensky Unit in the reef types at Lonplats.

CHAPTER THREE

METHODOLOGY

3.1 Sampling

Boreholes representative of the different reef types described in Chapter 2 were selected in consultation with the mine geologists at Lonplats' Mines. Five borehole cores were sampled from the core sheds of Karee and Eastern Platinum Mines. The boreholes that were considered for this research project are ZS 07, R 37, ML 44, TN 70 and TN 71. The boreholes represent the Thin, Brakspruit, Marikana and Westplats reef types respectively (Fig. 2.2). No single suitable borehole was available for Westplats reef type because of faulting, chlorite-filled joints, alteration, and the presence of discordant ultramafic bodies or proximity to potholes and so samples from two boreholes were combined for this study. TN 70 was fractured and faulted from 50 cm above the base of the pyroxenite but perfectly fresh below. TN 71 was faulted at the base and below the pyroxenite but fresh above. Thus a composite of these two adjacent boreholes (TN 70 and TN 71) had to be used where the faulted portions were omitted. Depending on the length of the reef types, samples were also taken from up to 21 m of the hanging wall above the Merensky pyroxenite and up to 8 m into the footwall of the pyroxenite, as shown in Fig. 2.2.

One hundred and two samples were collected. The number of samples in each reef type was chosen according to the thickness of the profile of the reef type itself. More samples were chosen from thick reef types such as the Marikana and Westplats reef types and fewer samples from narrow reef types such as the Brakspruit and the Thin reef types. Fifteen samples were selected from the Thin reef type, twenty one from both the Brakspruit and Marikana reef types and forty six from the Westplats reef type.

Continuous sampling was conducted through the Merensky pyroxenite from the four borehole cores. The hanging wall and footwall of the Merensky pyroxenite were sampled at intervals ranging from 1 to 5 m. Generally, 20 cm long samples were collected along the vertical extent of the borehole cores. Where the Merensky pyroxenite was thickest, samples were cut to a length of 40 cm. All samples were in the form of fresh half and quarter cores. The advantage of using quarter cores is that the Lonplats' Mines have already analyzed them for PGE. However, the usage of quarter cores is disadvantageous in regard to their quantity; 120 g. Sample weights of 20 cm- and 40 cm-long cores are typically 240 g and 480 g respectively.

Reference samples were also analyzed to ensure accuracy and precision of all analytical work undertaken. The reference samples included a two kilogram sample of the Merensky pyroxenite, and aliquots of three samples of pyroxenite, norite and anorthosite that have been routinely analyzed in conjection with several Bushveld related projects undertaken at the University of Witwatersrand. These samples were

included to ascertain that the present data are compatible with the previously published data bases from the University of the Witwatersrand. Precision and accuracy were also ensured by a selected number of duplicated analyses. In order to obtain the most meaningful analytical results, certain criteria were set up.

3.2 Criteria of choosing boreholes

3.2.1 Boreholes away from potholes, iron-rich ultramafic pegmatitic bodies and younger dykes:

Boreholes close to potholes, iron-rich ultramafic pegmatitic bodies and younger dykes were avoided. On selection of the boreholes, maps of these features were inspected to avoid possible effects from these complications to usual stratigraphy, geochemistry and mineralogy.

3.2.2 Intact boreholes:

The selection of boreholes ensured the wholeness of boreholes. Fractured and faulted boreholes were avoided. The presence of fractures and faults in the samples could imply the presence of hydrothermal systems.

3.3 Criteria of choosing samples

3.3.1 Fresh samples:

The freshness of the samples was of high priority. The samples had to be free of any alteration visible to the naked eye.

3.3.2 Vein-free samples:

Samples had to be devoid of any hydrothermal fluid systems that manifested themselves as veins of usually chlorite or quartz-feldspar-biotite pegmatitic veins.

3.3.3 Homogeneous samples:

To eliminate inhomogeneity, samples were cut at the contacts. As a result, some samples were longer and others shorter than the desired 20 cm length. However this procedure eliminated possible samples composed of more than one major rock type.

3.4 Processing of samples

2 cm long pieces of sample were set aside for the preparation of polished sections and polished thin sections for microscopic investigations of the sulphides and the host minerals as well as electron microprobe analyses (EMPA) of chromite minerals. Special 48 mm polished thin sections were utilized for the chromite mineral analyses. EMPA was used to analyse chromite minerals for Cr, V, Zn, Si, Ti, Al, Fe, Mg, Mn,

Ni and Ca. The remainder of the samples was used for further study and future reference.

Each 40 cm long sample was cut into six pieces of approximately 7 cm in length. Three alternate 7 cm pieces (Fig. 3.1) were combined and crushed to eliminate bias. This means that out of each 40 cm long sample, only three pieces (a total of about 20 cm) were crushed for analytical work.

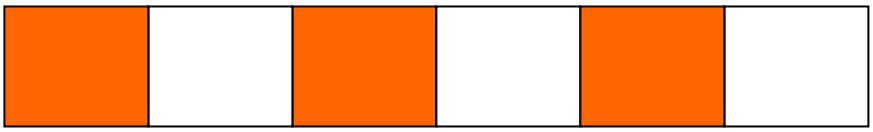

Figure 3.1 A sketch of a 40 cm long sample. Shaded pieces were combined for crushing and chemical analyses.

Coarsely-crushed (15 mm) samples were split into half. One aliquot was then milled into a fine (< 20 μm) size fraction which was used for whole-rock XRF analyses. Whole-rock analyses are important in providing an understanding of where the mineralization occurs within stratigraphies. The whole rock analyses included the determination of SiO_2, Al_2O_3, MnO, MgO, TiO_2, P_2O_5, K_2O, total iron as Fe_2O_3 and CaO as major elements and Cr, Ni, Na_2O, Zr, Nb, Co, Zn, Ba, Rb, Sr, S, C, Cl, V, PGE and Y as trace elements. All trace elements were analyzed by XRF at the University of the Witwatersrand except for S, PGE and C and Cl. PGE, C, S and Cl were analyzed at Set Point Laboratories by fire assay, LECO (Laboratory Equipment

Company Overhaul) combustion method and precipitation methods, respectively. Analyses of these latter trace elements by XRF fall short of accuracy. Milled samples of >110 g in weight were used for PGE analyses.

The second aliquot of the coarsely-crushed material was further crushed to 100 μm size. This sample fraction was washed and processed through a Franz magnetic separator to make plagioclase mineral separates for the determination of strontium isotopic information which was obtained by thermal ionisation solid source mass spectrometry. ICPMS (Inductively Coupled Plasma - Mass Spectrometry) and mass spectrometry were used to determine the absolute concentrations of Sr and Rb in plagioclase separates.

Analytical techniques, standards and other data are given in the appendix.

CHAPTER FOUR

PETROGRAPHY

4.1 Introduction

This chapter focuses on the examination of the cumulate rocks comprising the four reef types at Lonplats' Mines in thin and polished sections. Textural relationships and mineral contents are also described in this chapter. As mentioned in the previous chapters, the rocks of the four reef types are mainly pyroxenite, norite and anorthosite. Occasional pegmatitic pyroxenite is present as well. Chromitite layers occur mostly at contacts separating the different rock types within the reef types. Sulphides which are generally focused within specific intervals are also present. Minor magnetite is also contained in the rocks.

4.2 Cumulate terminology

Cumulate nomenclature was first developed by Wager et al. (1960) and further developed by Hunter (1996). The cumulate terminology was produced to describe igneous textures in rocks in slowly cooled layered complexes, such as the Bushveld Complex. Primary crystals that formed during crystal settling, which Jackson (1961) likened to clastic sediments in a sedimentation processes, are termed cumulus and the interstitial liquid is referred to as intercumulus. Wager et al. (1960) established the

terms that describe igneous rocks in layered intrusions: orthocumulates and adcumulates. Adcumulate and orthocumulate rocks are principal end-members of a continuum of rock types with increasing amounts of liquid trapped in the resultant pore spaces after accumulation.

An adcumulate is described as a rock in which accumulation of crystals is often monomineralic. The intercumulus liquid is removed as a result of crystal settling, overgrowth (adcumulate growth) and compaction of cumulus minerals. The cumulus phase comprises the entire rock. Orthocumulates, on the contrary, are rocks with the intercumulus phases that crystallize in pore spaces between the cumulus minerals and are often different from the cumulus phases. The intercumulus phases may enclose the primocrysts poikilitically.

4.3 Pyroxenite

Each reef type (vertical profile through the Merensky and Bastard units as well as through adjacent units) contains a maximum of two pyroxenite layers of variable thicknesses; the Merensky and Bastard pyroxenites. Pyroxenites are composed of approximately 79 – 95 % orthopyroxene. This cumulate phase occurs with sub-ordinate amounts of plagioclase, biotite, clinopyroxene and occasional chromite, magnetite and sulphides. Olivine and apatite are mineral phases that are rarely noted in these pyroxenites. The pyroxenites become feldspathic with an increase in height until they grade into overlying norite or anorthosite. The pyroxenites are generally

medium- to coarse-grained (2 mm to 5 mm) except where a pegmatitic pyroxenite exists. Pegmatitic pyroxenites are very coarse-grained because cumulus orthopyroxene grains reach a maximum size of 2 cm.

The mostly equidimensional orthopyroxenes range in grain shapes from euhedral to subhedral and a very minor amount is anhedral. The relations of the grain boundaries formed by the orthopyroxene grains are often triple junctions (Fig. 4.1a). On occasion, the orthopyroxene forms triple junctions with other adjacent minerals (Fig. 4.1b). In some cases, the orthopyroxene is present as isolated grains in plagioclase oikocrysts (Fig. 4.1c).

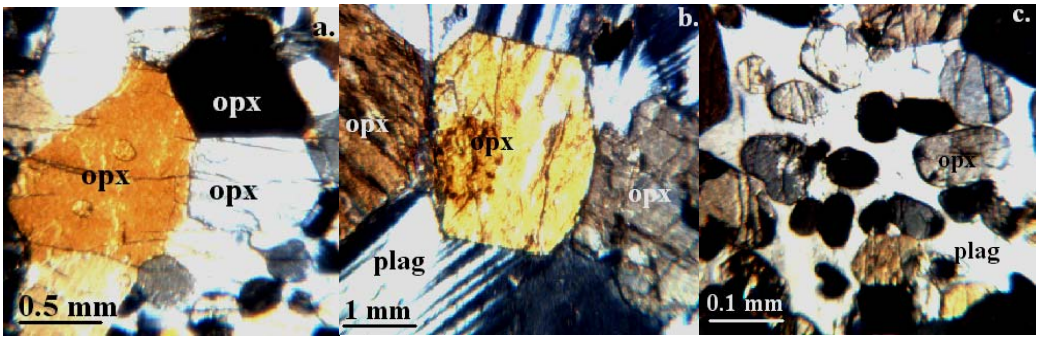

Fig 4.1 Relationship of orthopyroxene grains. a, orthopyroxenes form a triple junctions; b, triple junctions between orthopyroxene and plagioclase; c, an oikocrysts of plagioclase with isolated grains of orthopyroxene.

Plagioclase is a major intercumulus phase in the pyroxenites. Plagioclase in these mafic rocks can either be optically continuous (Fig. 4.1c) or exist as grains that grow against the orthopyroxenes and thereby impinge on the mafic minerals, forming cuspate grain boundaries (Fig. 4.2a). Plagioclase also occurs enclosed by

clinopyroxene resulting into a poikilitic texture (Fig. 4.2b). Clinopyroxene occurs as the second most abundant interstitial phase in the pyroxenites.

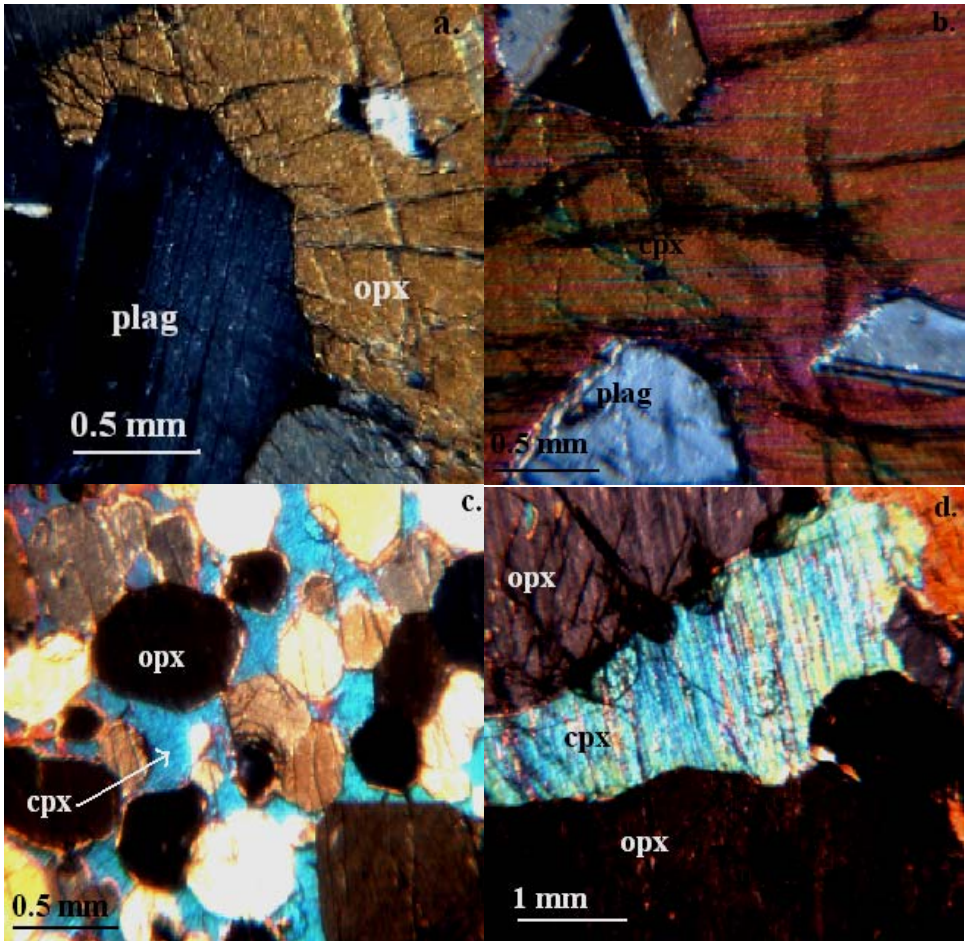

Fig. 4.2 a, Plagioclase (plag) grain impinging into an orthopyroxene (opx); b, clinopyroxene (cpx) poikilitically enclosing plagioclase in feldspathic pyroxenite ; c, clinopyroxene enclosing orthopyroxene and plagioclase; d, clinopyroxene interstitial to the orthopyroxene grains.

The clinopyroxene is present as a poikilitic grain enclosing orthopyroxene and on rare occasions, plagioclase (Fig. 4.2b and Fig. 4.2c). Figure 4.2d shows clinopyroxene

present as an intercumulus phase between cumulus orthopyroxene grains. Clinopyroxene can also occur in the pyroxenites as exsolution lamellae in the orthopyroxene (Fig. 4.3d). Clinopyroxene also replaces orthopyroxene on rare occasions.

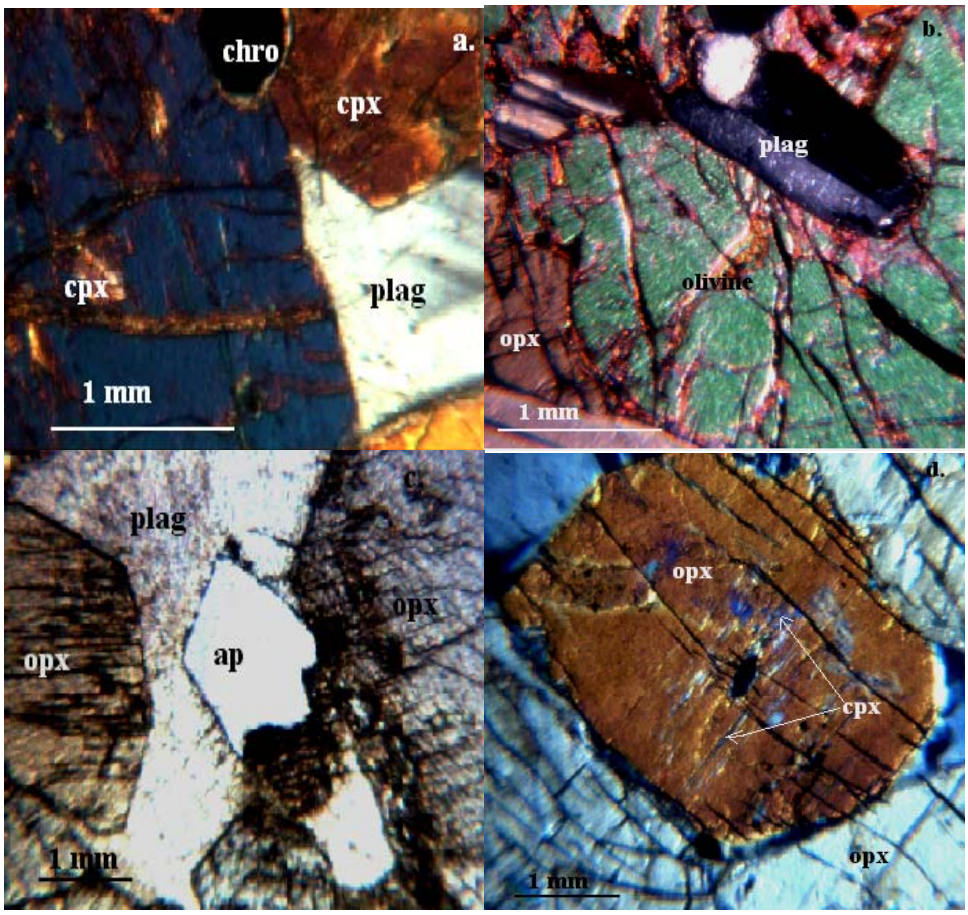

Fig. 4.3 a, Clinopyroxene with interstitial plagioclase; b, anhedral olivine enclosing plagioclase; c, idiomorphic apatite (ap) enclosed by plagioclase; d, cumulus orthopyroxene grain with exsolution lamellae of clinopyroxene, in the pegmatitic pyroxenite.

Poikilitic and ophitic textures are more common in pyroxenites than in pegmatitic pyroxenites. However, rare light green grains of clinopyroxene oikocrysts are present in the pegmatitic pyroxenites. Grain sizes of minerals in the pegmatitic pyroxenite reach a maximum of 2 cm. Biotite and sulphides as well as magnetite all occur as minor interstitial phases to the cumulus minerals in the pyroxenites. The two rarest minerals in the pyroxenites at Lonplats' Mines are olivine and apatite (Fig. 4.3b and Fig. 4.3c). Each of these two minerals has only been recognized in one thin section.

4.3.1 Sulphides

The main sulphide assemblage occurs mostly within, although not restricted to pyroxenites. Sulphides also occur in norite and rarely in anorthosite. The distribution of the sulphides in the pyroxenite is limited because the sulphides occur within a restricted interval, usually within the top meter of the Merensky pyroxenite. The base-metal sulphide assemblage occurs principally as interstitial phases in the pore spaces between silicate minerals in the pyroxenites. The common style of occurrence of the interstitial base metal sulphides is composite blebs of pyrrhotite, pentlandite, chalcopyrite and sometimes pyrite. Veins and inclusions of the sulphides in the silicate framework at Lonplats' Mines are not common modes of occurrences.

The sulphide mineralogy at Lonplats' Mines is approximately 45% pyrrhotite, 35% pentlandite, 17% chalcopyrite and 3% pyrite. This composition is determined by summing up the estimated abundances of sulphide minerals in individual composite

grains. The proportions in which individual sulphide minerals exist in composite grains vary from grain to grain. An abundant sulphide mineral phase in one grain may be the least abundant in another sulphide grain, e.g. pyrrhotite may be abundant in one composite sulphide grain but pentlandite may be the abundant phase in the next grain. An average of these varied compositions is then used to estimate the overall composition of the sulphide assemblage. Although Vermaak and Hendriks (1976) have reported subordinate amounts of cubanite, mackinawite, sphalerite, galena, and rare sulfarsenides, such minerals have not been seen under an optical microscope in the Lonplats' thin sections for this project.

Irregular blebs

Blebs of sulphides (Fig. 4.4a) interstitial to the pyroxene and plagioclase usually consist of composite intergrowths of pyrrhotite, pentlandite, chalcopyrite and rarely pyrite. The interstitial sulphides account a large fraction of the space in the pore that they occupy. Rare association with biotite in the occupied pore spaces is encountered also. The sulphides can also exist as very fine-grained irregular blebs (Fig. 4.4b). Minor inclusions of orthopyroxene and plagioclase occur in the sulphide blebs.

Inclusion particles

Minute particles of sulphides (Fig. 4.4c) are occasionally present as inclusions in orthopyroxene and plagioclase minerals.

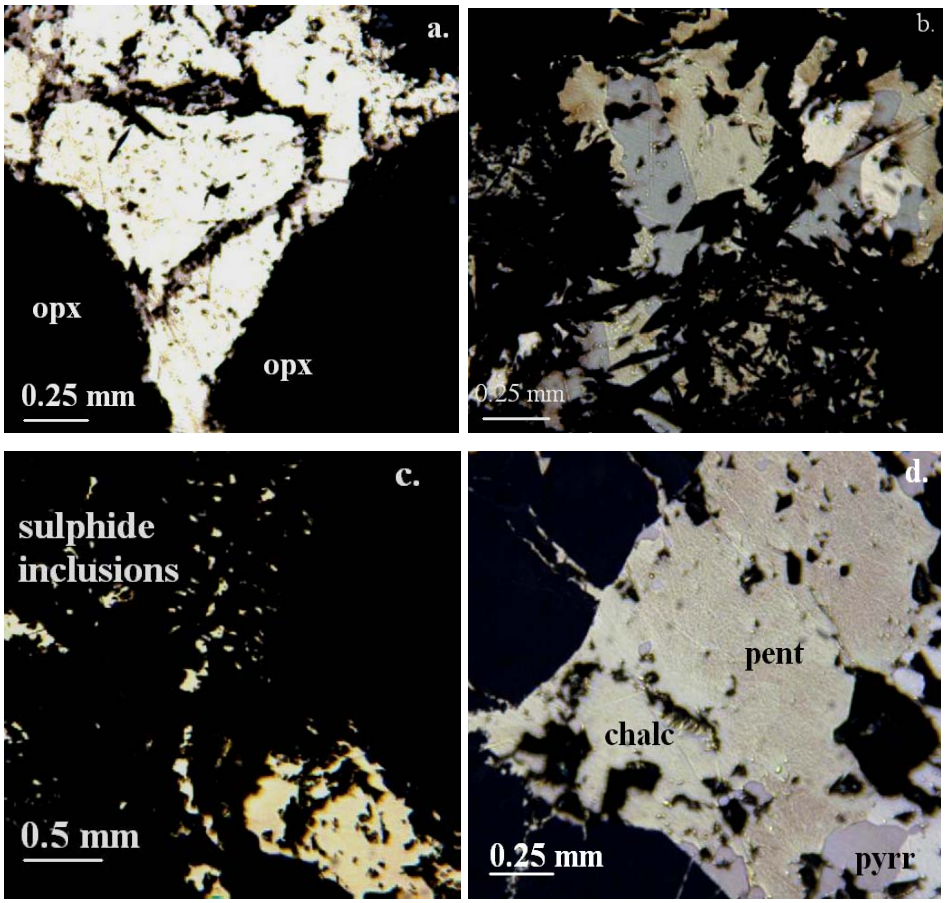

Fig. 4.4 Modes of sulphide occurrences. a, irregular blebs; b, fine-grained irregular blebs; c, sulphide inclusions in the orthopyroxene; d, veins off-shooting from the main sulphide body into orthopyroxene grains.

Veins

The sulphide veins (Fig. 4.4d) at Lonplats' Mines are microscopic (< 0.1 mm thick) and are mainly composed of chalcopyrite. However, veins composed of both chalcopyrite and pentlandite are also present but rare. The veins occur in various fashions of offshoots from irregular sulphide blebs (Fig. 4.4d) and as isolated in the silicate minerals.

4.3.1.1 Pyrrhotite

Pyrrhotite is the most abundant base metal sulphide type. It comprises 45% of the sulphide assemblage. As the dominant sulphide mineral, pyrrhotite often occurs in the core (Fig. 4.5a) of irregular blebs that are usually manifested as composite intergrowths of sulphides. Although pyrrhotite is often coarse-grained to medium-grained, it is also present fine-grain irregular blebs (Fig. 4.4b).

4.3.1.2 Pentlandite

As the second most abundant sulphide mineral, pentlandite often is present, not only as exsolution lamellae (Fig. 4.5b) in pyrrhotite grains, but also present as part of the sulphide intergrowths. Figure 4.5c illustrates this intergrowth pattern. Pentlandite, intergrown with chalcopyrite usually occurs around the pyrrhotite cores.

4.3.1.3 Chalcopyrite

Chalcopyrite, the third most important mineral in the sulphide assemblage, occurs in several styles or modes. Chalcopyrite can be present as isolated grains (Fig. 4.5d). Chalcopyrite can manifest itself as veins (Fig. 4.4d) in the silicate phases. Chalcopyrite also forms part of the composite overgrowths (Fig. 4.6a) and also forms rims around the composites grains of sulphide, especially pentlandite (Fig. 4.6b).

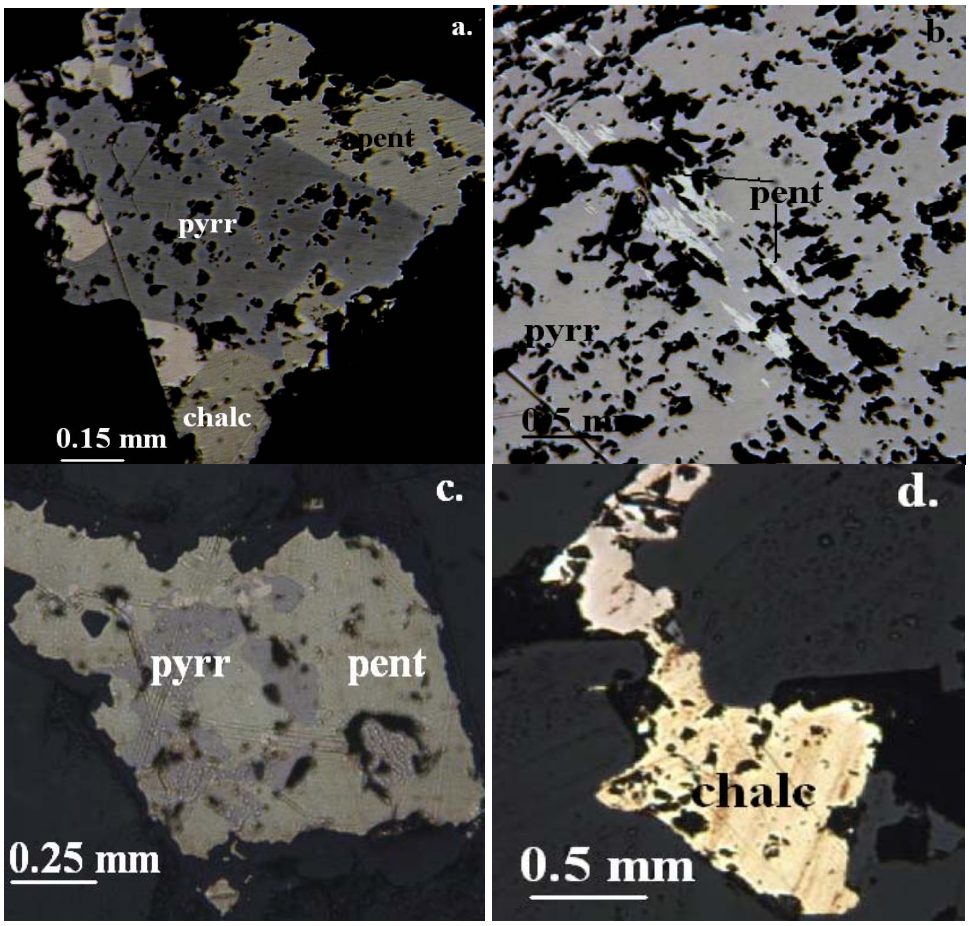

Fig. 4.5 a, Pyrrhotite (pyrr) as the core of the sulphide aggregate with pentlandite and chalcopyrite; b, exsolution lamellae of pentlandite (pent) in pyrrhotite; c, pentlandite intergrown with pyrrhotite; d, isolated chalcopyrite (chalc) grain between plagioclase.

4.3.1.4 Pyrite

Pyrite is the rarest of the four main sulphides in the mineral assemblage. Pyrite grains are often present as subhedral grains (Fig. 4.6c) in the composite grains of pyrrhotite,

pentlandite and chalcopyrite. A rare feature manifested as a worm-like texture akin to a mymerkite is shown by intergrowths of mainly pyrite and chalcopyrite (Fig. 4.6d).

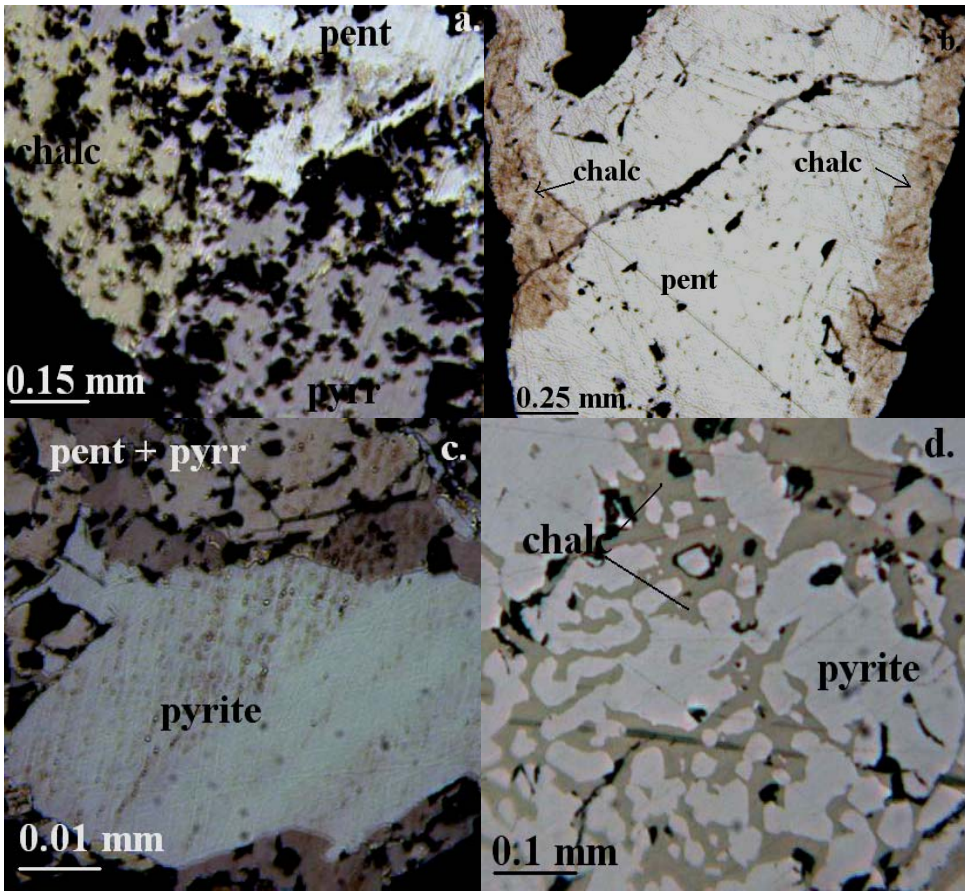

Fig. 4.6 a, Pyrrhotite and pentlandite rimmed by chalcopyrite; b, rims of chalcopyrite around pentlandite; c, pyrite grain enclosed in composite pentlandite and pyrrhotite; d, intergrowths of chalcopyrite and pyrite.

Another less common feature is the replacement of pyrite by chalcopyrite, also evident in the sulphide textures (Fig. 4.7a). Microbrecciation occurs solely in the pyrite grains (Fig. 4.7b, c and d). The fragmented pyrite grains are overgrown by pyrrhotite or chalcopyrite along the resultant fractures.

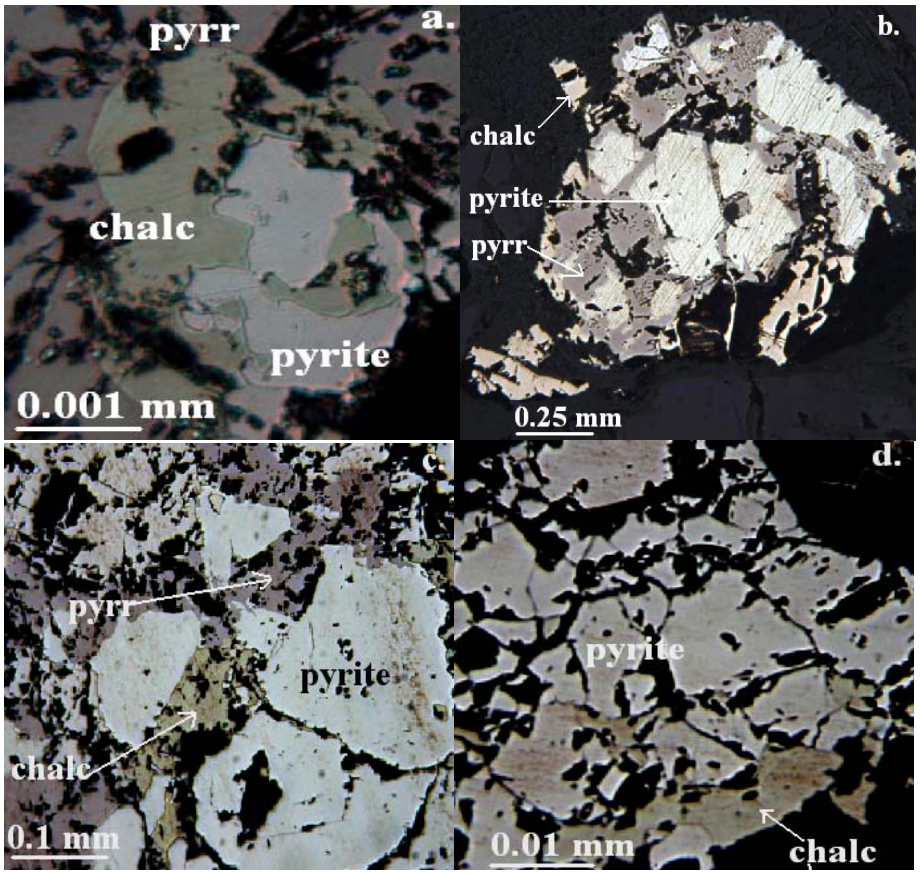

Fig. 4.7 a, Chalcopyrite replaces pyrite and is in turn rimmed by pyrrhotite; b brecciated pyrite replaced by pyrrhotite; c, brecciated pyrite replaced by pyrrhotite and chalcopyrite; d, microbrecciated pyrite.

4.3.1.5 Associated minerals

The sulphides at Lonplats' Mines are associated with chromite and to a lesser extent, magnetite. Figure 4.8 shows the sulphides nucleating around euhedral spinel grains; chromite and magnetite. Bottom left of Figure 4.8c shows what seems to be intergrowths of magnetite and the sulphides. The sulphide composites are also interstitial to both chromite and magnetite. Where magnetite is present, a mutual association with the sulphides is commonly demonstrated.

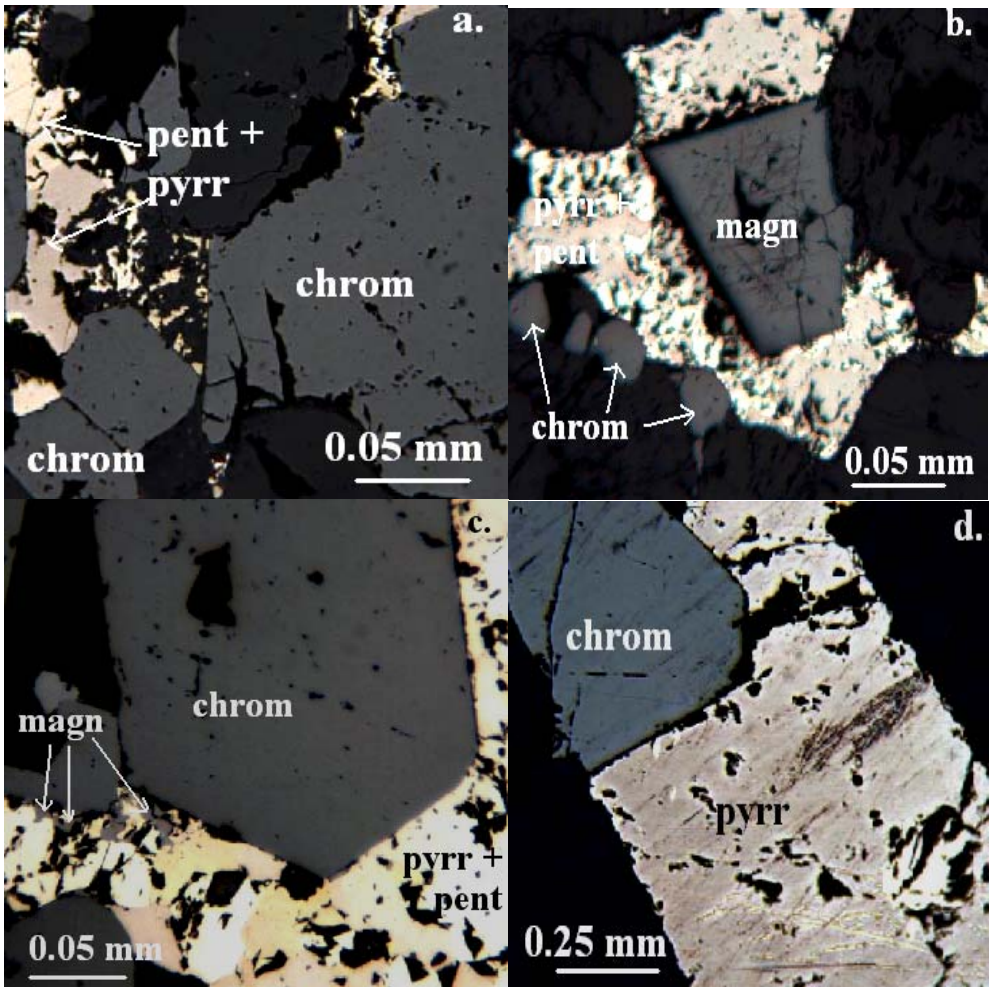

Fig. 4.8 Chromite and magnetite associated with sulphides. a, sulphides interstitial to chromite; b, sulphides forming around magnetite; c, intergrowths of sulphides and magnetite; d, pyrrhotite forming around chromite.

4.4 Anorthosite

The anorthosites in the reef types, including the hanging wall and the footwall to the Merensky pyroxenite, have plagioclase abundances of up to 96%. The anorthosites contain minor euhedral orthopyroxene resulting in the so-called spotted anorthosites and also contain poikilitic orthopyroxene grains making up mottled anorthosites. The

oikocrysts in the anorthosite range in size from 1cm to 3cm. The anorthosites are medium-grained. However, occasional larger plagioclase grains (1 cm across) occur amid the mosaic (Fig. 4.9a) of finer grains of plagioclase at times giving the rocks a random size distribution of grains.

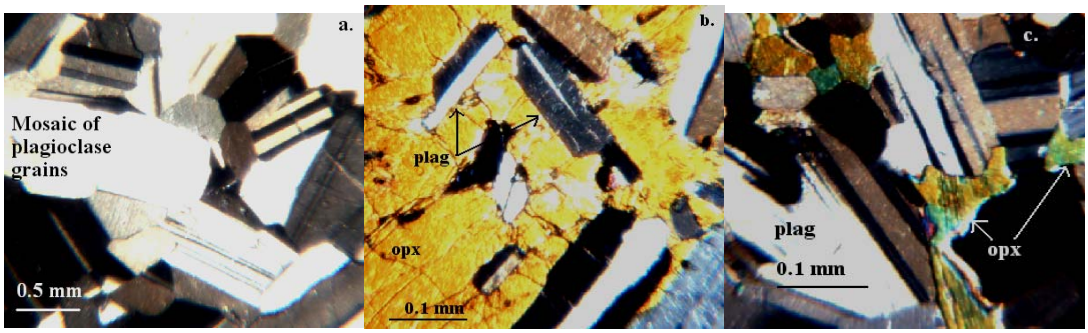

Fig. 4.9 a, A mosaic of plagioclase grains; b, oikocryst of orthopyroxene enclosing tabular plagioclase; c, interstitial orthopyroxene in small pore spaces.

An appreciable proportion of primary plagioclase grains are tabular. However the original grain shape is often obliterated by the impingement of the plagioclase grains against one another. The impingement of the grains results into triple junctions, subsequently forming an interlocking mosaic (Fig. 4.9a). The mosaic displays no preferred orientation of the plagioclase grains. Idiomorphic plagioclase grains enveloped by intercumulus orthopyroxene give the anorthosites a poikilitic texture (Fig. 4.9b), hence the mottles. Orthopyroxene can also occur as small interstitial grains (Fig. 4.9 c) in the anorthosites; free from enclosed minerals.

Minute amounts of clinopyroxene are present as exsolution, replacement and intercumulus phases in the anorthosites. A very minor amount of sulphide minerals

can be present in the anorthosites that are adjacent to the mineralized pyroxenite. Sporadic chromite occurs in the anorthosites at grain boundaries and rarely enclosed by orthopyroxene.

4.5 Norite

Norites are among the least abundant rocks in the four reef types. Norites range between leuconorites and melanorites. Definitions of melanorites and feldspathic pyroxenites as well as definitions of leuconorites and spotted anorthosites are not rigorous. Therefore, for this immediate purpose, only rocks that contain approximately equal amounts of cumulus plagioclase and orthopyroxene will be considered.

Norites in the four reef type profiles are generally medium-grained. The primary orthopyroxene and plagioclase minerals comprising the norites are inequidimensional. Plagioclase and orthopyroxene are subhedral to anhedral. Cumulus plagioclase minerals form interlocking mosaics as shown in Fig. 4.10a and occur with orthopyroxene grains. Plagioclase grains in the mosaic impinge onto one another to a significant degree whereas the grain boundary relations of orthopyroxene grains are variable. Very few triple junctions are displayed in the norites. Although orthopyroxene and plagioclase minerals are cumulus, plagioclase minerals can have an intercumulus component. Some of the plagioclase is interstitial to both the

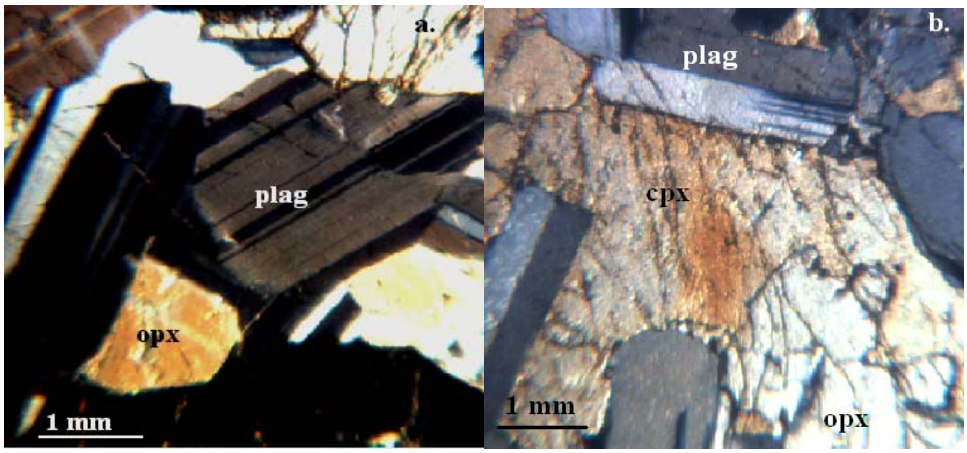

Fig. 4.10. a, Mosaic of cumulus plagioclase with orthopyroxene; b, intercumulus clinopyroxene enclosing resorbed orthopyroxene and plagioclase grains.

displayed in the norites. Clinopyroxene that are interstitial to plagioclase and orthopyroxene (Fig. 4.10b) are also present as twinned grains (Fig. 4.11b). Biotite (Fig. 4.11a) and sulphides are present as minute interstitial phases.

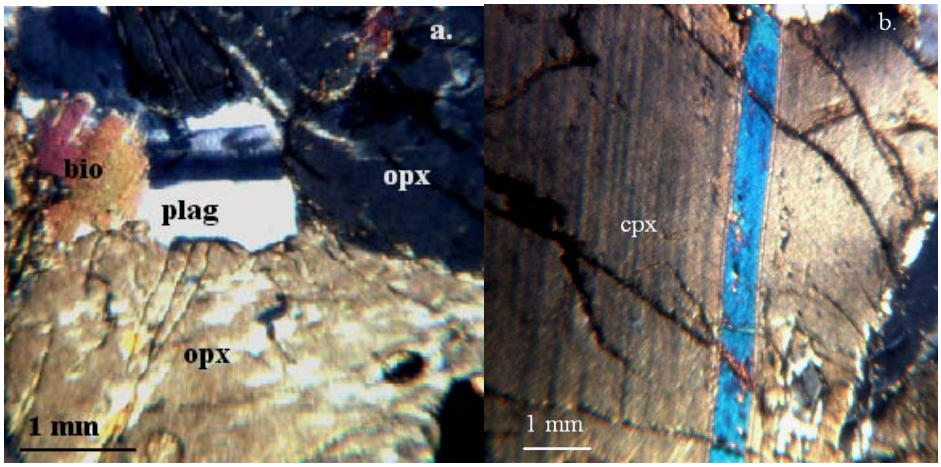

Fig. 4.11. a, Intercumulus plagioclase and biotite; b, twinned clinopyroxene.

4.6 Chromitite

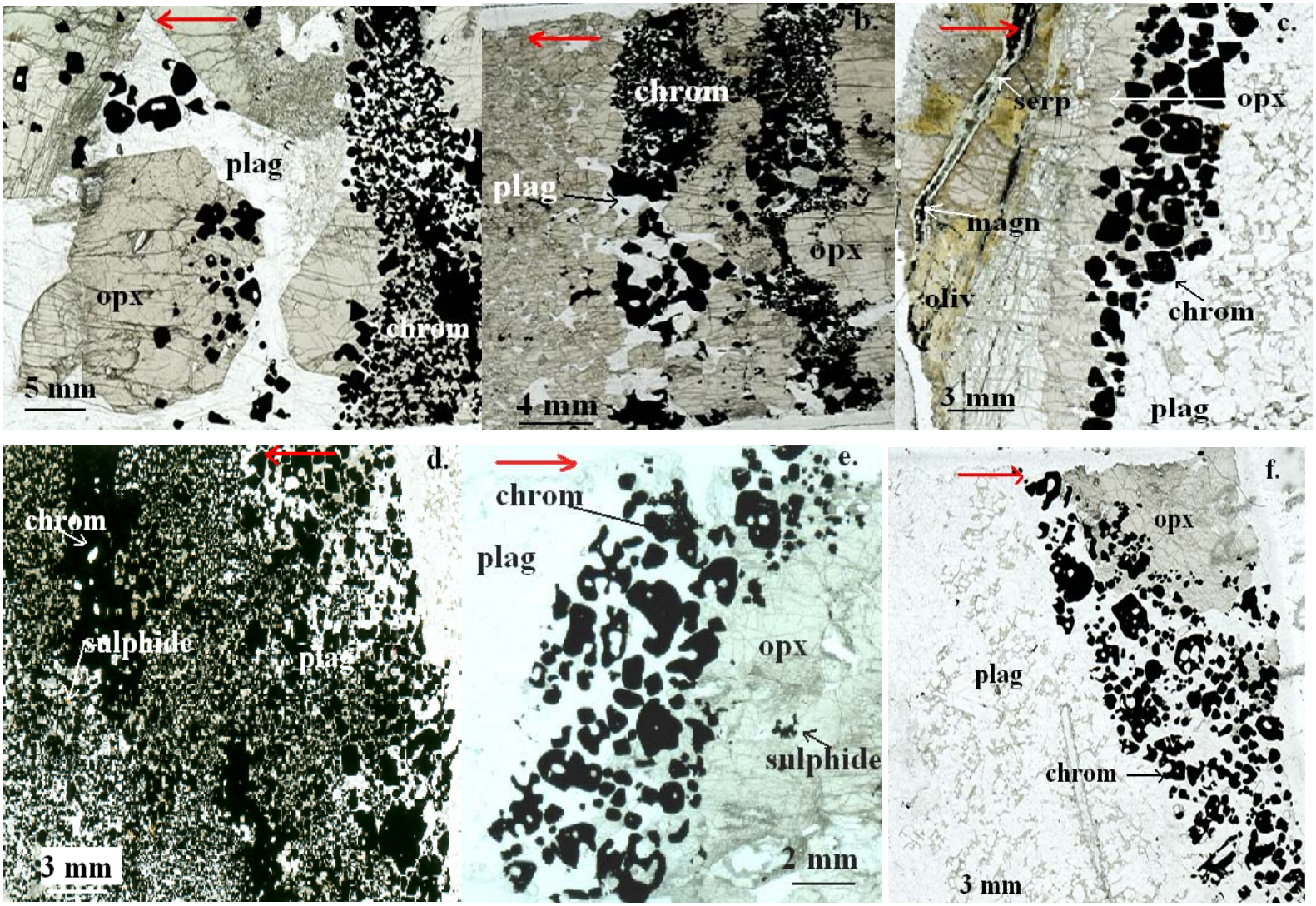
plag
opx
chrom
5 mm
b.
chrom
plag
opx
4 mm
c.
serp
opx
magn
oliv
chrom
3 mm
plag
d.
chrom
sulphide
plag
3 mm
e.
chrom
plag
opx
sulphide
2 mm
f.
opx
plag
chrom
3 mm

← Fig. 4.12 Chromitite layers from the different reef types. a, b and c, chromitite layers (basal, intermediate and upper) at different stratigraphic levels from the Brakspruit reef type; d, basal chromitite layer from the Thin reef type; e, basal chromitite layer from the Marikana reef type; f, intermediate chromitite layer from the Marikana reef type. Arrows show upward direction.

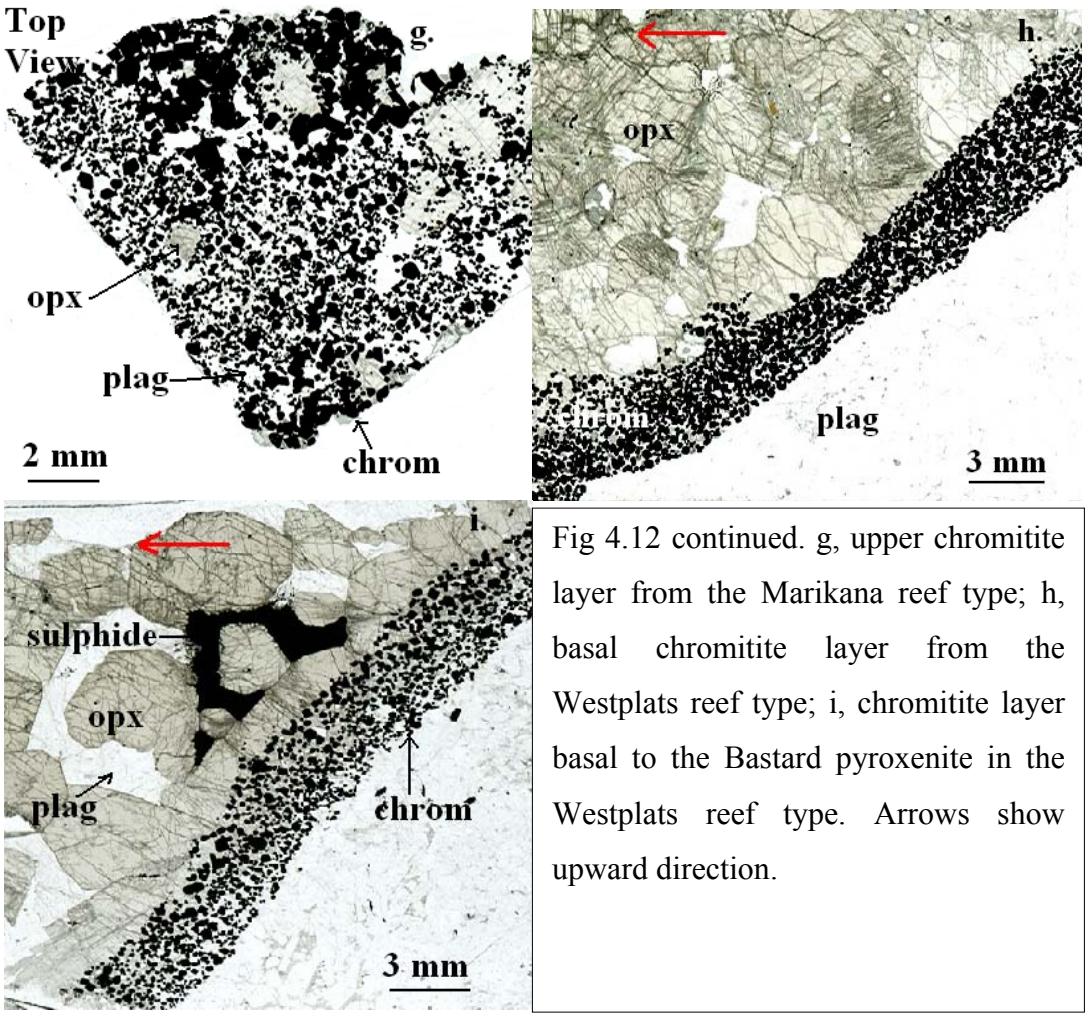

Fig 4.12 continued. g, upper chromitite layer from the Marikana reef type; h, basal chromitite layer from the Westplats reef type; i, chromitite layer basal to the Bastard pyroxenite in the Westplats reef type. Arrows show upward direction.

The four reef types all contain at least one chromitite layer (Fig. 4.12). Rigorous determination of the modal proportions of chromitite in these layers by point counting included an average of 500 counts in the respective polished thin sections. The

chromitite layers contain a wide range of modal proportions. Thin chromitite layers (~2 mm) contain an average of 37% chromite and semi-massive layers contain a mean of 62% chromite.

The chromitite layers are often hosted in pyroxene or at contacts between anorthosites and pyroxenites (Fig. 4.12c, e, f, h and i). Contacts between the chromitite layers and their hosts are often sharp but can also be irregular. A chromitite layer can divided into more than one layer (Fig. 4.12b). The thicknesses of the chromitite layers range from 1 mm to 2.5 cm. The Thin reef type has the thickest chromitite layer and the Westplats reef type contains the thinnest chromitite layer.

The chromitite layers are fine-grained to medium-grained. The morphology of the chromite grains vary from subhedral, anhedral and rarely euhedral and these chromite

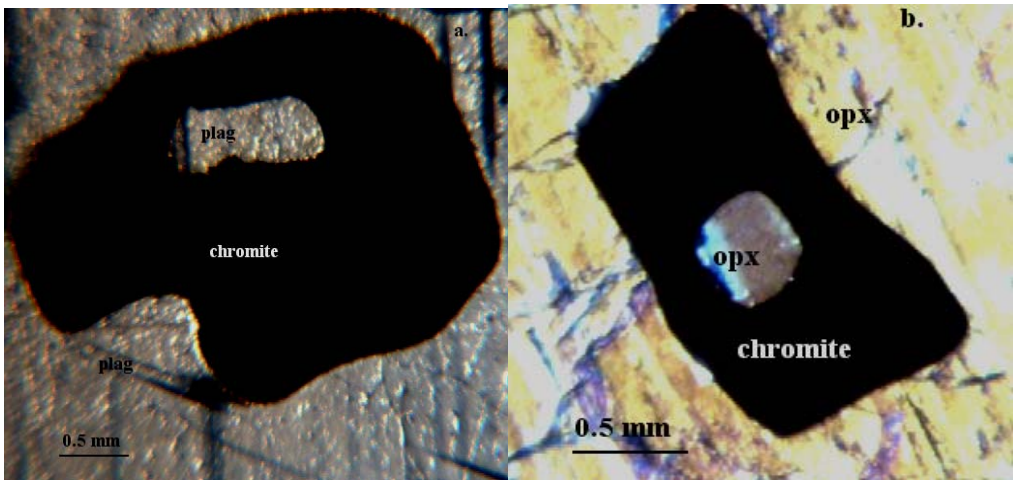

Fig. 4.13 Inclusions of plagioclase and orthopyroxene in irregular-shaped chromite hosted by these silicate phases, respectively.

grains rarely share mutual grain boundaries (Fig. 4.12) even when they are form a layer. In rare instances, the chromite grains occur as clusters (Fig. 4.12d) and form bigger grains. The chromite minerals also occur as disseminated grains (Fig. 4.12a). Inclusions of plagioclase and pyroxene that vary in size and shape may occur in the chromite grains (Fig. 4.13a and b). The inclusions exhibit optical continuity with the surrounding silicate host to the chromite minerals.

CHAPTER FIVE

WHOLE-ROCK GEOCHEMISTRY

5.1 Introduction

This chapter presents whole-rock XRF data produced for the rocks of the five boreholes that represent the four reef types (see Chapter Two) at Lonplats' Mines. Major- and trace-element data are presented in Appendix A and B. Although field observations were used to characterize these reef types, the plots produced from the geochemical data will be utilized for observations of chemical variations of the reef types. Harker plots of different elements versus magnesium concentrations for each reef type are presented here. Also plotted in these Harker diagrams are the mineral compositions from Boerst (2001) who studied the Merensky Reef at Impala Mines.

Orthopyroxene and plagioclase, which concentrate mostly lithophile elements, are the principal contributors to the modal silicate mineralogy of the rocks in the Merensky, and the adjacent units and hence, also to the chemical composition. Minor amounts of chromite, clinopyroxene, biotite and olivine as well as sulphides also contribute to the geochemistry of these units. The contribution of pyroxene and plagioclase is reflected in the element oxide contents; SiO_2, MgO, FeO, CaO, Na_2O and Al_2O_3.

5.2 Major-element trends

5.2.1MgO and FeO

Mg and Fe^{+2} both concentrate in pyroxenes. A very small amount of iron is accounted for by the spinel and sulphide minerals. In Fig. 5.1, a positive linear correlation between FeO considered as total iron and MgO is shown in each of these binary diagrams.

Pyroxenites in the Merensky Unit, and in adjacent units, have MgO contents that range from 19 wt % to 24 wt %. The FeO (total) content in the pyroxenites of the four reef types, ranges from 10 wt % to 12 wt %. Norites, which are few in abundance, contain a range of MgO and FeO (total) concentrations of 8.7 wt % to 12 wt % and 3 wt % to 8 wt %, respectively. Anorthosites have the least amounts of mafic minerals and thus are composed of lesser MgO (0.71 wt % to 4 wt %) and FeO (1wt % to 2 wt %) contents.

There are several samples that plot above the simple joining line between the mineral compositions of orthopyroxene and plagioclase minerals. This is especially observed in the pyroxenites and is a result of these rocks containing more than usual amounts of FeO (total). The elevated amounts of FeO (total) may be attributed to the occurrence of spinel minerals and less to the presence of clinopyroxene. Clinopyroxene contains less FeO (total) than orthopyroxene.

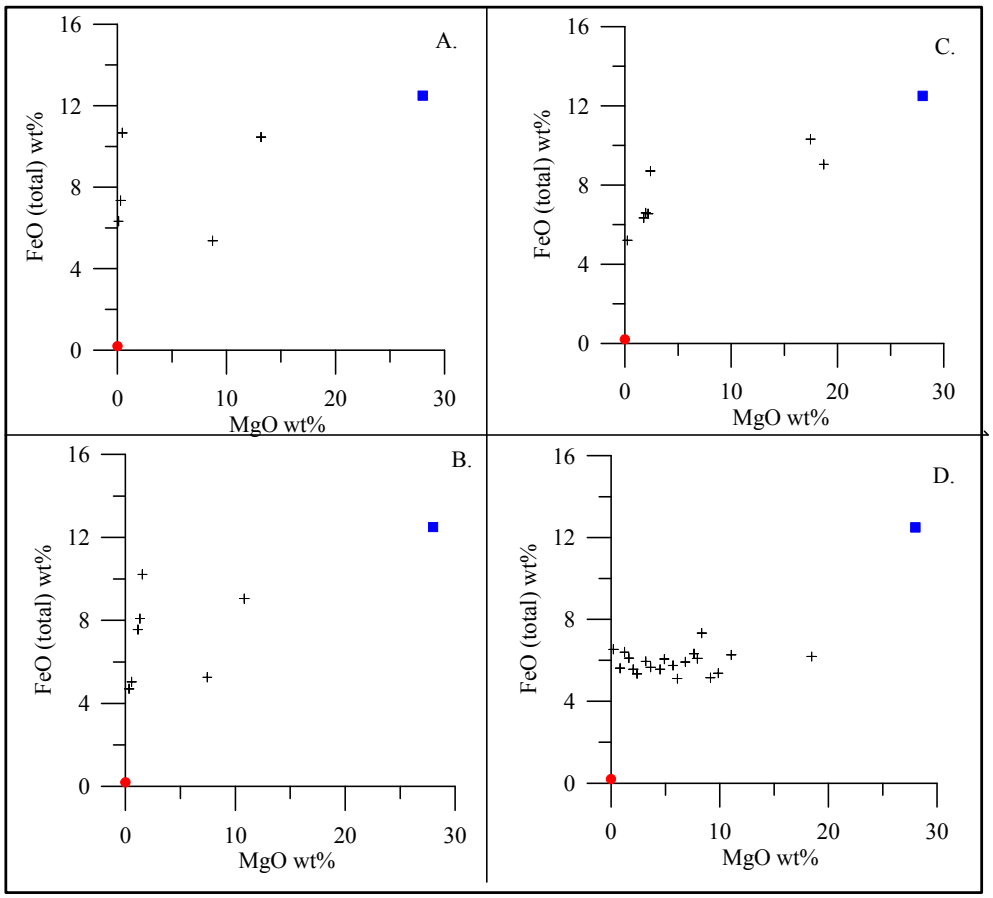

Fig. 5.1. FeO (total) contents in the rocks of A, Thin; B, Brakspruit; C, Marikana; and D, Westplats reef types. Plagioclase (filled circle) and Orthopyroxene (filled square) compositions are also shown, from Boerst (2001).

5.2.2 MnO and TiO_2

Manganese and titanium are lithophile minor elements present in abundances of less than 1 wt % and their presence is mainly accounted for by pyroxenes. This is indicated by a positive linear relationship of MnO and TiO_2 with MgO in Figures 5.2 and 5.3. Although TiO_2 is more compatible in chromites than it is in pyroxenes, the contribution of chromite towards TiO_2 abundances is less than the contribution of

pyroxenes because chromite is present in limited amounts. TiO_2 in the pyroxenite at Lonplats' Mines can reach a maximum of 0.3 wt %. Pyroxenites with common chromite contain 0.4 to 0.6 wt % of TiO_2. This is demonstrated in a group of pyroxenites that are registered above the tie-line between orthopyroxene and plagioclase compositions. The Brakspruit, Marikana and the Westplats reef types contain such a group of pyroxenites (Fig. 5.2). MnO is present in low concentrations of 0.25 wt %, at maximum (Fig.5.3).

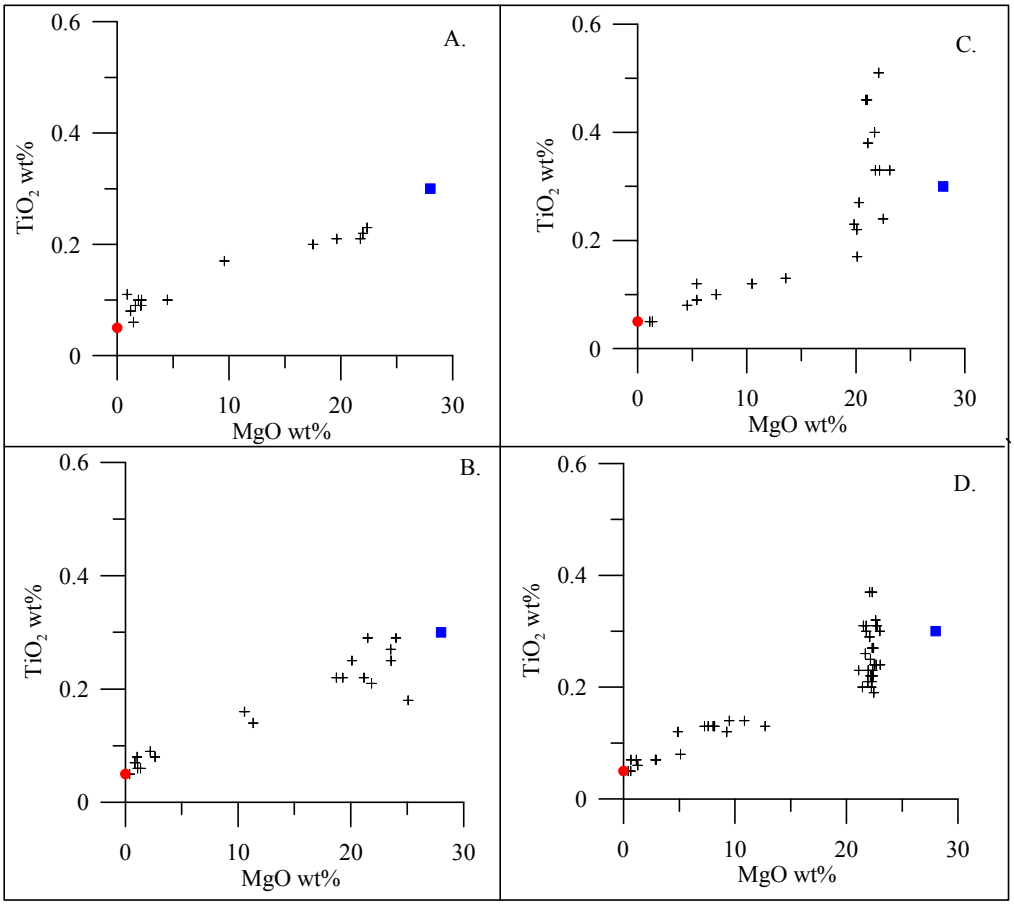

Fig. 5.2 TiO_2 contents in the rocks of A, the Thin; B, Brakspruit; C, Marikana; and D, Westplats reef types. Plagioclase (filled circle) and Orthopyroxene (filled square) compositions are also shown, from Boerst (2001).

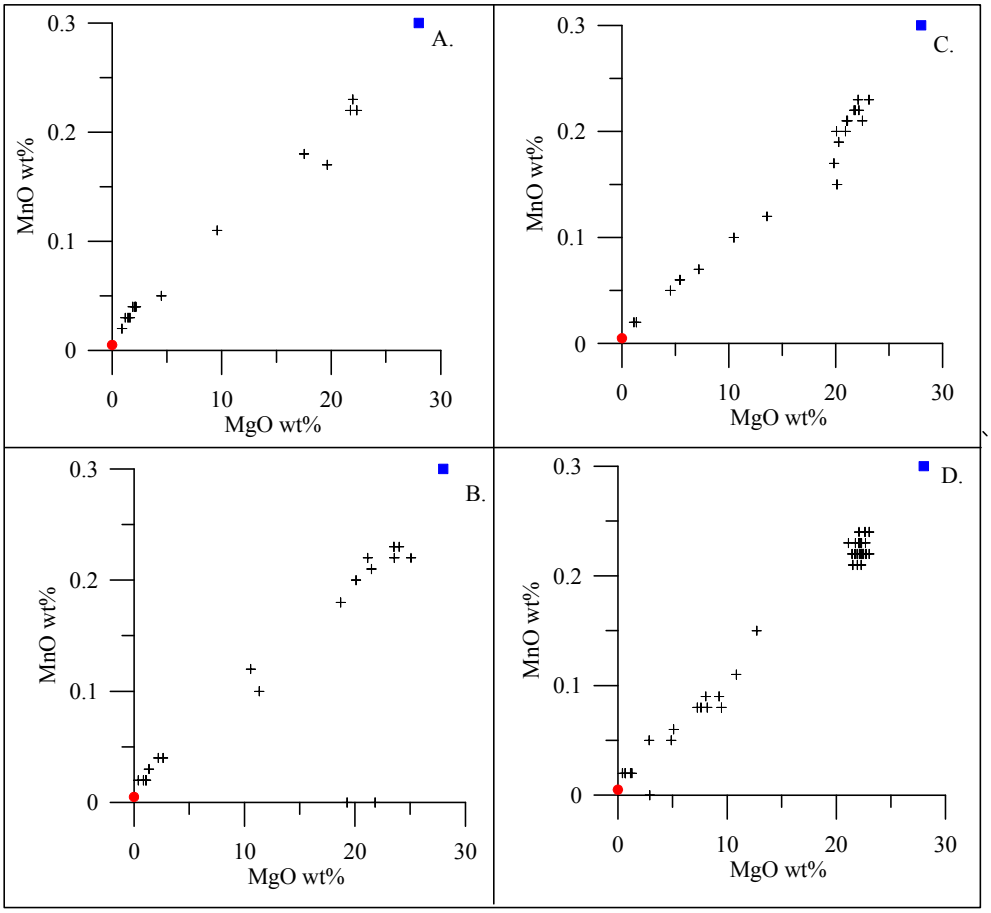

Fig. 5.3 MnO contents in the rocks of A, the Thin; B, Braksprui; C, Marikana; and D, Westplats reef types. Plagioclase (filled circle) and Orthopyroxene (filled square) compositions are also shown, from Boerst (2001).

5.2.3 Al_2O_3 and CaO

Al_2O_3 and CaO are elements that are more abundant in anorthosite and norite than in pyroxenites. Figures 5.4 and 5.5 show decreasing trends of both Al_2O_3 and CaO with increasing MgO for each reef type. Anorthosites contain Al_2O_3 concentrations that

reach a maximum of 32 wt %. Because norites are intermediate rocks, alumina is present in average amounts of 17 wt % to 24 wt %. Al_2O_3 concentrations in

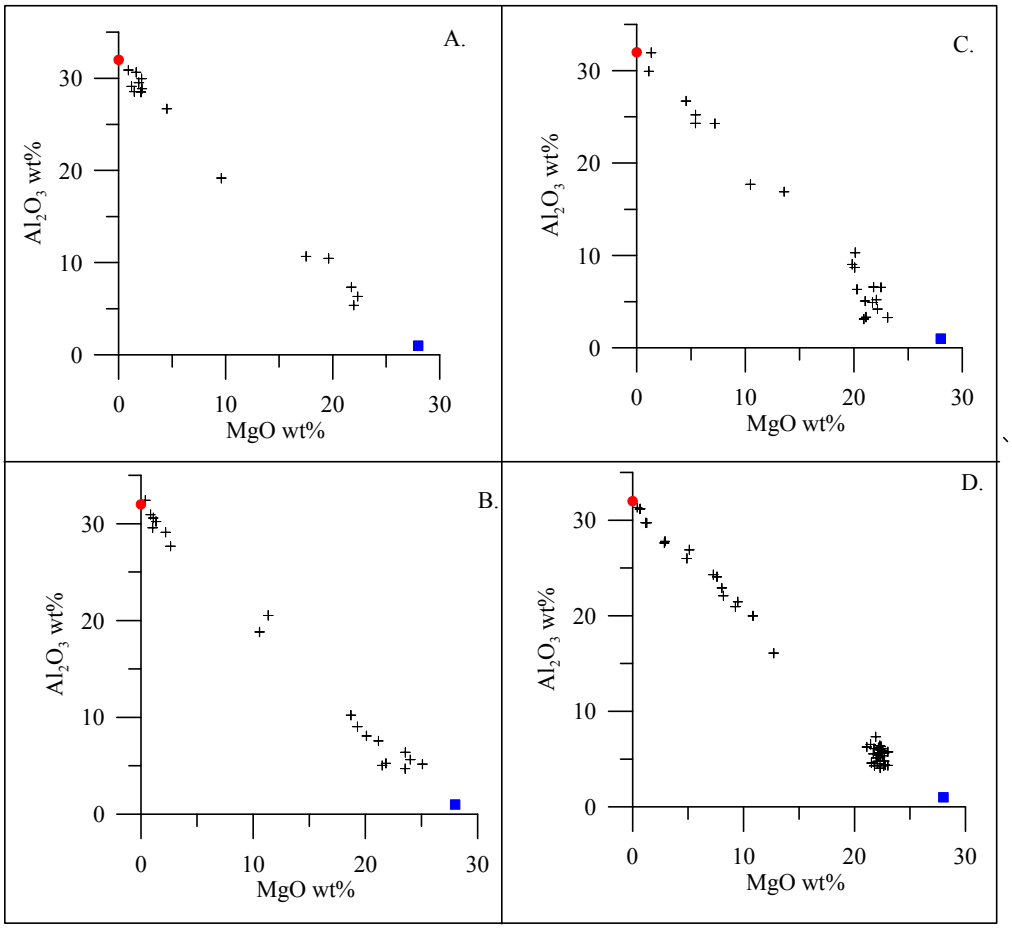

Fig. 5.4 Al_2O_3 contents in the rocks of A, the Thin; B, Brakspruit; C, Marikana; and D, Westplats reef types. Plagioclase (filled circle) and Orthopyroxene (filled square) compositions are also shown, from Boerst (2001).

pyroxenites reach a maximum of 7 wt % and 10 wt % in feldspathic pyroxenites. Very small fractions of alumina can be accounted for in orthopyroxene, chromite and biotite. CaO occurs mostly in the plagioclase. However, a small amount is also contributed by clinopyroxene which is never abundant. As expected, more CaO, which can be up to 16 wt %, occurs in anorthositic rocks.

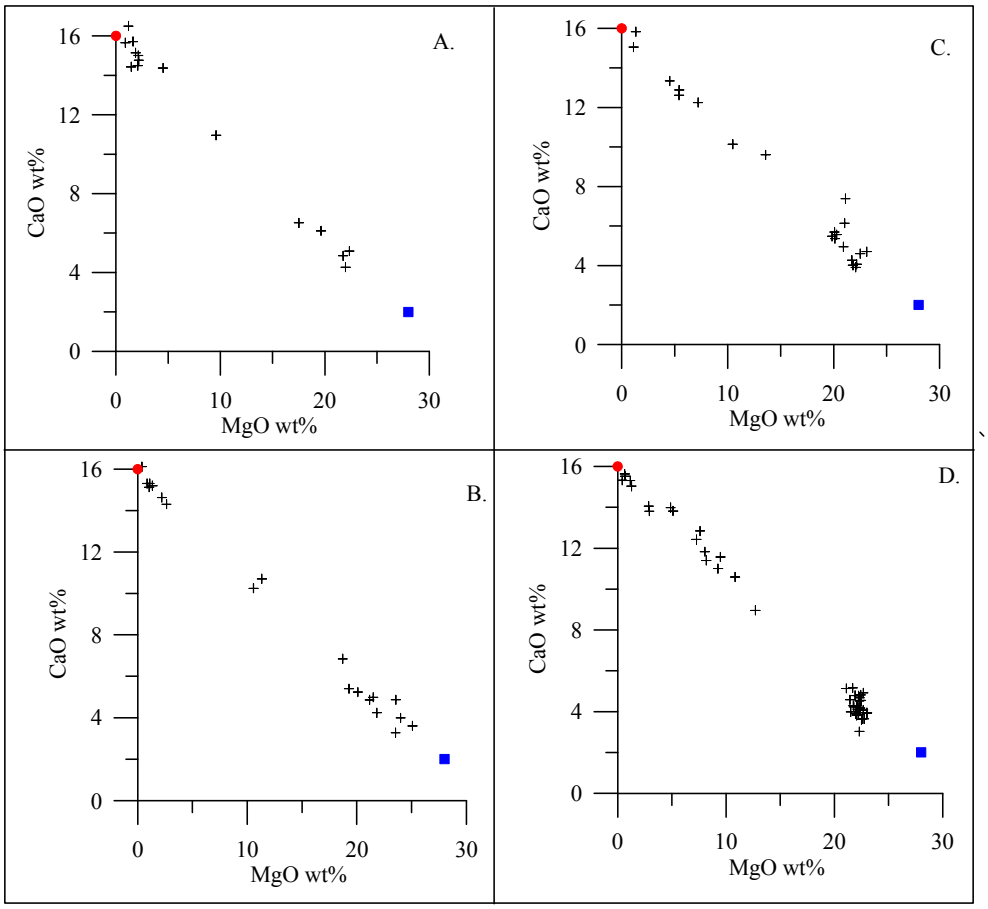

Fig. 5.5 CaO contents in the rocks of A, the Thin; B, Brakspruit; C, Marikana; and D, Westplats reef types. Plagioclase (filled circle) and Orthopyroxene (filled square) compositions are also shown, from Boerst (2001).

5.2.4 Na_2O and K_2O

A fair amount of Na_2O and K_2O is indicated in anorthosites, norites and less in pyroxenites. However, these alkali elements occur here in small amounts ($Na_2O \leq 2.5$ wt % and $K_2O \leq 0.5$ wt %). 2.5 wt % is the maximum amount of Na_2O that occurs in anorthosites and less than 1 wt % is present in pyroxenites. A negative correlation is

observed between sodium and magnesium (Fig. 5.6). K_2O shows more variable concentrations when plotted against MgO. Two trends are displayed (Fig. 5.7); a

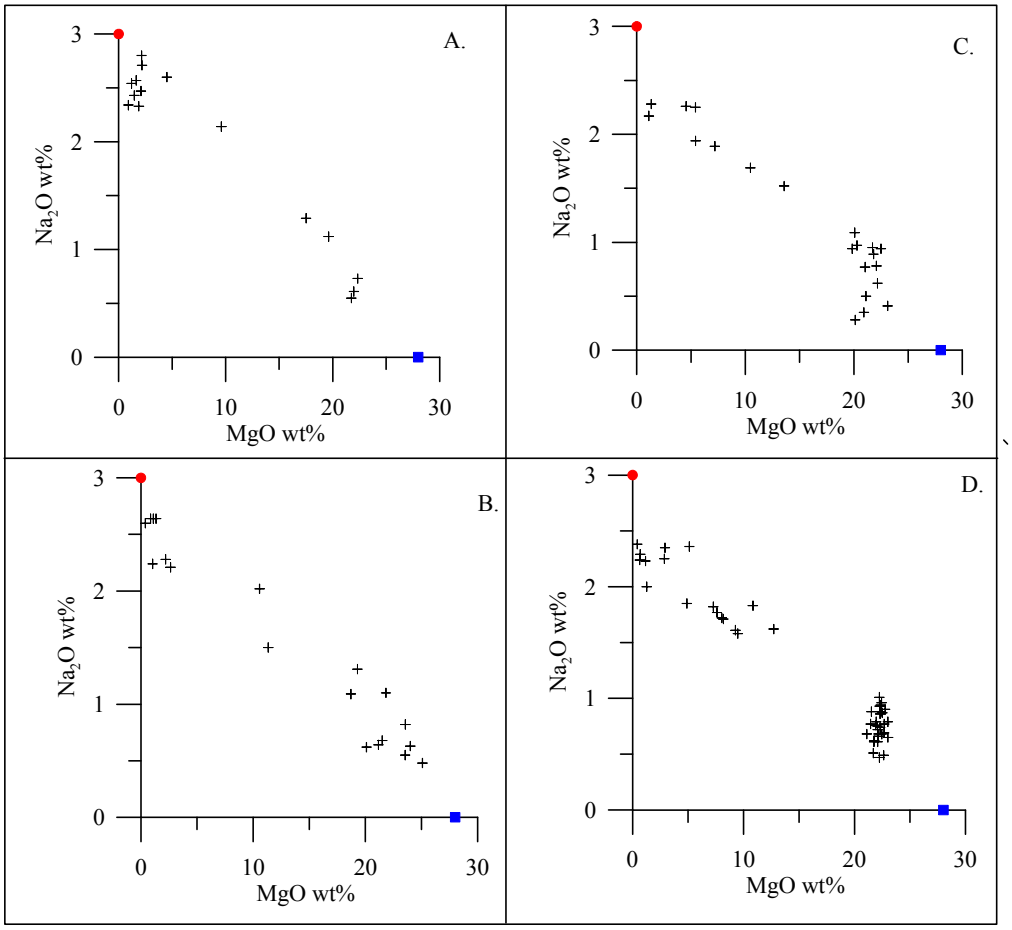

Fig. 5.6 Na_2O contents in the rocks of A, the Thin; B, Braksprui t; C, Marikana; and D, Westplats reef types. Plagioclase (filled circle) and Orthopyroxene (filled square) compositions are also shown, from Boerst (2001).

trend that is negatively correlated with MgO and a trend that is shown by a cluster of MgO rich rock. This is less pronounced in the Thin reef type. All rocks plot above the simple tie-line between the compositions of plagioclase and orthopyroxene. Na_2O

and K_2O are present in solid solution in plagioclase and a minor amount of K_2O is present in biotite.

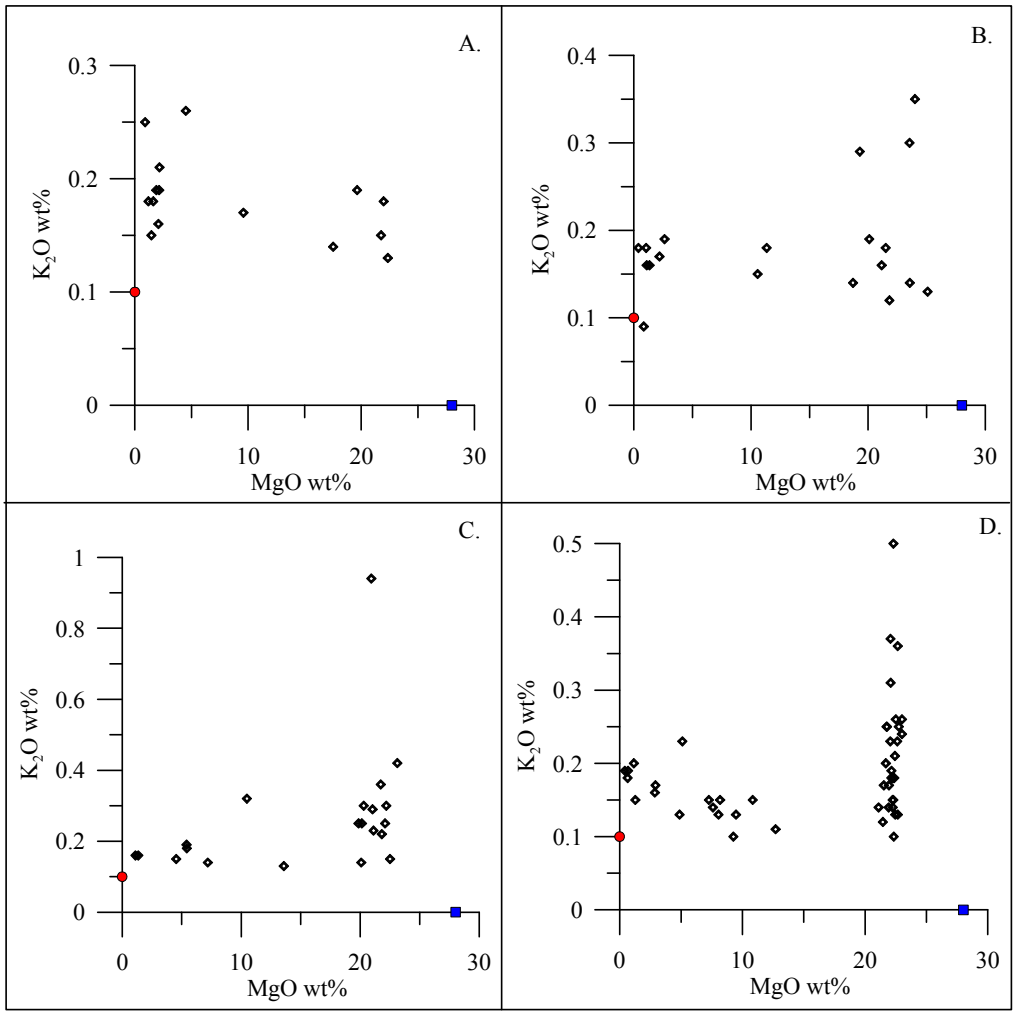

Fig. 5.7 K_2O concentrations in the rocks of A, Thin; B, Brakspruit; C, Marikana; and D, Westplats reef types. Plagioclase (filled circle) and Orthopyroxene (filled square) compositions are also shown, from Boerst (2001).

5.3 Trace-element trends

Trace elements discussed here are classified into three categories.

1. A group of trace elements that is generally incompatible in the major silicate and oxide phases in the rocks of the four reef types; Ba, Rb, Y, Zr and P.

2. A group of trace elements that is controlled by major phases such as pyroxene, plagioclase and chromite; Ni, Sr, Cr and V as well as Zn.

3. A group of trace elements that is concentrated by the sulphide minerals; S, Ni, Cu, and Co.

Figure 5.8 to Figure 5.20 show trends of the trace elements in the four reef types. The trace element abundances are plotted against MgO contents so that variation of these elements in different rocks of the reef types is demonstrated.

5.3.1 Trace elements incompatible in silicate phases

Data for incompatible elements are shown in Figures 5.8 through to 5.12. The incompatible elements that occur in the rocks of the four reef types are Ba, Zr, Rb, Y and Nb as well as P. Ba, Zr and Rb are present in concentrations of tens of parts per million (ppm) and even less. Nb and Y occur in abundance less that 12 ppm. P occurs in abundances of no more than 0.06 wt%. Nb is excluded in the discussions because it occurs in concentrations that are close to the detection limits. All these incompatible elements are lithophile. Any affinity will mostly be to silicate and phosphate phases.

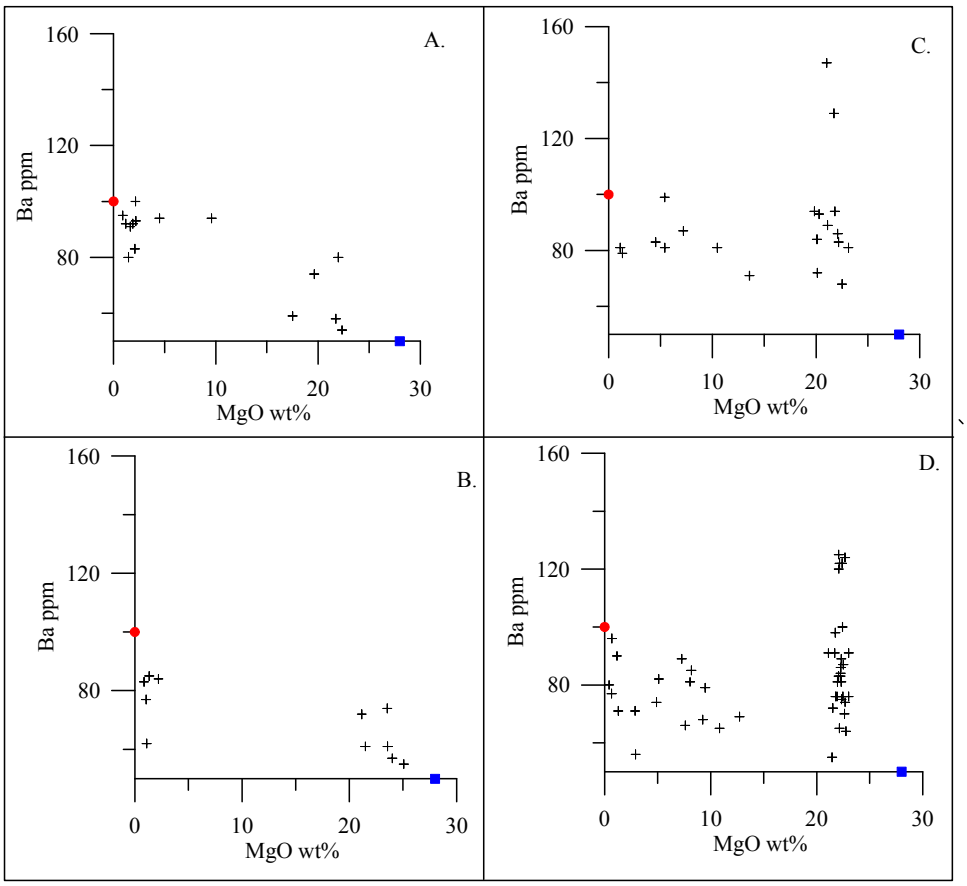

Fig. 5.8 Ba contents in the rocks of A, the Thin; B, Brakspruit; C, Marikana; and D, Westplats reef types. Plagioclase (filled circle) and Orthopyroxene (filled square) compositions are also shown from Boerst (2001).

Anorthosites are generally low in incompatible elements, especially Rb, Zr and Y. These elements are present in abundances of less than 9 ppm in the anorthosites in all the reef types. However pyroxenites contain varied concentrations of Ba, Rb, Zr and Y. Pyroxenites contain Rb that average 15 ppm. Y in these mafic rocks reaches maxima of 12 ppm.

Although Ba shows a poor mutual dependence on MgO concentrations (Fig. 5.8), it fractionates into plagioclase (D = 0.23, from Rollinson, 1993) and hence anorthosites

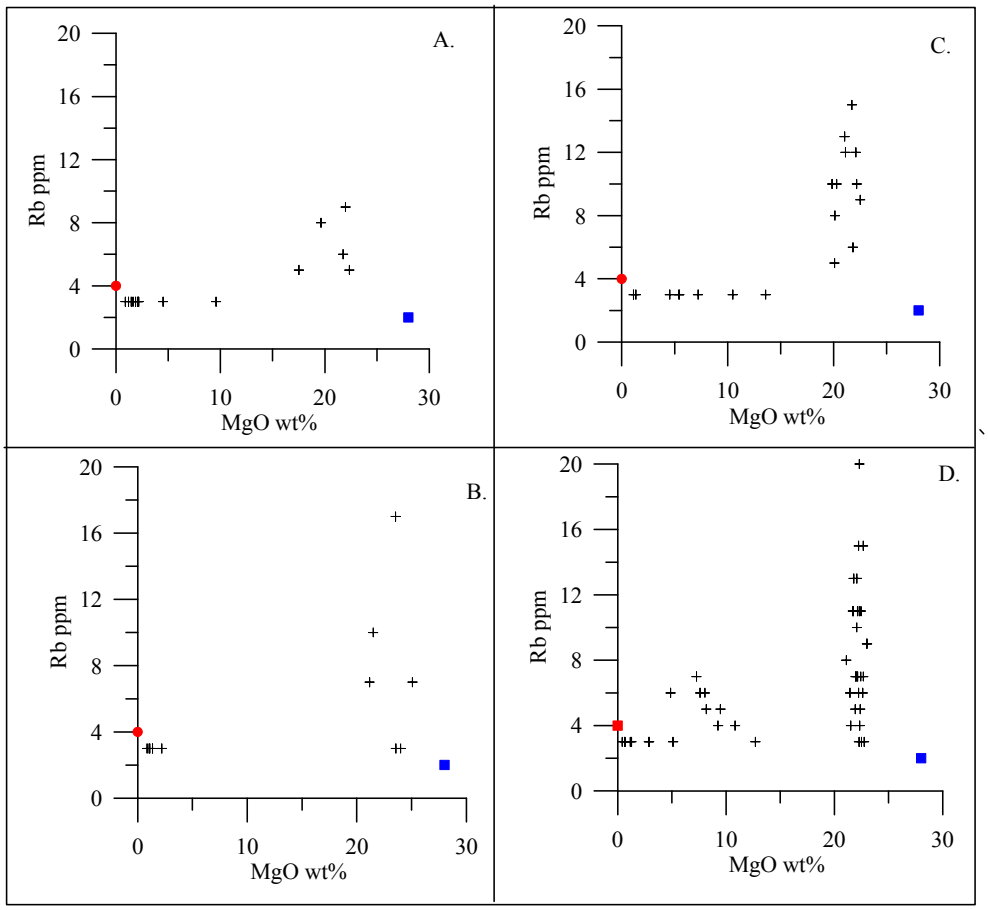

Fig. 5.9 Rb contents in the rocks of A, the Thin; B, Brakspruit; C, Marikana; and D, Westplats reef types. Plagioclase (filled circle) (Cawthorn, 1996) and Orthopyroxene (filled square) (Boerst, 2001) compositions are also shown.

have appreciable amounts of Ba. However, there are pyroxenites that are rich in Ba relative to other rocks (Fig. 5.8). Ba in the rocks of the different reef types range from

50 ppm to 120 ppm. Some of the pyroxenites have rather elevated Ba contents of up to 140 ppm.

Although the elements that are discussed above are mainly incompatible, they can have an affinity to minerals that occur in small modal quantities. Rb is compatible in biotite. However, Rb can also partition, to a lesser degree into plagioclase. Rb shows poor mutual dependence on MgO (Fig. 5.9). Y may be concentrated into apatite, in very limited amounts. The abundances of Y in the reef types are generally low and signal the rarity of apatite in these rocks. MgO rich rocks are rich in Y compared to anorthosites and norites (Fig. 5.10). In terms of Y, rocks plot above the simple tie-line between plagioclase and orthopyroxene.

Zr partitions well into zircon, sphene and rutile. However, no microscopic evidence of any of these mineral phases was found in the samples. Zr is the most variable in the mafic rocks ranging from 10 ppm to 50 ppm. Rb and Y show a gradual increase with MgO contents in the rocks. Zr increases abruptly as MgO contents increase, usually at 20 wt % of MgO in all reef types but the Westplats reef type. Norites in the Westplats reef type (Fig. 5.11) have elevated Zr amounts of 30 ppm. More Zr is in the pyroxenites than in the anorthosites and norites. The presence of the incompatible elements already discussed above may also indicate the quantities of trapped liquid in the rocks of the different reef types.

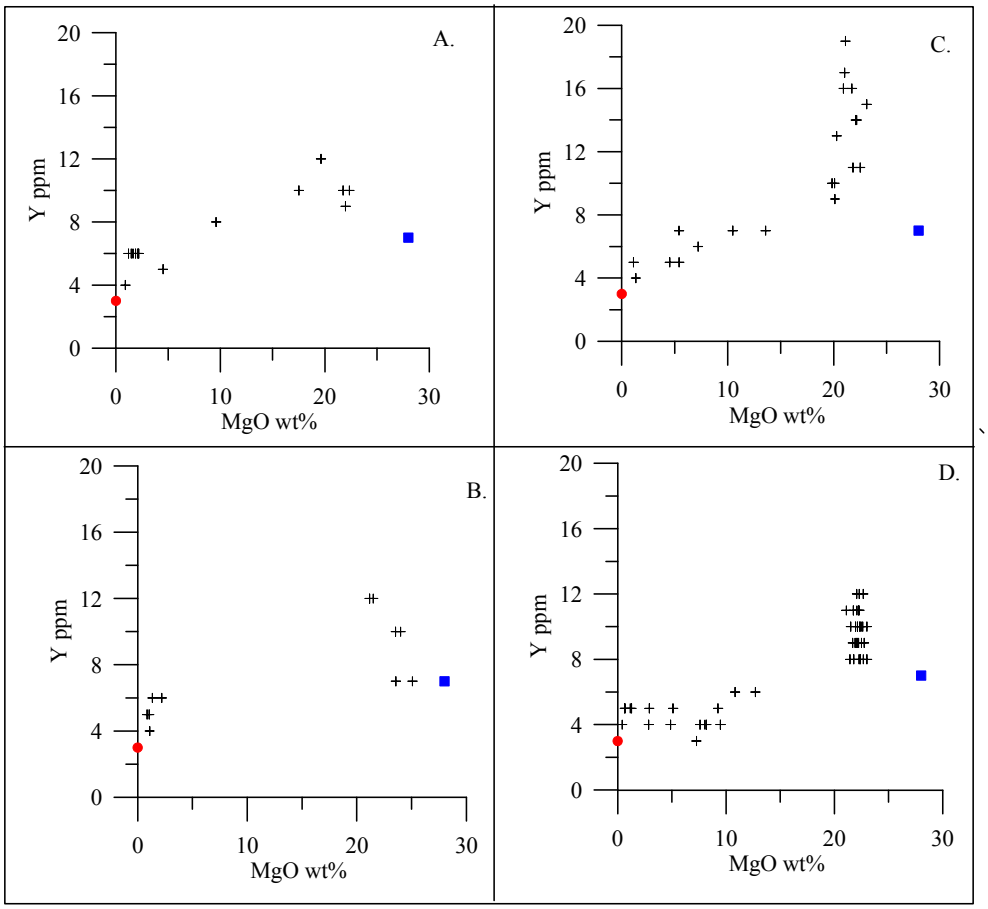

Fig. 5.10 Y contents in the rocks of A, the Thin; B, Brakspruit; C, Marikana; and D, Westplats reef types. Plagioclase (filled circle) and Orthopyroxene (filled square) compositions are also shown from Boerst (2001).

Although generally present in trace amounts and is incompatible with most minerals, P_2O_5 is solely concentrated in apatite. Apatite occurs sparingly and thus amounts of phosphorus in the rocks are also limited. Anorthosites, norites and pyroxenites contain P_2O_5 contents averaging 0.035 wt %. However, very few rocks have P_2O_5 concentrations that reach maxima of 0.06 wt % and even 0.2 wt %. The highest P_2O_5 amounts are in the rocks of the Westplats reef type. Figure 5.12 shows that P_2O_5 has

a varied relation with respect to MgO contents of the rocks. No strong linear correlations

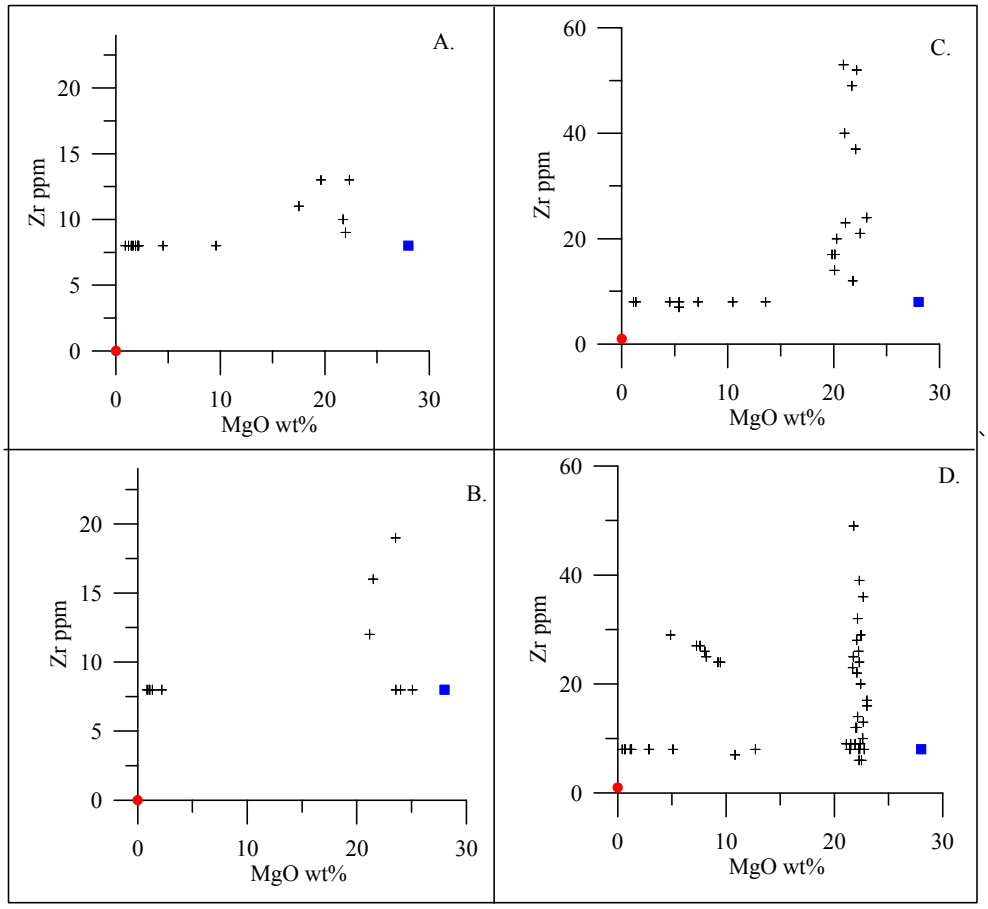

Fig. 5.11 Zr contents in the rocks of A, the Thin; B, Brakspruit; C, Marikana; and D, Westplats reef types. Plagioclase (filled circle) and Orthopyroxene (filled square) compositions are also shown from Boerst (2001).

are observed regarding these two elements in the rocks of the different reef types. However, pyroxenite typically contains the most phosphorus relative to the felsic rocks. Detection limit for P_2O_5 is 0.01 with an absolute error of -0.02%.

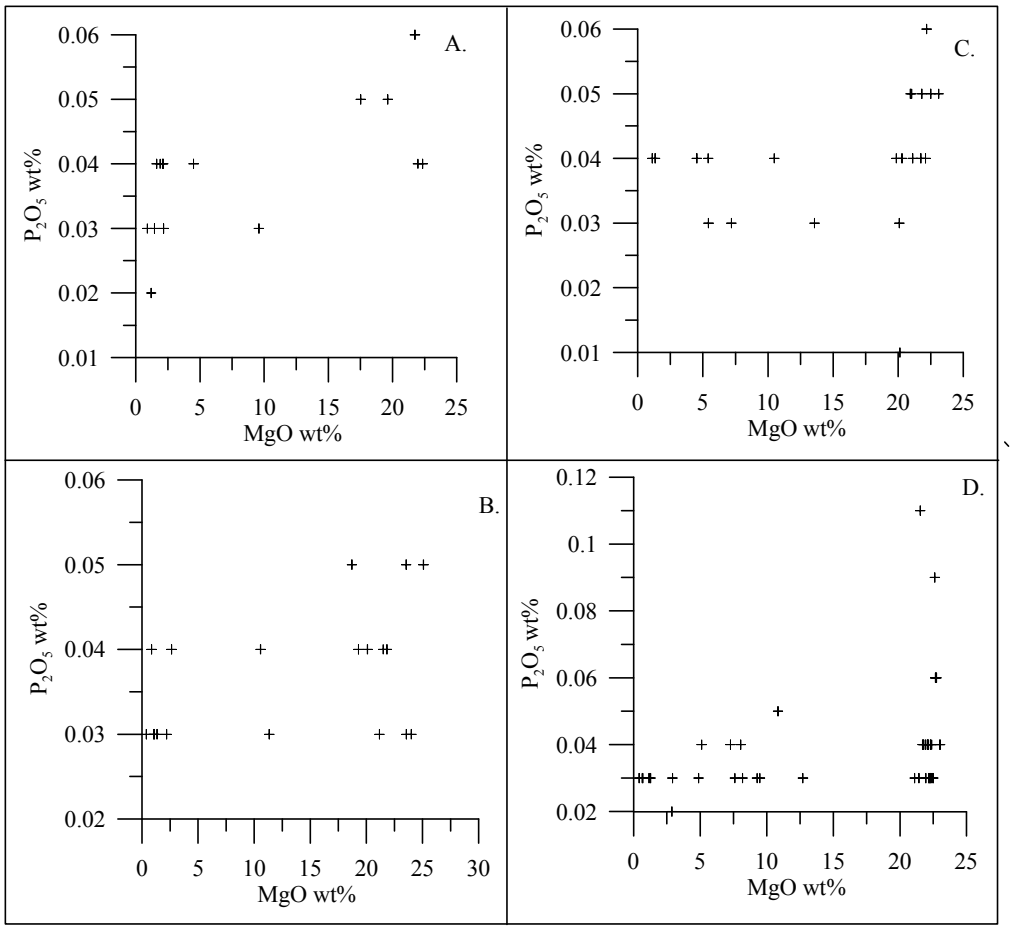

Fig. 5.12 P_2O_5 contents in the rocks of A, the Thin; B, Brakspruit; C, Marikana; and D, Westplats reef types.

5.3.2 Trace elements compatible in silicate phases

Trace elements that are discussed in this section are elements that are compatible with major phases such as pyroxene, plagioclase and chromite but generally partition sparingly in other minerals e.g. Sr is compatible with plagioclase, but not with pyroxene. Figure 5.13 shows that Sr is negatively correlated with MgO. Anorthosites

have more Sr (450 ppm) and norites have Sr contents of approximately 200 ppm. In like manner, Sr is less abundant in the pyroxenites (~ 90 ppm).

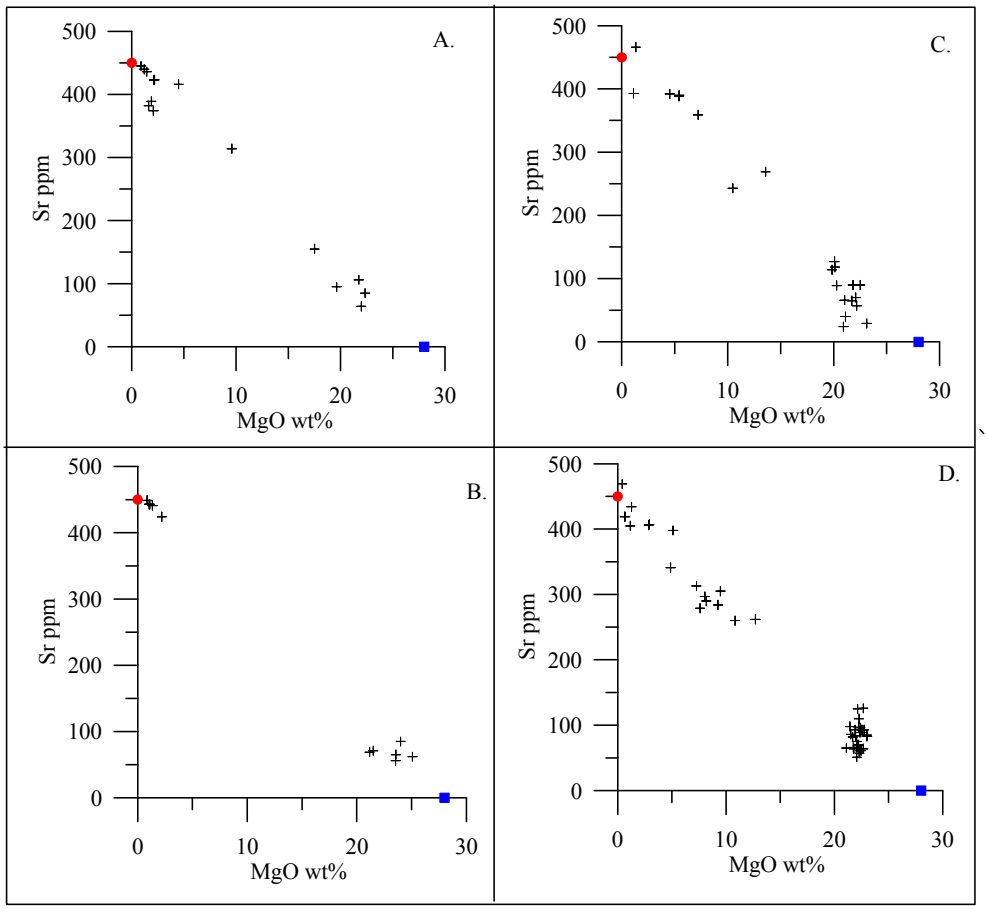

Fig. 5.13 Sr contents in the rocks of A, the Thin; B, Brakspruit; C, Marikana; and D, Westplats reef types. Plagioclase (filled circle) and Orthopyroxene (filled square) compositions are also shown, from Boerst (2001).

Apart from the strong compatibility with chromite, Cr is also compatible in clinopyroxene, and to a lesser extent, in orthopyroxene and magnetite. Clinopyroxene and magnetite occur in limited amounts and therefore their input of Cr is also limited. Cr shows a strong mutual dependence on MgO (Fig. 5.14). Most of the rocks in the

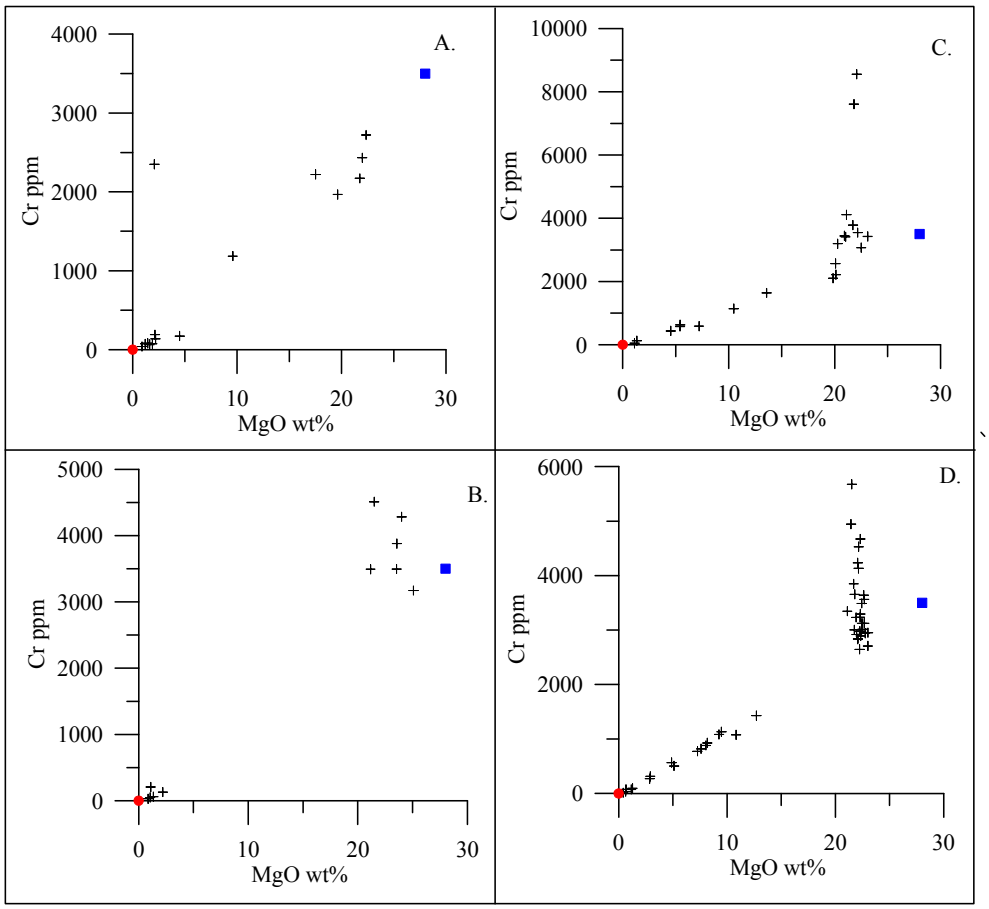

Fig. 5.14 Cr contents in the rocks of A, the Thin; B, Brakspruit; C, Marikana; and D, Westplats reef types. Plagioclase (filled circle) and Orthopyroxene (filled square) compositions are also shown, from Boerst (2001).

different reef type register along the simple tie-line between the compositions of plagioclase and orthopyroxene and several plot above this line. Rocks that occur above this simple line contain chromite. Rocks in the reef types with chromitite layers contain Cr quantities of up to 6000 ppm (8000 ppm in the Westplats reef type, Fig. 5.13) whilst pyroxenites with disseminated chromite contain a maximum of 4000 ppm of Cr. On occasion, anorthosites that are immediate to the chromitite layers can

contain unusually high concentrations of Cr because they host minor disseminated chromite minerals.

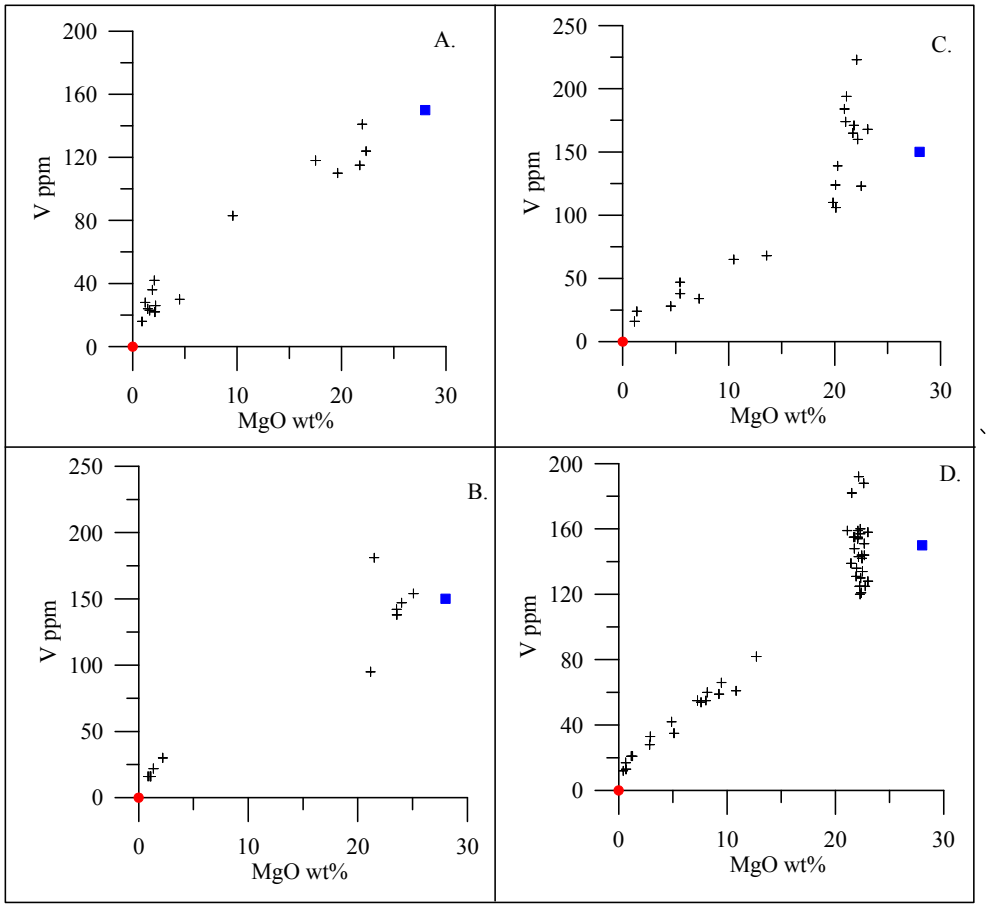

Fig. 5.15 V contents in the rocks of A, the Thin; B, Brakspruit; C, Marikana; and D, Westplats reef types. Plagioclase (filled circle) and Orthopyroxene (filled square) compositions are also shown, from Boerst (2001).

Vanadium is a lithophile element that strongly fractionates into iron oxide minerals such as magnetite and chromite. V also fractionates into orthopyroxene. V follows the same pattern that Cr shows with increasing MgO (Fig. 5.15). V abundances reach maxima of 200 ppm in the mafic rocks of all four reef types. Some of the mafic rocks

plot above the tie-line joining the compositions of plagioclase and orthopyroxene. These signal the presence of iron oxide minerals. Anorthosites and norites contain V concentrations of less than 40 ppm and 80 ppm correspondingly.

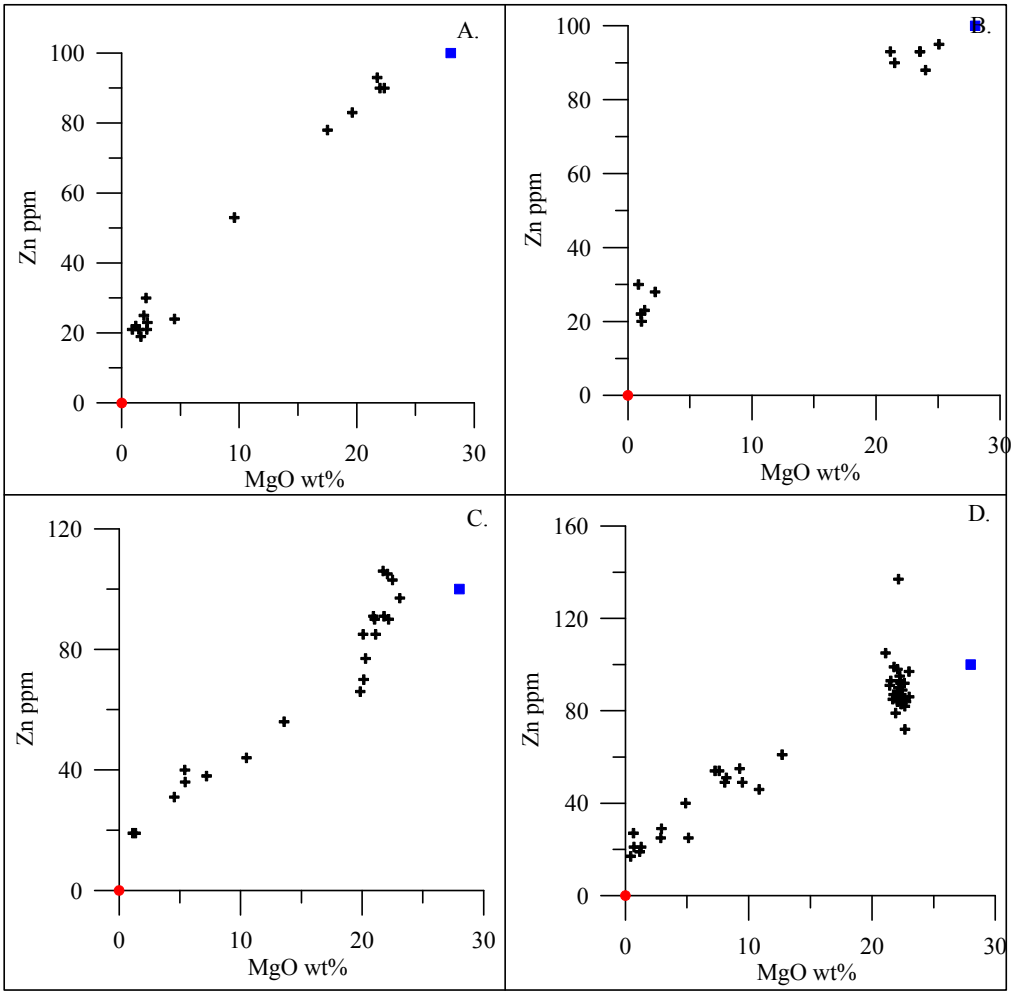

Fig. 5.16 Zn contents in the rocks of A, the Thin; B, Brakspruit; C, Marikana; and D, Westplats reef types. Plagioclase (filled circle) and Orthopyroxene (filled square) compositions are also shown, from Boerst (2001).

Zn in the rocks of the four reef types shows a positive relationship with MgO (Fig. 5.16). This is because Zn also partitions into pyroxenes. Anorthosites contain

abundances of 20 ppm Zn whilst norites have Zn concentrations of about 60 ppm. Pyroxenites have contents of 70 ppm to 100 ppm Zn.

5.3.3 Trace elements compatible in sulphides

Figures 5.17 to 5.20 show the variations of Cu, Ni, and Co and S. These are elements that are incorporated into sulphide minerals. Ni, Cu and S contents for sulphides are also presented in this chapter. From the whole-rock trace-element data, Ni in sulphide is calculated by assuming that the Ni to MgO ratio is 23 in pyroxenites with only pyroxene and plagioclase and with no sulphides have. Thus, the nickel content concentrated in sulphide minerals is calculated by removing 23xMgO from the whole rock Ni abundances (Cawthorn, 1999a). Ni, Cu and S ratios are used in order to understand the geochemistry of the sulphide mineral assemblages that occur in the reef types.

S in the rocks of the reef types range from less than 0.1 wt % to 0.7 wt % (Fig. 5.17). S abundances are an indication of the amount of sulphide mineralization there is in rocks. Mineralized rocks have S contents of more than 0.1 wt %. Norites anorthosites that contain sulphide minerals have sulphur amounts of generally less than 0.1 wt %.

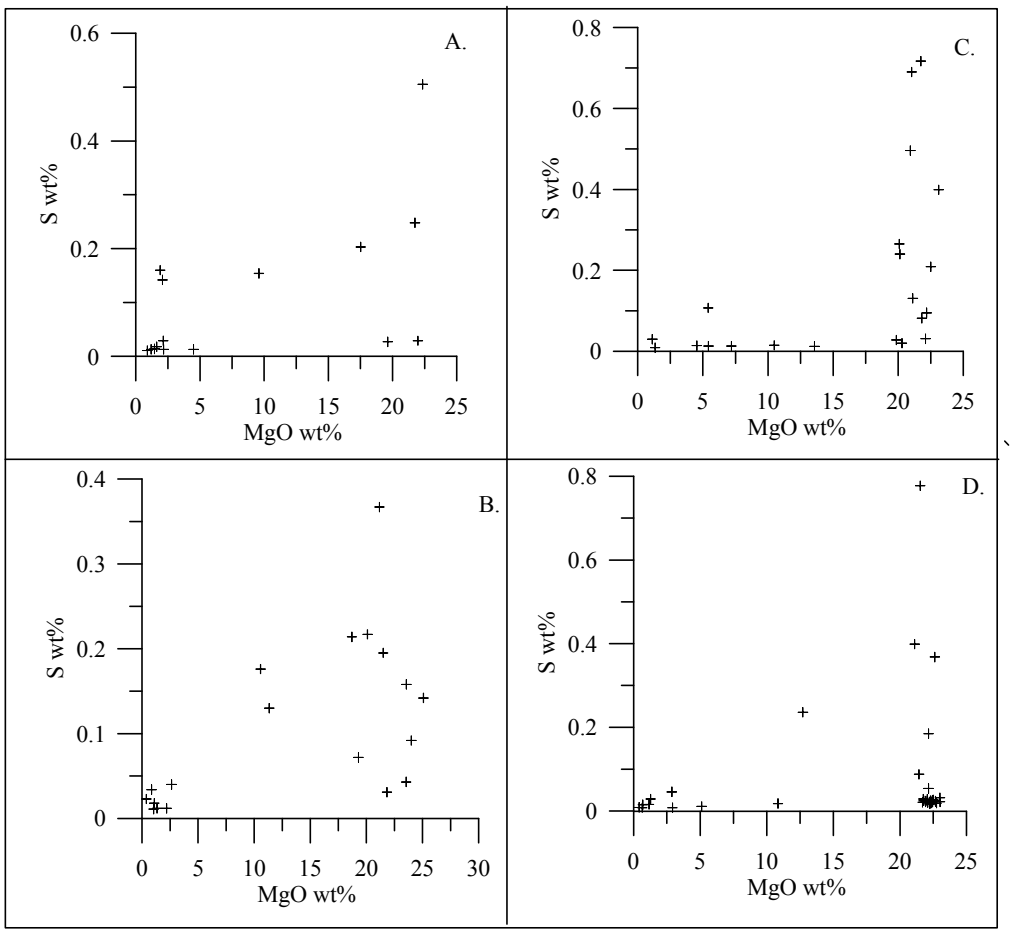

Fig. 5.17 S contents in the rocks of A, the Thin; B, Brakspruit; C, Marikana; and D, Westplats reef types. Plagioclase (filled circle) and Orthopyroxene (filled square) compositions are also shown, from Boerst (2001).

Very few anorthosites and norites contain sulphide minerals. The Marikana and Westplats reef types contain the most S contents relative to rocks in other reef types. Cu in the rocks of the reef types ranges from 10 to 1800 ppm. Cu is a chalcophile element and thus mostly partitions into sulphide minerals.

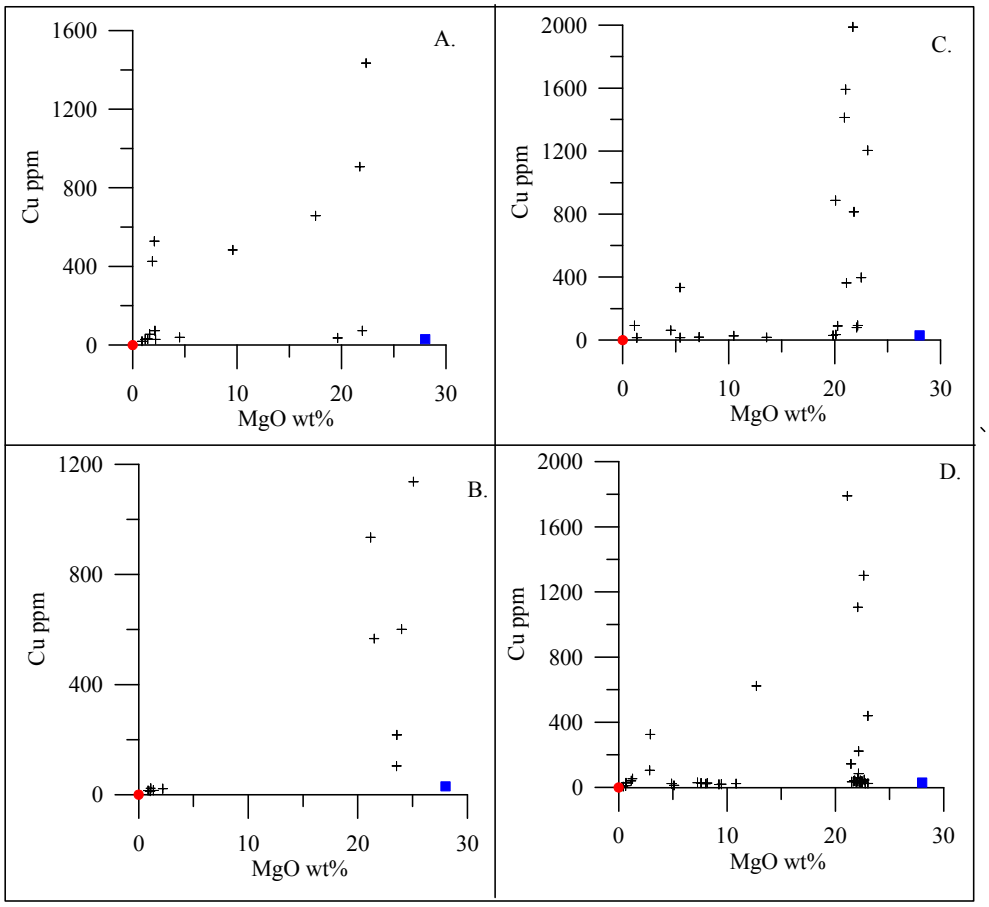

Fig. 5.18 Cu contents in the rocks of A, the Thin; B, Brakspruit; C, Marikana; and D, Westplats reef types. Plagioclase (filled circle) and Orthopyroxene (filled square) compositions are also shown, from Boerst (2001).

Barren rocks, irrespective of their mafic or felsic affinity, contain Cu abundances of up to 100 ppm and rocks mineralized with sulphides contain up to 18 times Cu contents (≤ 1800 ppm) (Fig. 5.18). Cu does not necessarily have a positive correlation with MgO as with Ni.

Nickel is a siderophile element that can be concentrated in olivine and orthopyroxene. Ni is enriched in olivine more than it is in orthopyroxene. However, olivine

contributes a limited amount of Ni because it is very scarce in the samples that were analyzed. Ni contents on the rocks of the four reef types range from 16 ppm to 4000 ppm (Fig. 5.19). Pyroxenites that are barren of mineralization contain a maximum of 700 ppm Ni. Rocks that contain more that this concentration are regarded as sulphide-bearing rocks. These are rocks that plot above the plain line joining the compositions

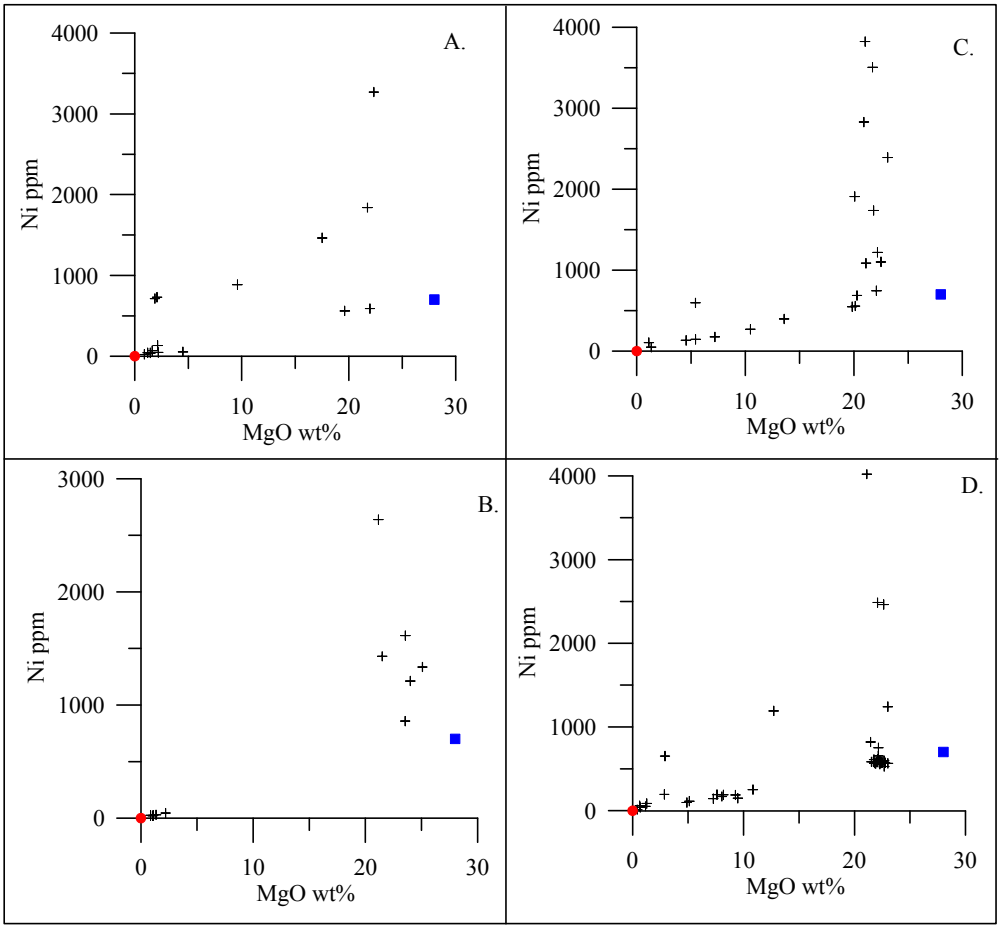

Fig. 5.19 Ni contents in the rocks of A, the Thin; B, Brakspruit; C, Marikana; and D, Westplats reef types. Plagioclase (filled circle) and Orthopyroxene (filled square) compositions are also shown, from Cawthorn (1999).

of plagioclase and orthopyroxene. Very few norites and anorthosites contain significant Ni amounts (~ 1000 ppm). In general, Ni shows a strong mutual dependence on MgO.

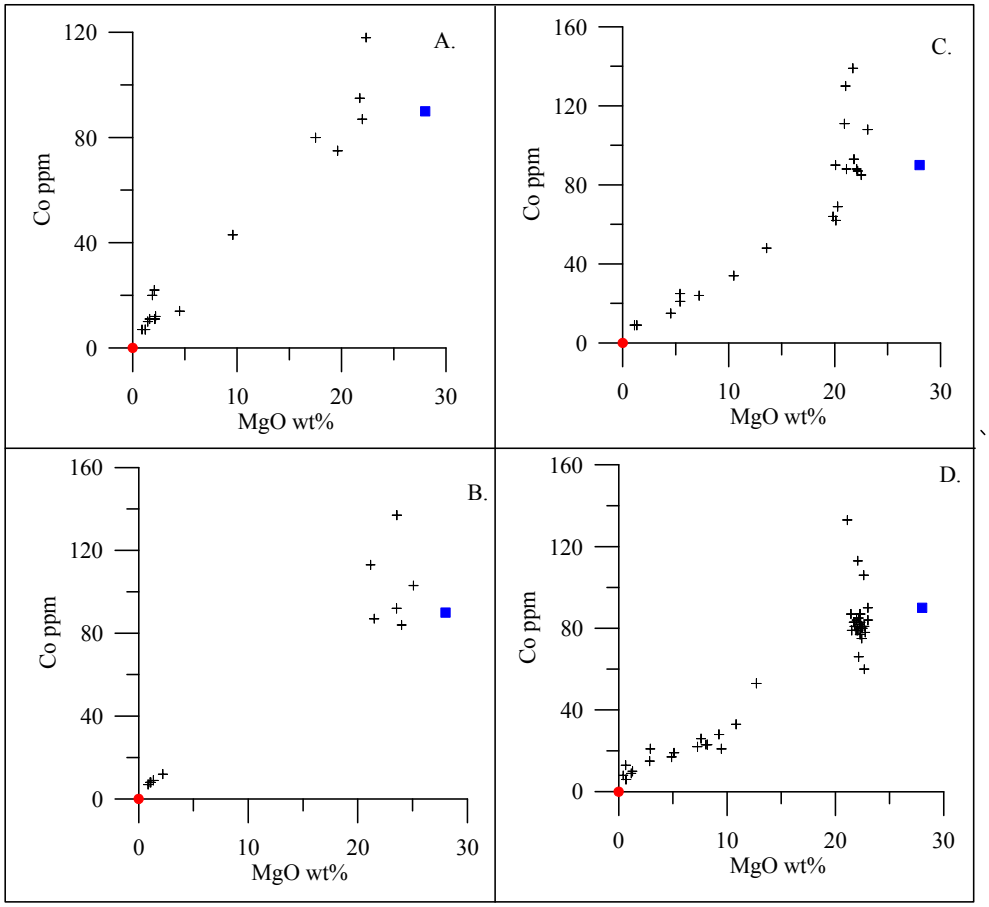

Fig. 5.20 Co contents in the rocks of A, the Thin; B, Brakspruit; C, Marikana; and D, Westplats reef types. Plagioclase (filled circle) and Orthopyroxene (filled square) compositions are also shown, from Boerst (2001).

Co shows a positive correlation with MgO in all the reef types (Fig. 5.20). Co can fractionate into orthopyroxene. Excess Co in rocks of the four reef types is evident in samples that register above the plagioclase-orthopyroxene compositional line.

Anorthosites contain less than 20 ppm Co and pyroxenites are composed of up to 80 ppm Co. Co in norites and mineralized pyroxenites is approximately 40 ppm and up to 120 ppm, respectively.

Figures 5.21 to 5.24 show S, Cu, Ni, and Co plotted against height and all these elements show a correlative pattern. The Merensky pyroxenite with its base at 0 m, where a chromitite layer occurs, is enriched with S, Cu, Ni, and Co. The enrichment of these elements is especially observed toward the base of thin (up to 2 m) Merensky pyroxenite and toward the top of the Merensky pyroxenite where the Merensky pyroxenite is thick (11 m). The highest peaks of sulphur are observed in the Marikana and the Westplats reef types (Fig. 5.23 and 5.24). A decrease of S with increasing height is observed at the top of the Merensky pyroxenite that grades into the overlying anorthosites and norites.

A less prominent rise of S is noted at the level of the Bastard pyroxenite for all but the Brakspruit reef type (Fig. 5.22). Anorthosites and norites contain insignificant S (Fig. 5.19 to 5.22) in the different reef types. The rise in S in the Thin and Westplats reef types in coupled with increases of Cu, Ni and Co at the level of the Bastard pyroxenite. S in the Marikana reef type increases with a slight elevation of Ni and Co but not Cu. In the Westplats reef type, a S peak is realized principally at the top of the Merensky pyroxenite. However, there are peaks of Ni, Cu and Co that are not parallel to the behaviour of S at the level of 5 m in the Merensky pyroxenite (Fig. 5.24).

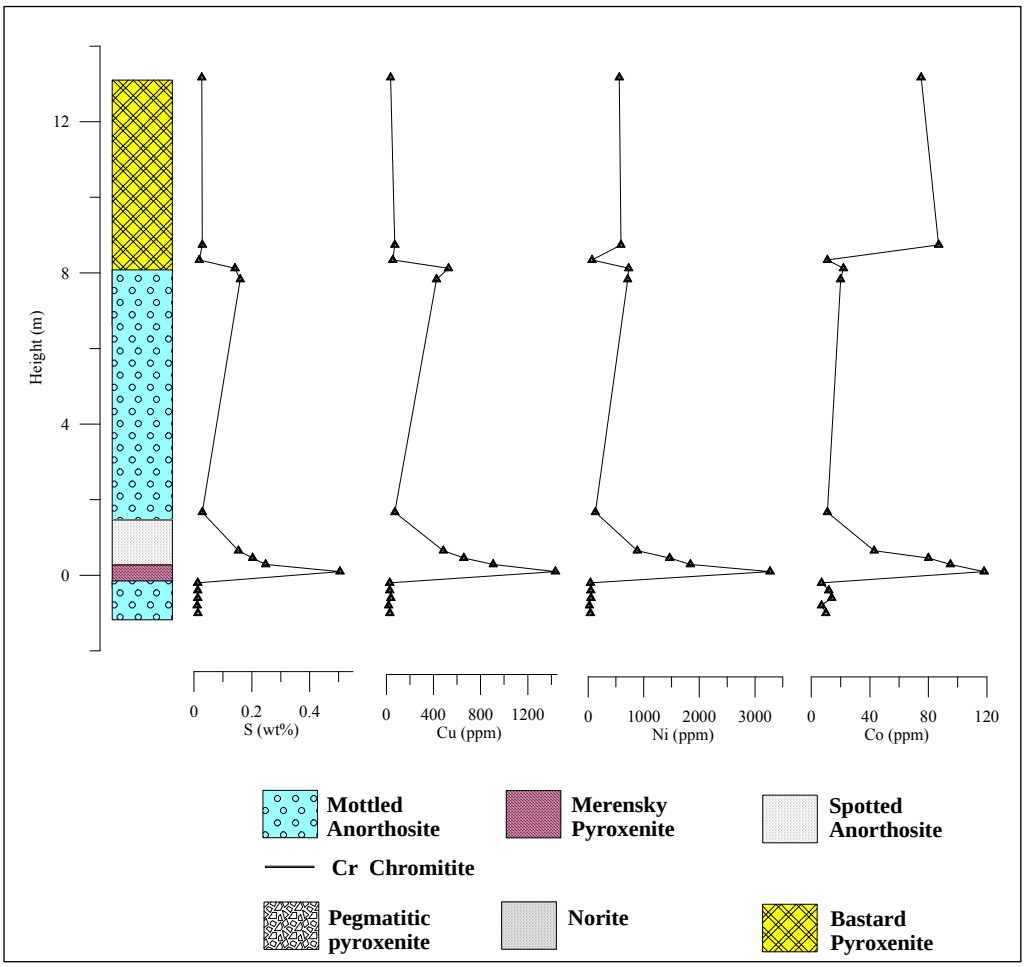

Fig. 5.21 Whole-rock compatible trace-element data for the Thin reef type. The base of the basal chromitite layer in the Merensky Unit is considered as datum.

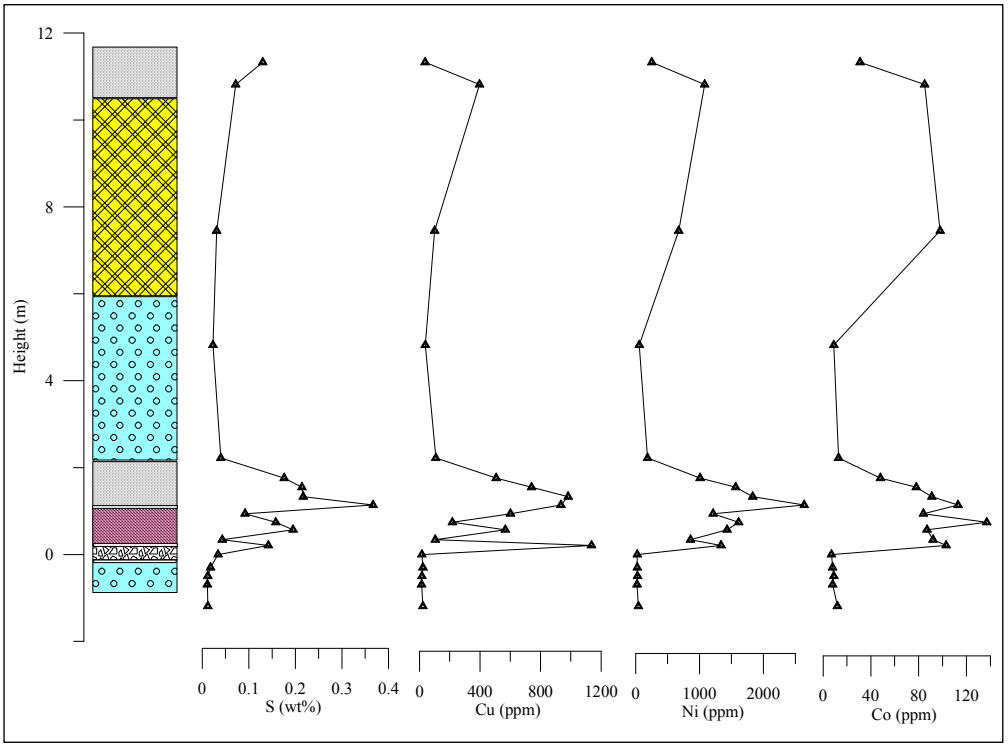

Fig. 5.22 Whole-rock compatible trace-element data for the Brakspruit reef type. The base of the basal chromitite layer in the Merensky Unit is considered as datum.

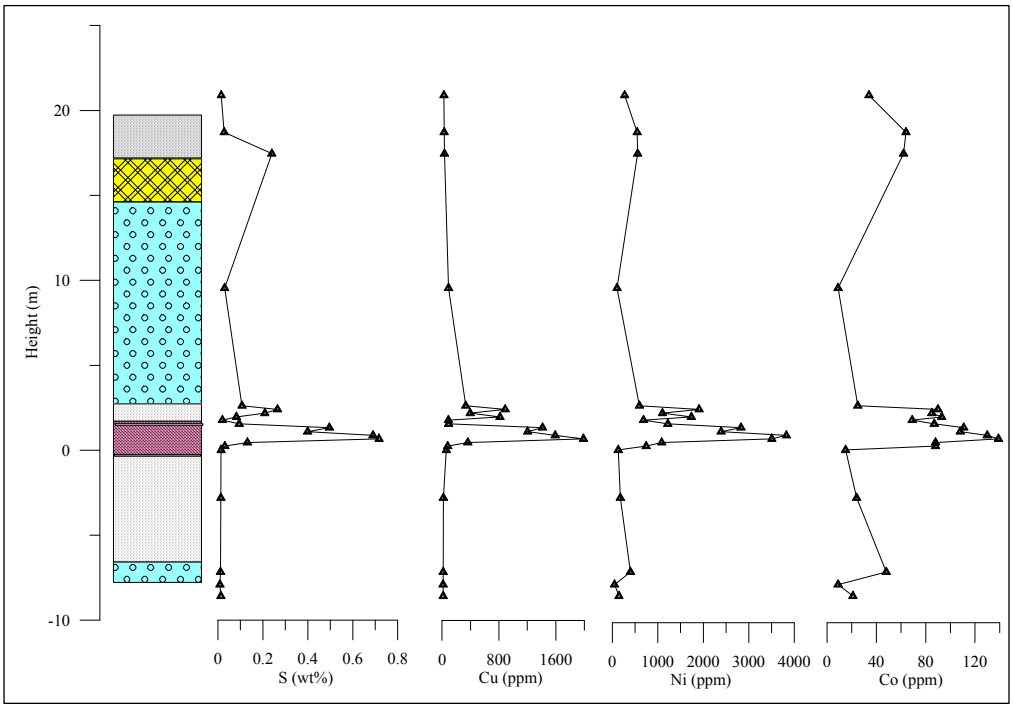

Fig. 5.23 Whole-rock compatible trace-element data for the Marikana reef type. The base of the basal chromitite layer in the Merensky Unit is considered as datum.

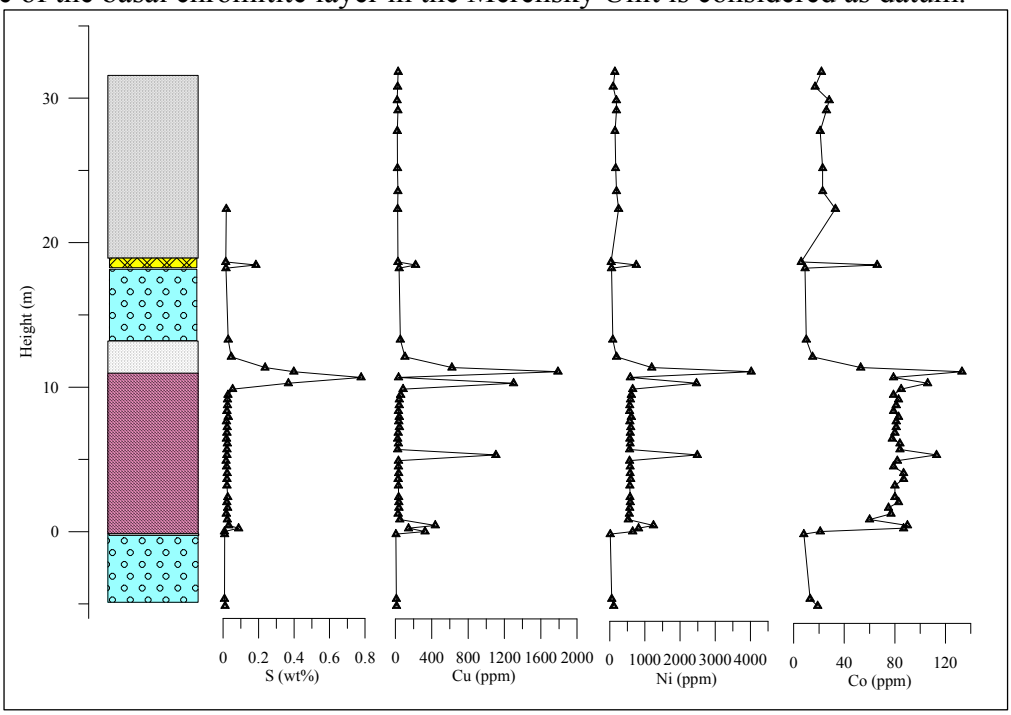

Fig. 5.24 Whole-rock compatible trace-element data for the Westplats reef type. The base of the basal chromitite layer in the Merensky Unit is considered as datum.

5.4 Chlorine

Chlorine data for the thick reef type of the Westplats reef type are presented in Fig. 5.25. According to this figure, anorthosites have no more than 0.02 wt % of Cl and pyroxenites contain Cl ranging from 0.02 wt % to 0.04 wt%. However, very few samples contain Cl concentrations that reach this maximum. Most of the pyroxenites have average abundances of 0.03 wt %. Overall, Cl contained in all the samples of the Westplats reef type is minimal.

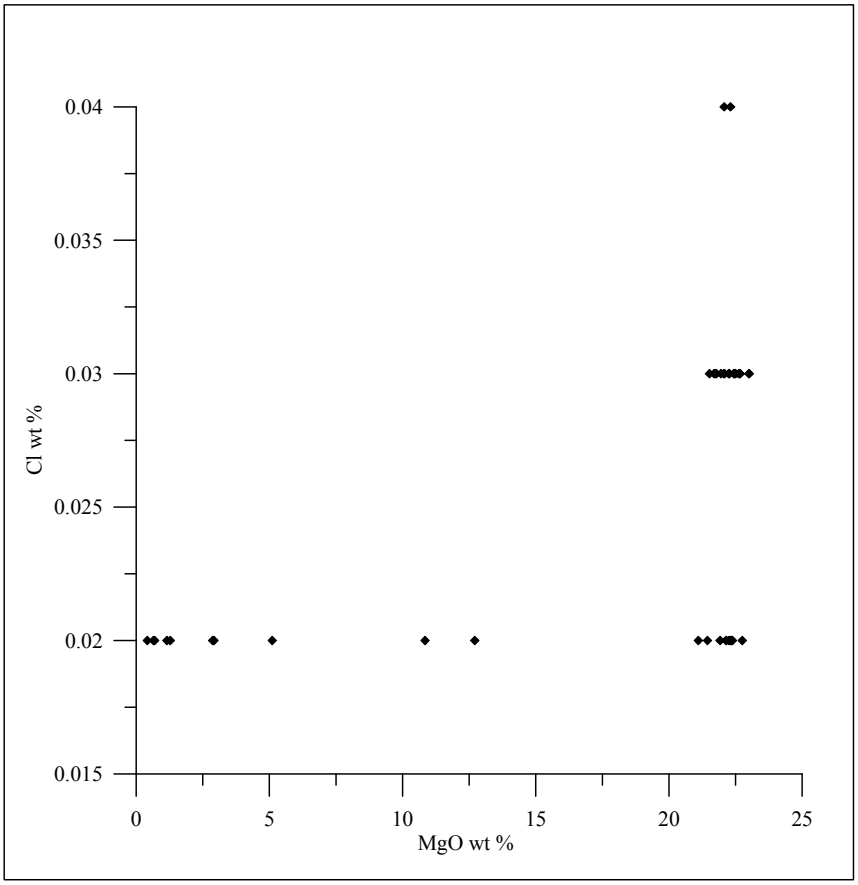

Fig. 5.25 Chlorine data for the Westplats reef type.

5.5 Platinum-group elements

Only Au, Pt and Pd were analysed and the analyses are shown in Table 5.1 and Figure 5.26 represents these PGE analyses plotted with S contents of the rock samples in the Westplats and Marikana reef types. Au is the least abundant element relative to Pt and Pd in all analyzed samples irrespective of the reef type. However, in the Marikana reef type, pyroxenites contain more Au than do the footwall and hanging wall anorthosites. Pd, which is generally the second least common element, is more abundant in the Merensky pyroxenite relative to the Bastard pyroxenite in the

Westplats reef type, as well as in the footwall and hanging wall anorthosites in the Marikana reef type. However, there are some samples of the Merensky pyroxenite that are low in Pd. Pt which is the most abundant element, is most common in the Merensky pyroxenite. However, as with Pd, there are Merensky pyroxenite samples that are very low in Pt. According to Table 5.1, the pyroxenites that are low in PGE are located below and/ or above the mineralized zone of the Merensky Unit. Pyroxenites with sulphides contain the most PGE (Fig. 5.26).

Table 5.1 Au, Pt and Pd data for the Westplats and Marikana reef type. Height in m. is shown with the basal chromitite layer of the Merensky Unit taken as datum. MR-Sref 1 represents a reference sample of a sulphide-bearing pyroxenite.

Reef type/ Height	Rock type	Au ppm	Pt ppm	Pd ppm
Westplats reef type				
18.46	Bastard pyroxenite	0.06	0.47	0.43
11.35	Merensky pyroxenite	0.10	0.08	0.05
10.27	Merensky pyroxenite	0.52	2.69	1.1
3.65	Merensky pyroxenite	0.03	0.02	0.02
1.65	Merensky pyroxenite	<0.01	0.04	0.02
1.24	Merensky pyroxenite	<0.01	0.03	0.02
0.44	Merensky pyroxenite	0.01	0.05	0.02
Marikana reef type				
2.61	Hanging wall anorthosite	0.05	0.05	0.05
1.77	Merensky pyroxenite	0.04	0.18	0.04
1.33	Merensky pyroxenite	0.6	4.98	3.01
0.87	Merensky pyroxenite	0.69	5.85	3.44
0.67	Merensky pyroxenite	0.86	5.72	3.08
-8.59	Footwall anorthosite	<0.01	0.01	0.01
MR-S ref1	Pyroxenite	0.4	3.16	1.8

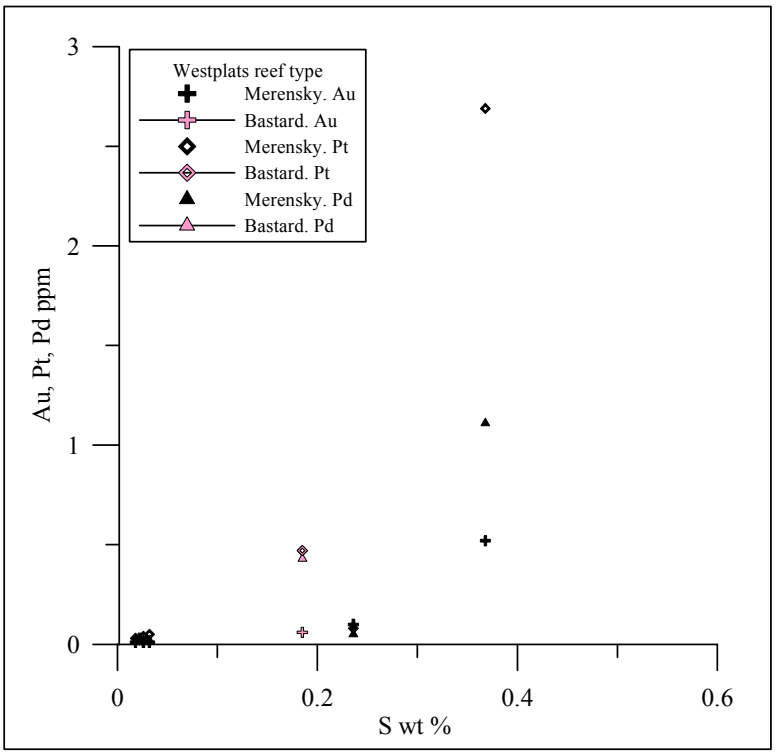

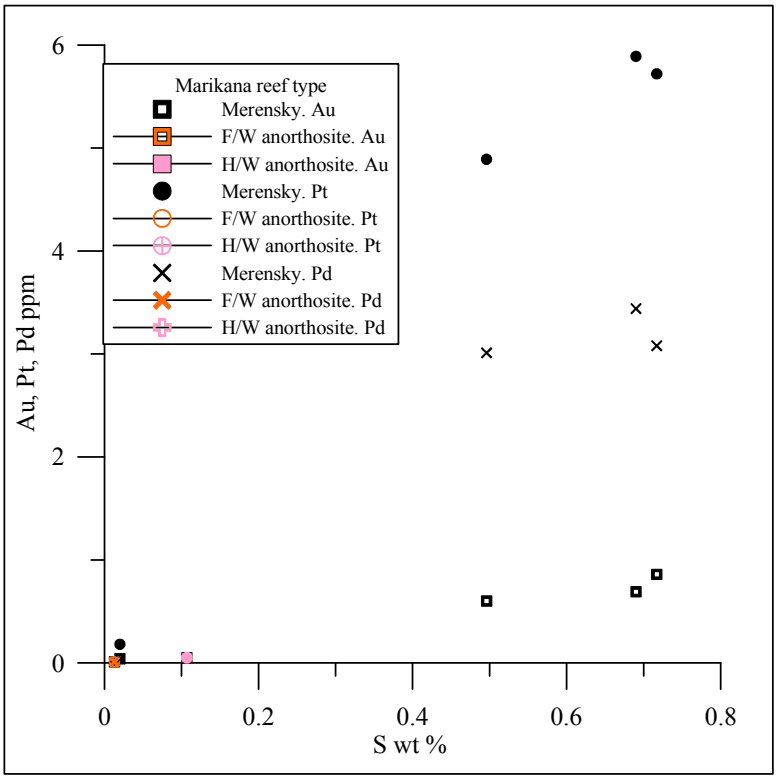

Fig. 5.26 PGE data for the Westplats and Marikana reef types.

5.6 Calculation of Ni in sulphide

From figures 5.27 and 5.28 are plots of Ni versus MgO contents and these are used to determine the Ni: MgO ratio and therefore the amount of Ni contained in orthopyroxene and sulphides. It can be deduced from these figures that the Ni to MgO ratios in the different reef types are also slightly different. The Thin and Brakspruit reef types show Ni: MgO ratios of 27 and 25 respectively. The Marikana and the Westplats reef types show Ni: MgO of 28 and 26, correspondingly. Each of these ratios is used to determine the excess Ni that is contained in the sulphides in the four reef types, respectively. 27XMgO, 25XMgO, 28XMgO and 26XMgO is removed from the whole-rock Ni contents for the Thin, Brakspruit, Marikana and Westplats reef types respectively to determine the amount of Ni present in sulphides.

The calculated Ni is used for the determining the S: Ni and Ni: Cu ratios. These ratios are used to characterize the sulphides in the respective reef types. There is a slight variation in the Ni: Cu (Fig. 5.29) and S to metal (calculated Ni and Cu) ratios according to the varied reef types (Fig. 5.30 to 5.31).

Table 5.2 presents the standard deviations calculated for the Ni: Cu, S: Ni and S: Cu ratios for the different reef types. The standard deviations calculated for the Ni: Cu show that the dispersion of the set of Ni: Cu ratios is not significant except for the Brakspruit reef type. A significant standard deviation in the S: Ni ratios is evident in all the reef types; a considerably scatter is indicated in the S: Ni data. Because of this

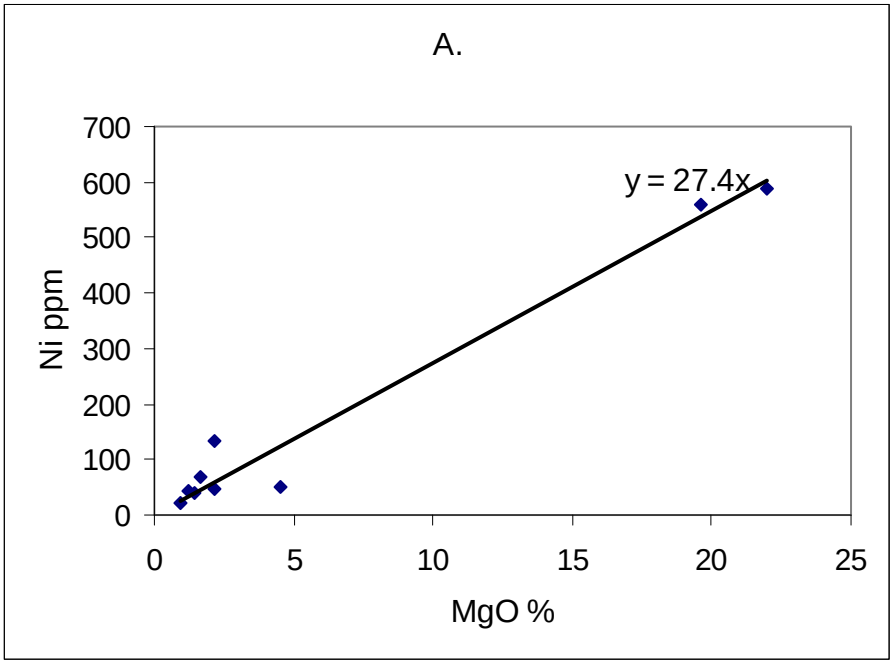

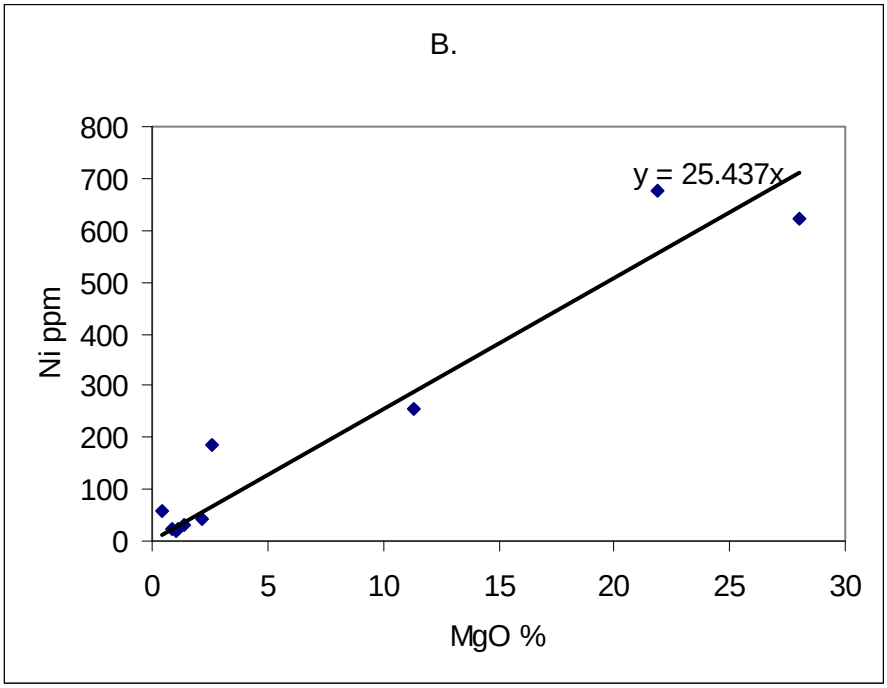

Fig. 5.27 Average Ni/ MgO (y) ratios for A, Thin reef type; B, Brakspruit reef type in non-sulphide-bearing rocks taken as < 700 ppm Ni.

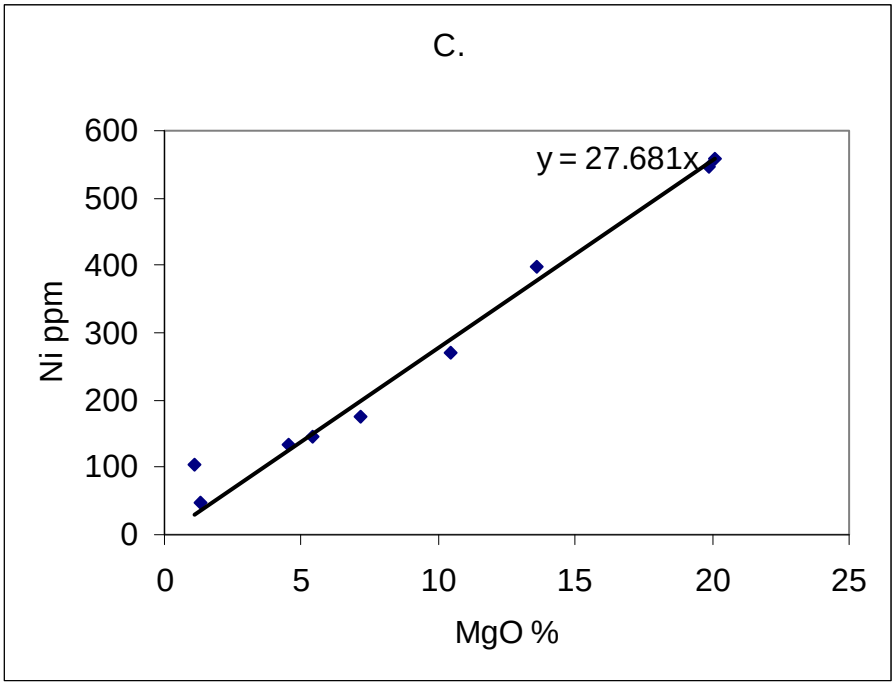

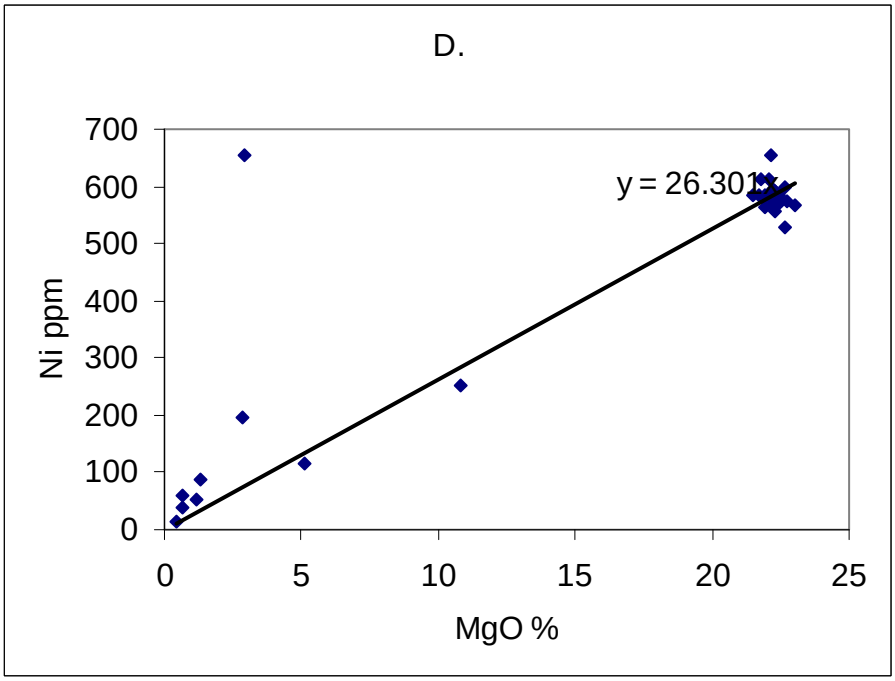

Fig. 5.28 Average Ni/ MgO (y) ratios for C, Marikana reef type; D, Westplats reef type in non-sulphide-bearing rocks taken as < 700 ppm Ni.

Table 5.2. *Standard deviation values for Ni: Cu, S: Ni and S: Cu ratios for the four reef types.

	Thin	**Brakspruit**
	Std Deviation*	Std Deviation*
Ni: Cu	0.22	0.53
S: Ni	0.42	1.00
S: Cu	0.23	0.38
	Marikana	**Westplats**
	Std Deviation*	Std Deviation*
Ni: Cu	0.24	0.42
S: Ni	1.14	1.71
S: Cu	0.95	0.75

scatter, some degree of uncertainty results in the ratios and therefore interpretations should be dealt with caution.

The Ni: Cu ratios for the sulphides in the four reef types range from 1.4:1 to 1.8:1 (Fig. 5.29). This is not a significant difference and considering the small standard deviation, the ratios can be calculated as an average of 1.6:1. However, it is evident that the pegmatitic Brakspruit reef type contains sulphides of the least Ni: Cu ratios and sulphides from the other three reef types exhibit Ni: Cu ratios that reach 1.8:1. However, the standard deviation in the ratios of Ni: Cu for the Brakspruit are elevated compared to those of the other reef types and uncertainty is propagated in this value (1.4: 1).

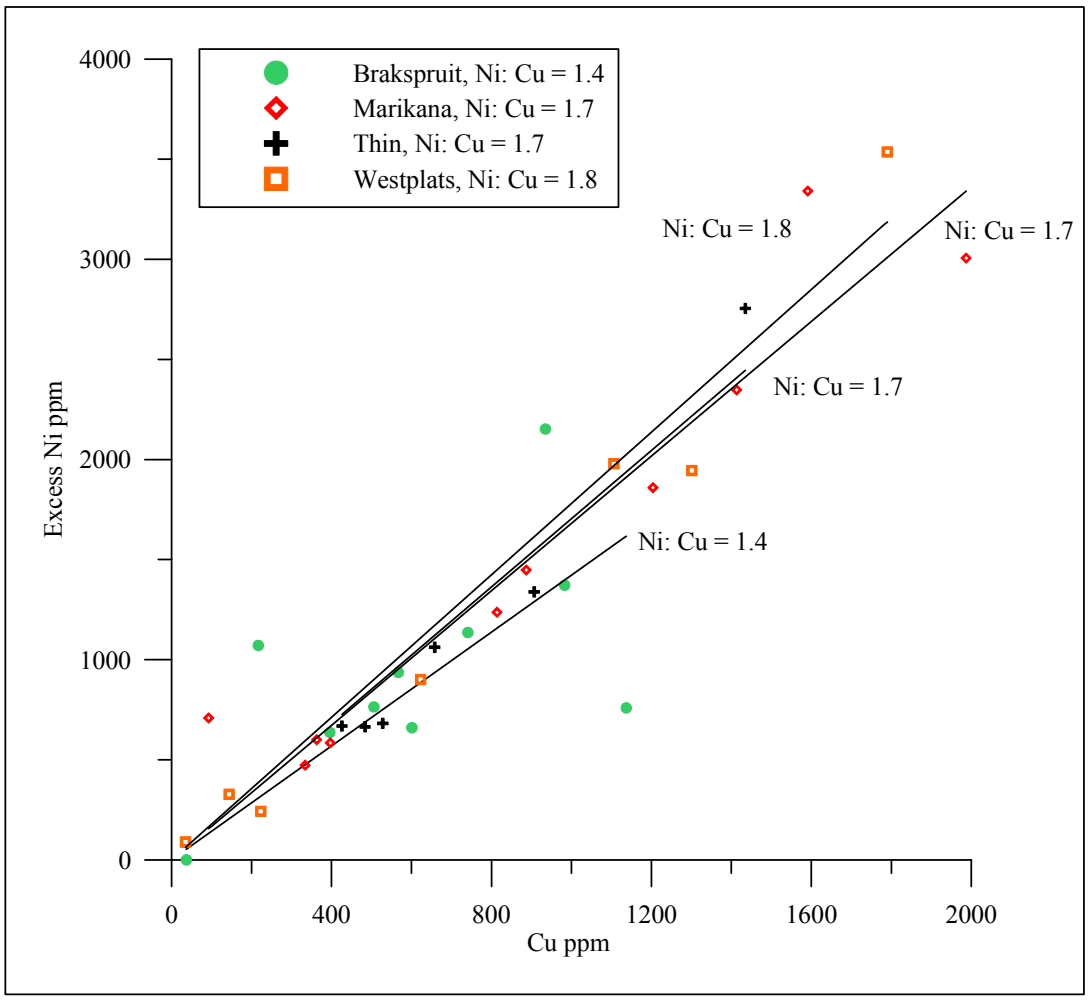

Fig. 5.29. Excess Ni to Cu ratios for sulphides in the different reef types.

S: Cu (3.6) ratio generally higher in the Marikana reef type (Fig.5.30), with a considerable standard deviation. The S to Cu values for the Thin, Brakspruit and Westplats reef types are 3.2, 2.5 and 2.2 with standard deviations of 0.23, 0.38 and 0.75 respectively. S: Ni ratios range from 1.2:1 to 2.1: 1 and the average of the values can be taken as 1.6. The Westplats reef type shows the least values for S: Ni and the other three reef types have sulphides with S: Ni ratios that approach 2: 1. The

standard deviations in the S: Ni ratios are significant that those on other ratios and therefore the S: Ni ratios cannot be dealt with rigorously.

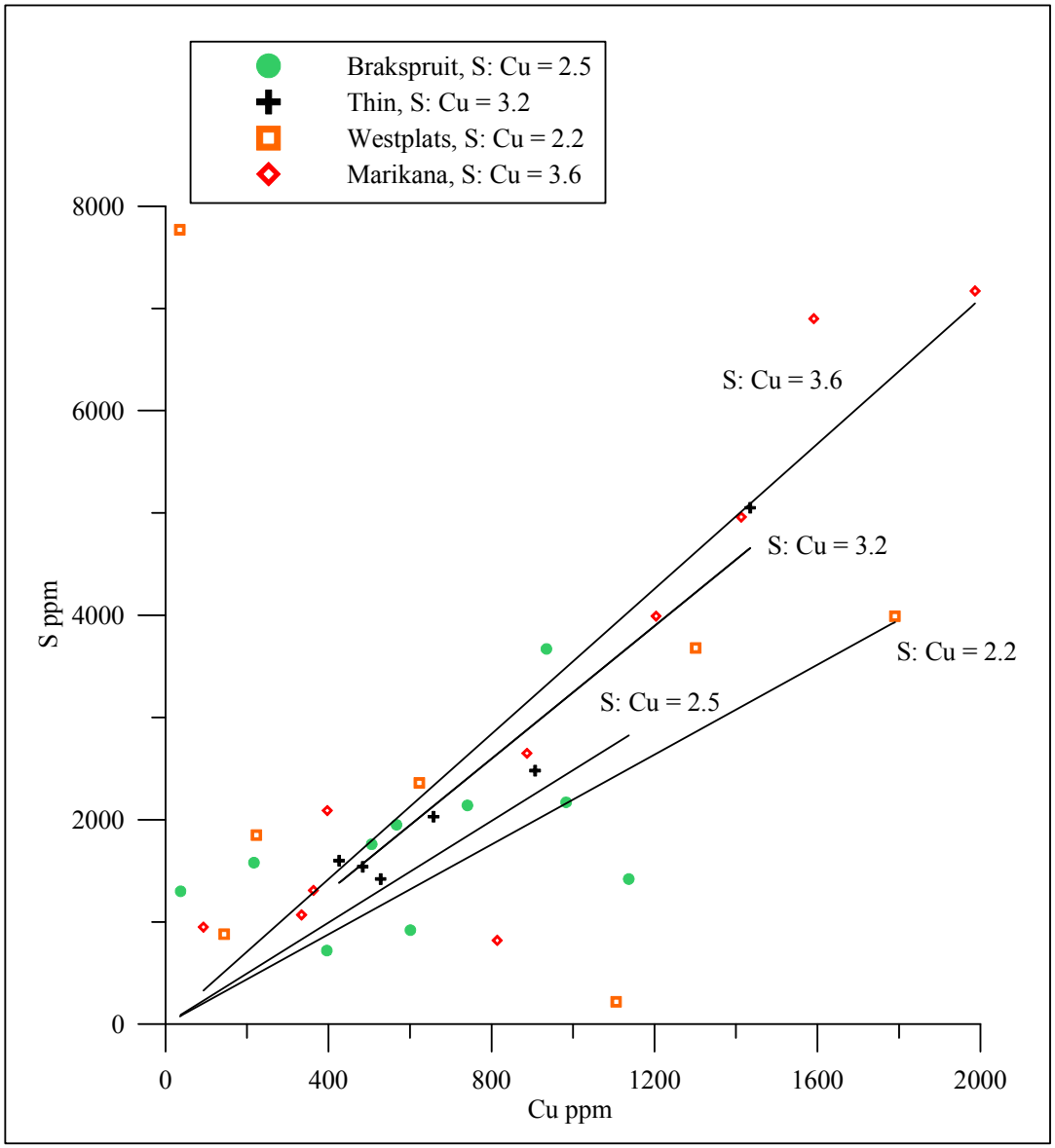

Fig. 5.30 S to Cu ratios for sulphides in the four reef types.

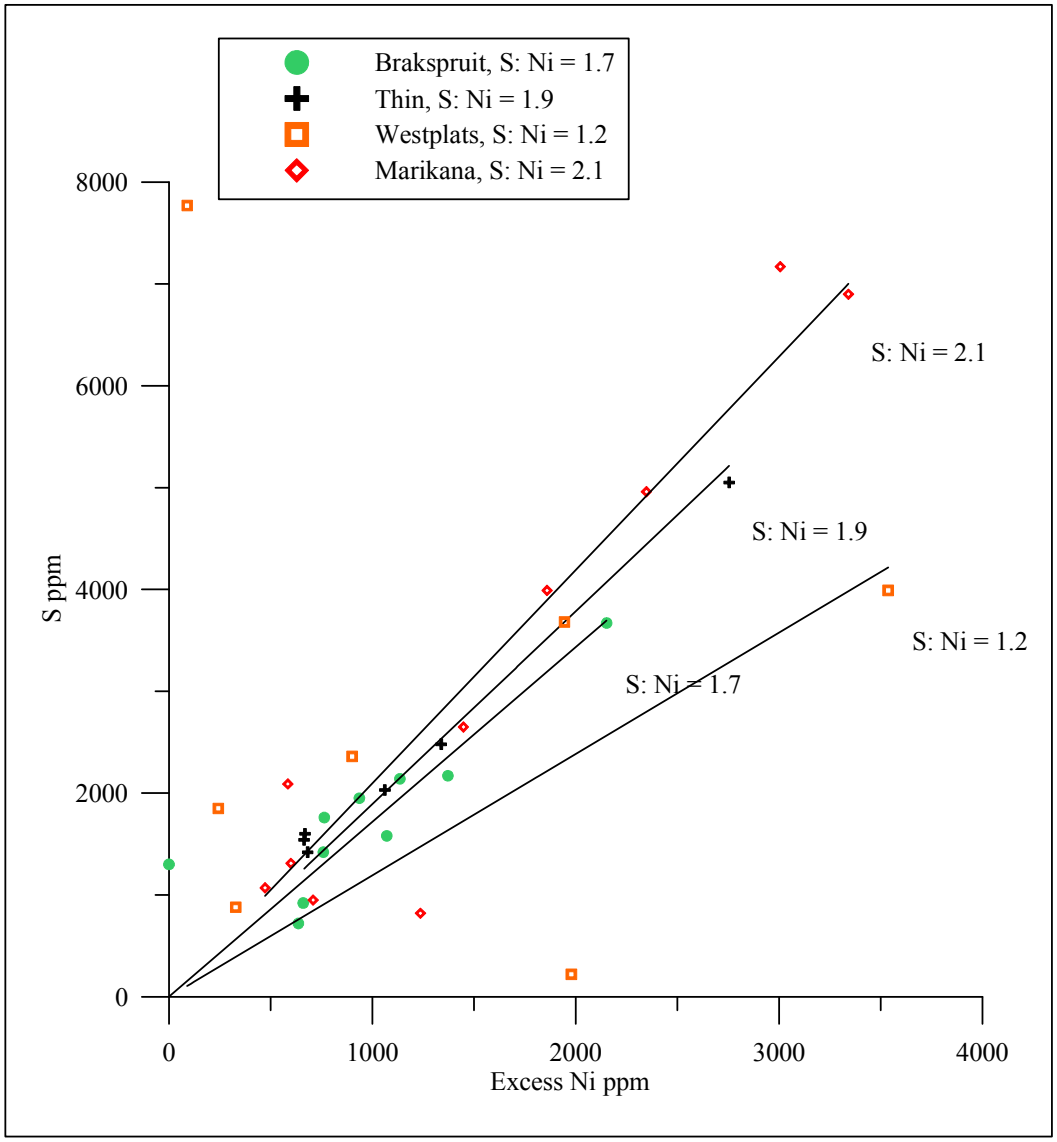

Fig. 5.31. S to Ni (excess) ratios for sulphides in the different reef types.

CHAPTER SIX

MINERAL CHEMISTRY

Mineral separates of plagioclase and polished thin sections of chromitite layers were prepared for mass spectrometry and electron microprobe analyses respectively. The initial strontium isotope ratios that were obtained from analyses of plagioclase separates were used to investigate the effect of addition of magma in a magma chamber. The mineral chemistry of the chromites will help to establish the correlation of the chromitite layers across the four reef types representing the Merensky Unit at Lonplats' Mines. Data for chromite mineral chemistry obtained from SpectRau, University of Johannesburg, are presented in Appendix C, and isotope data from the plagioclase separates are shown in Tables 6.3 and 6.4.

6.1 Chromite compositions

Eight sections through chromitite layers from the Merensky Unit were analysed for mineral chemistry. Three chromitite layers are from the Brakspruit reef type (R 37). Another three are from the Marikana reef type (ML 44). The remaining two are from the Westplats (TN 71) and Thin (ZS 07) reef types respectively. The chromitite layers are situated no more than a meter from the base of the Merensky Unit. In fact, four mark the base of the unit.

Basal layers of all reef types occur at the arbitrary level of 0 m in the stratigraphic sections drawn in this study. The upper and intermediate chromitite layers of the Brakspruit reef type occur at 0.94 m and 0.43 m, respectively. The other two chromitite layers in the Marikana reef type occur at 0.24 m and 1.9 m respectively.

An average of 30 analyses was conducted on each of the eight chromitite layers. Both the rims and the cores of the chromite grains were analyzed where grains were large enough. The semi-massive chromitite layers were analyzed along their horizontal and vertical extents.

All chromite grains are cumulus and unaltered. Various sizes of chromite grains were considered in the analyses of the grains. The minimum size of the chromite grains is 0.1 mm. Some of the grains that form network structures can be up to 2.5 mm in size. In some instances, the network structures that are formed by annealed grains make it hard to distinguish between the different chromite grains.

Mineral phases such as pyroxene and plagioclase that host the chromite grains were carefully noted to observe their effect on the chemistry of the chromite. Olivine is a rare host to the chromite grains. Where network structures exist in the semi-massive chromitite layers, it is difficult to discern the host. The presence of inclusions of pyroxenes and plagioclases, which are usually less than 0.1 mm in the chromite grains is minimal.

The chromite grains were analyzed for Cr, Fe, V, Zn, Ti, Al, Mg, Mn, Ni, Ca and Si. Minor elements such as Si, Ca, Zn, Ni and Mn will not be dealt with in this section because they occur in very minute amounts in chromites. Although occurring in amounts of generally just under 1wt% in chromites and a few having Ti contents of about 2wt%, analyses of Ti is reasonably reliable and therefore will be briefly handled.

Plots of cations and cation ratios calculated from stochiometry can be more rigorously interpreted than binary oxide diagrams and will therefore be used instead. A program of spinel stochiometric calculations, including ferrous: ferric ratios was used to convert element oxides into cations in the chromite grains. The principle of using an ideal formula of XY_2O_4, taking X = (Fe^{2+}, Ni, Mn, Co, Zn) and Y = (Cr^{3+}, Fe^{3+}, Al) is applied in the stochiometric calculation. Iron is divided into ferrous and ferric to suit the condition $n_Y = 2n_X$ where n_Y is total atoms of trivalent cations and n_X is total divalent cations per unit cell. A shortcoming about the stochiometric calculations is the uncertainty in major elements that propagates into larger uncertainty in the estimation of the ferric iron content (Wood and Virgo, 1989). Nothing can be done about this but to appreciate that this problem is a potential hindrance in interpreting small differences in ferric iron concentrations.

The Cr # and Mg # used here to categorize the chromitite layers are also calculated by equations (1) and (2) respectively, using atomic proportions.

$$Cr\# = \frac{100Cr}{Cr + Al} \qquad (1)$$

$$Mg\# = \frac{100Mg}{Mg + Fe^{+2}} \qquad (2)$$

6.1.1 Rims and Cores

The extent of possible systematic zoning is evaluated in Fig. 6.1. Tie-lines are drawn from rims to their corresponding cores of a few chromite grains where grain size is

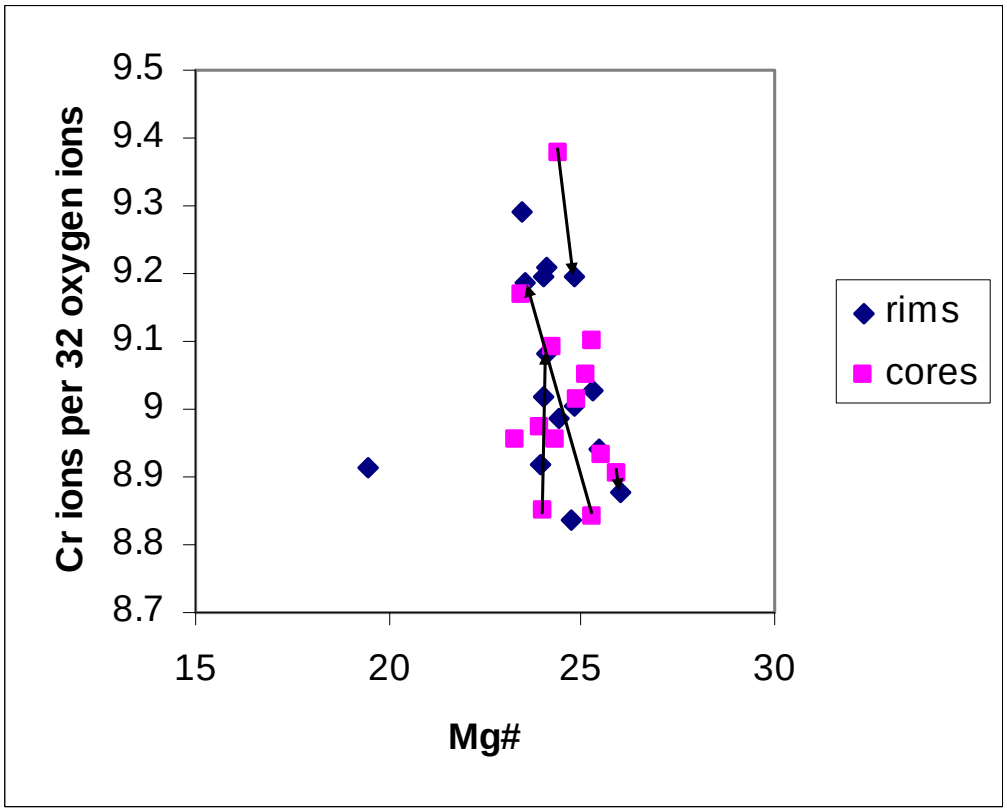

Fig. 6.1. Rim and core compositions of chromite grains from the basal layer in the Marikana reef type. Tie-lines are drawn from the cores to the rims of chromite grains.

large enough. It is shown by Fig. 6.1 that differences between the compositions of rims and their cores are not systematic.

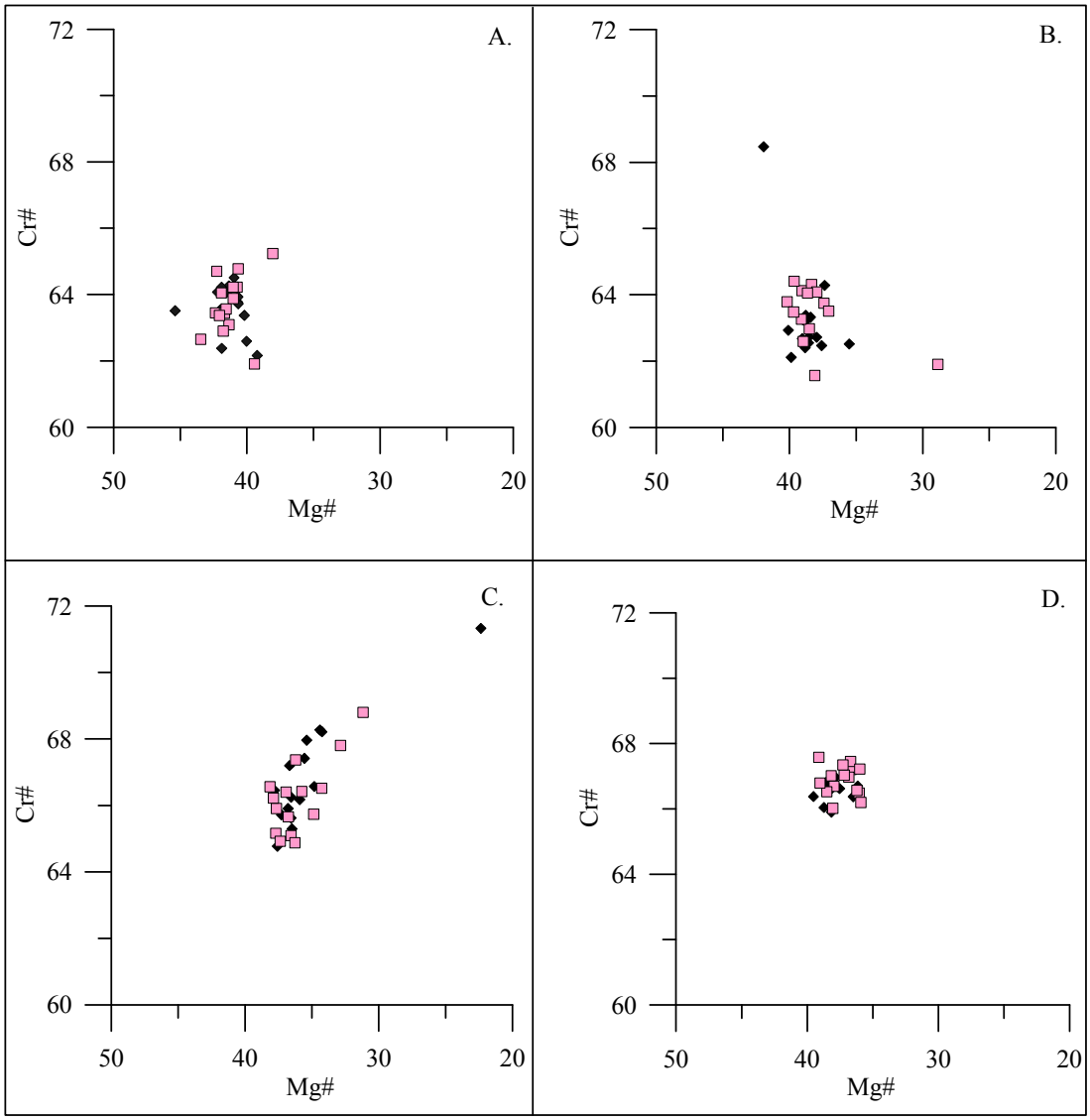

Fig. 6.2 Compositions of rims (diamonds) and cores (squares) of chromites in basal chromitite layers of the Thin (A), Brakspruit (B), Marikana (C) and Westplats (D) reef types.

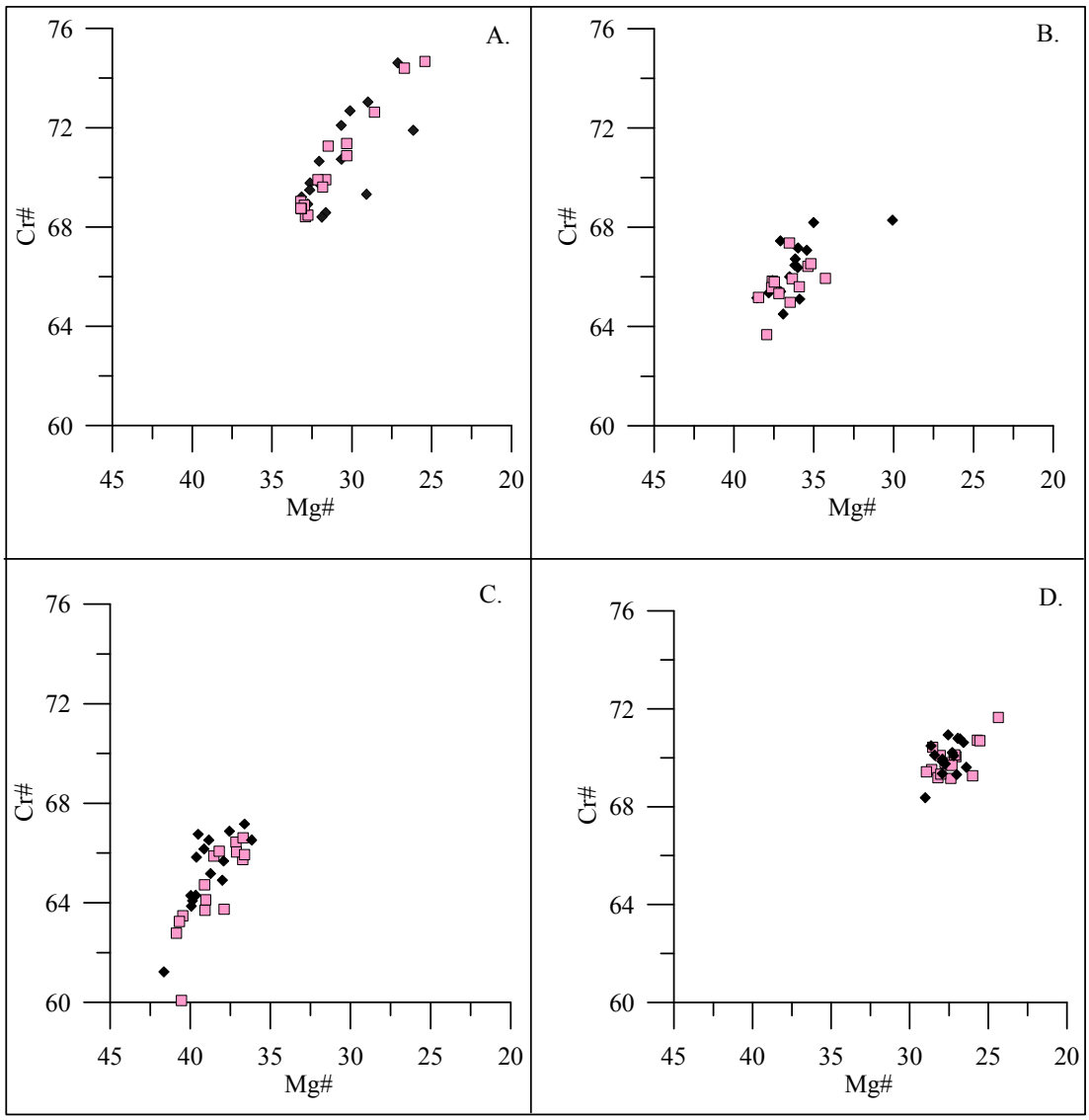

Fig. 6.3 Compositions of rims (diamonds) and cores (squares) of chromites in the intermediate chromitite layers of the Brakspruit (A) and Marikana (B) reef types. C and D show compositions of upper chromitite layers of these two reef types respectively.

Note that for ease of comparison, all sets of figures of this type have identical values and scales on both axes. Figures 6.2 and 6.3 show that rim and core compositions are randomly distributed in their respective fields. This may imply that there no major

chemical variations between compositions of rims and compositions of chromite cores except for very few chromite grains that are isolated from their chromite populations (Fig 6.2B and C).

6.1.2 Chromite host minerals

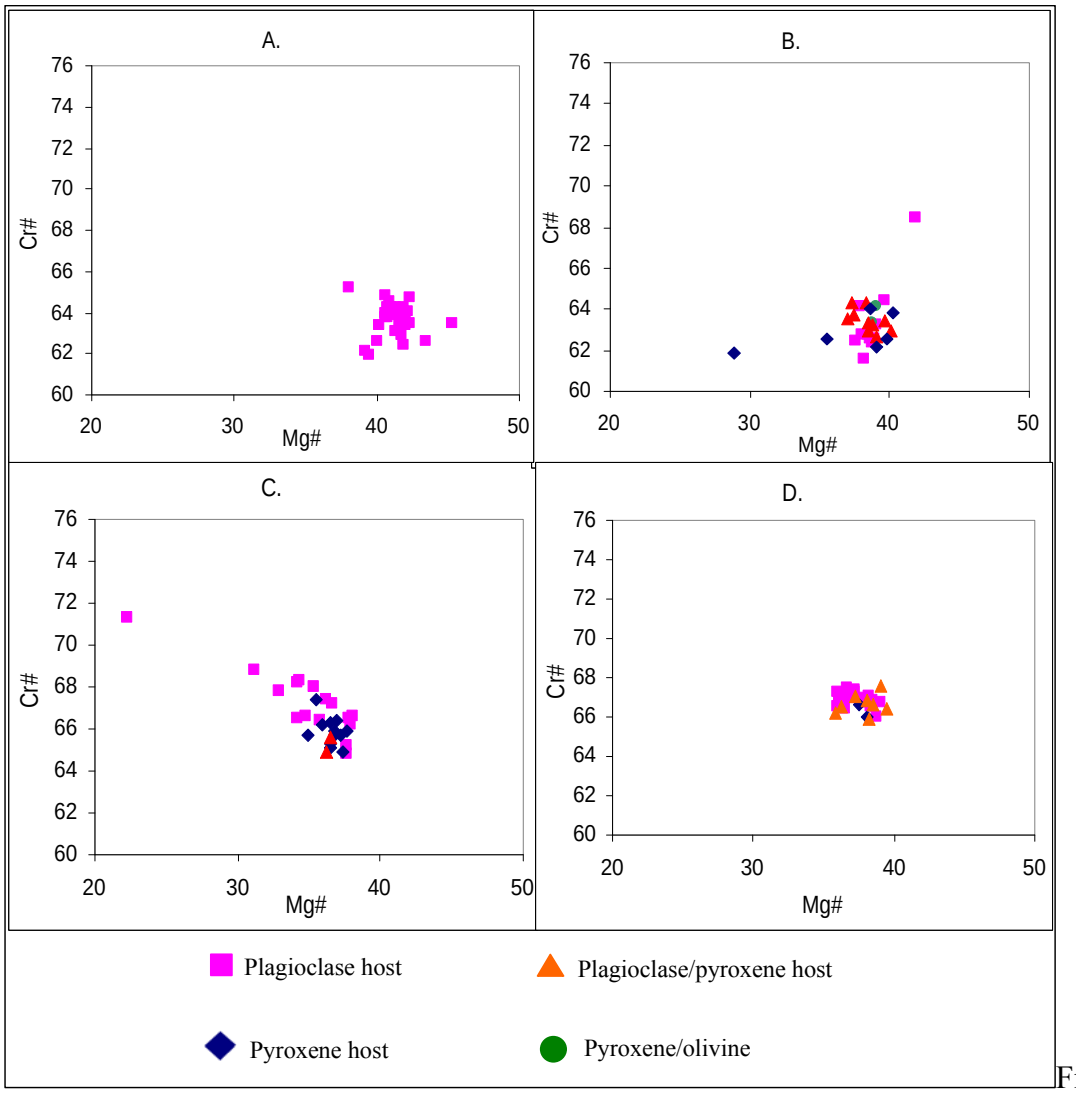

Fig. 6.4 A compound plot of Cr# against Mg# for basal chromitites of the Thin (A), Brakspruit (B), Marikana (C) and Westplats (D) reef types with different hosts.

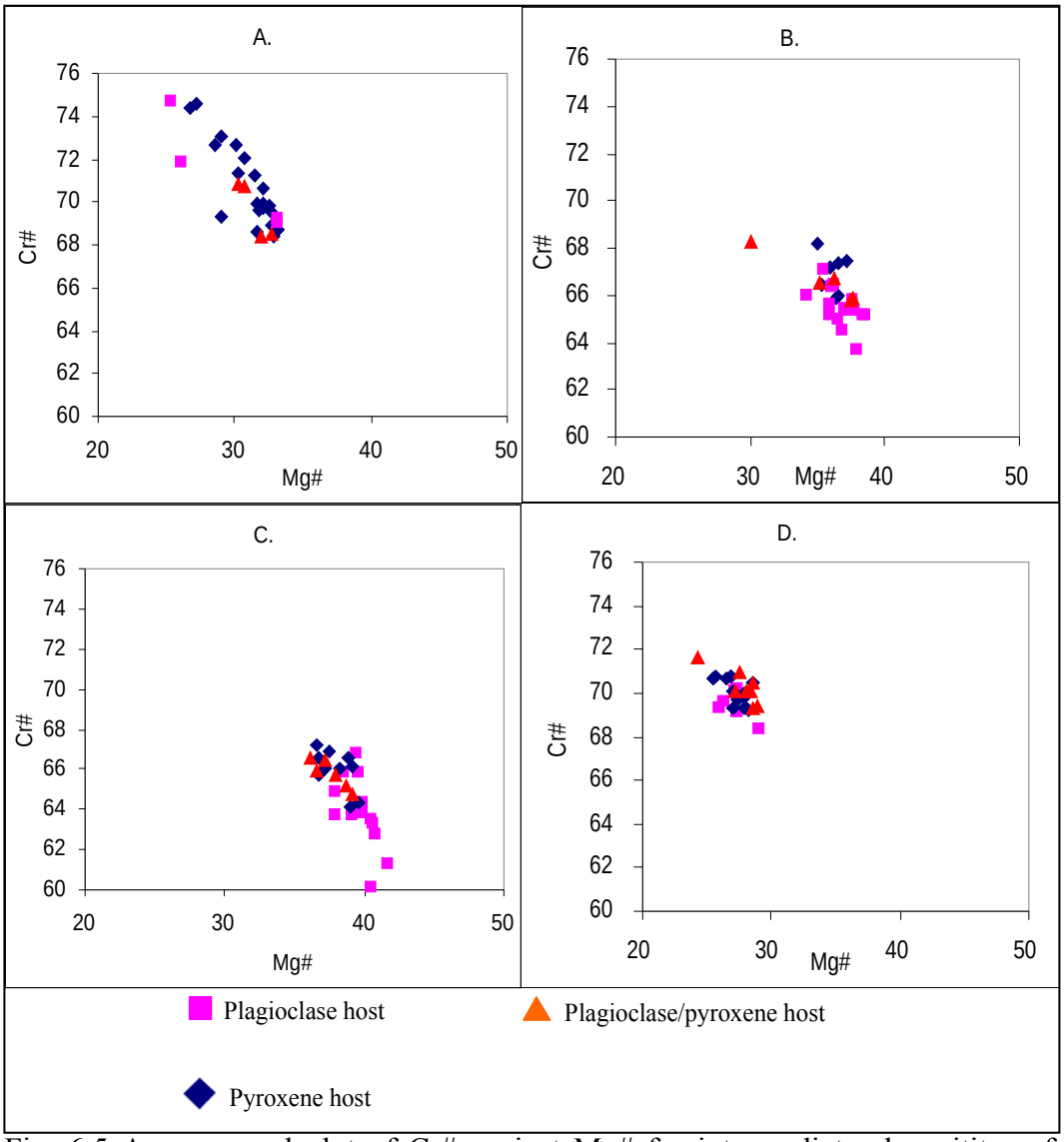

Fig. 6.5 A compound plot of Cr# against Mg# for intermediate chromitites of the Brakspruit (A), Marikana (B) reef types, and upper chromitites of the Brakspruit (C) and Marikana (D) reef types with different hosts.

Figures 6.4 and 6.5 illustrate the chromite compositions as a function of the different mineral phases that are hosts to the chromite grains from the layers in each reef type. Common mineral hosts to chromites are plagioclase and orthopyroxene. In some instances, chromite grains may occur between plagioclase and orthopyroxene or

rarely between orthopyroxene and olivine (e.g. Fig. 6.4) in polymineralic rocks. Having taken this into consideration, there is no major systematic difference observed in terms of Cr# and Mg# in the chemistry of chromites that are hosted by the different minerals.

6.1.3 Chromite populations

The chromite grains can be classified chemically into populations. Each chromitite layer has its distinct compositional range. However, overlaps between populations also exist (Fig. 6.6 to 6.9). The discussion will start from the basal chromitite layers of the Thin, Brakspruit, Marikana, and Westplats reef types. Thereafter, the focus will be placed on the intermediate and upper chromitites of the Brakspruit and Marikana reef types.

Chromite grains from the Thin reef type, have Mg# and Cr# ranging from 38 to 48 and 62 to 65, respectively (Fig. 6.6). Chromite compositions in this reef type have the lowest Cr# and the highest Mg# (Fig. 6.6), and these are classified as type 1a chromites (see Table 6.1). The chromites of the basal layer in the Brakspruit reef type are grouped as type 1b because they have similar Cr# as the Thin reef type chromites but have slightly different Mg# ranging from 30 to 40. Overlap exists between these two populations.

Chromites from the Westplats reef type have affinities of type 2a chromites (Table 6.1). These have intermediate Cr# and Mg# (Fig. 6.6). Chromites in the basal and intermediate layers from the Marikana reef type are both classified as type 2b chromites as they have intermediate Cr# but lower Mg# (33 to 37). These three populations of chromite grains from the Westplats and Marikana reef types also show some overlap.

Table 6.1 Classification of chromite grains from the four reef types.

	Type 1	Type 2	Type 3
A	$62 \leq$ Cr# ≤ 65 $38 \leq$ Mg# ≤ 45 *Thin, basal*	$65 \leq$ Cr# ≤ 68 $35 \leq$ Mg# ≤ 40 *Westplats, basal* *Brakspruit, upper*	$68 \leq$ Cr# ≤ 75 $27 \leq$ Mg# ≤ 35 *Brakspruit, intermediate*
B	$62 \leq$ Cr# ≤ 65 $35 \leq$ Mg# ≤ 40 *Brakspruit, basal* *Brakspruit, upper*	$64 \leq$ Cr# ≤ 69 $33 \leq$ Mg# ≤ 37 *Marikana, basal* *Marikana, intermediate*	$68 \leq$ Cr# ≤ 72 $24 \leq$ Mg# ≤ 30 *Marikana, upper*

The chromitite layers of the Brakspruit reef type are distinct, relative to each other, in their chemistry. The basal, intermediate and upper chromitite layers of the Brakspruit reef type plot in different fields (Fig. 6.6). The basal chromitite layer in this reef type is already discussed above. The chromite grains in the intermediate chromitite layer from the Brakspruit reef type have the highest values of Cr # and lower Mg# values and are assembled in the type 3a group. Chromite compositions in the upper layer from the Brakspruit reef type are spread over type 1 and type 2 groups.

Chromite grains in the upper layer of the Marikana reef type have compositions that define type 3b and are distinct from the basal and intermediate chromitite layers and have high Cr# values and the highest Mg# which vary from 24 to 30. The intermediate and basal chromitite layers in the Marikana reef type have chromites classified as type 2b.

6.1.4 Cation compositions

Cation compositions for the eight chromitite layers are presented in Fig. 6.7 and Fig. 6.8, plotted against Mg#. There is generally little variation between the cation compositions in the respective populations of the different basal chromitite layers (Fig. 6.7). However, there are distinctions in several chromite grains. These grains are considered as outliers and will therefore be ignored. Cr cations in the Thin, Brakspruit and Marikana reef types show a slightly decreasing trend with decreasing

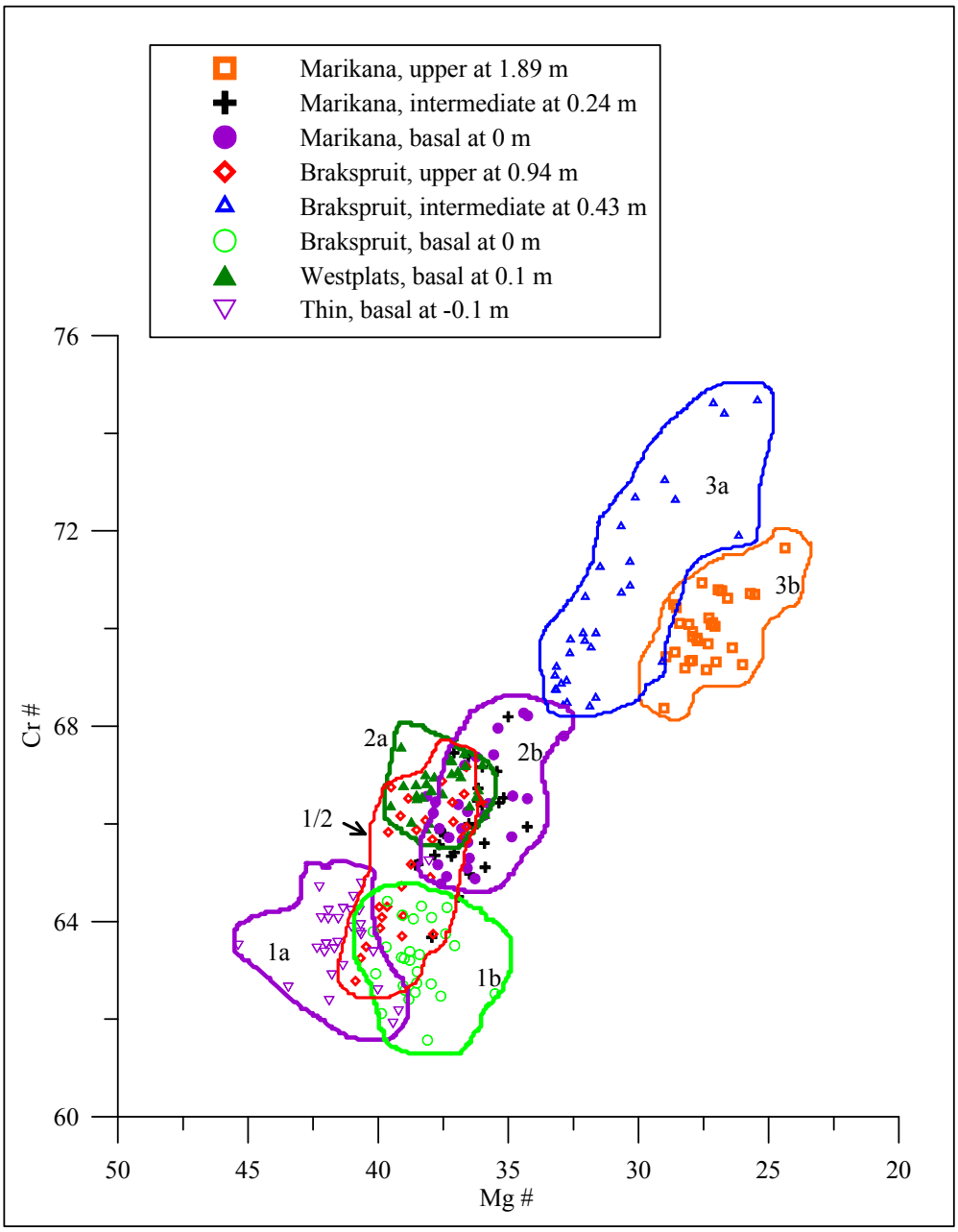

Fig. 6.6 Cr# and Mg# of chromite grains from different reef types. Height at which the chromitite layers occur is shown in the legend.

Mg# (Fig. 6.7). Al cation proportions also show a decreasing trend with chromites in the Marikana reef type being the most illustrative of this trend. The Marikana and the

Westplats reef type chromitites are comparable with Al cation values of 4 to 5. Chromites in the Thin and Brakspruit reef type, from the basal layers have Al cation compositions that range from 5 to 5.7. Ti cation compositions for the four basal chromitite layers are similar.

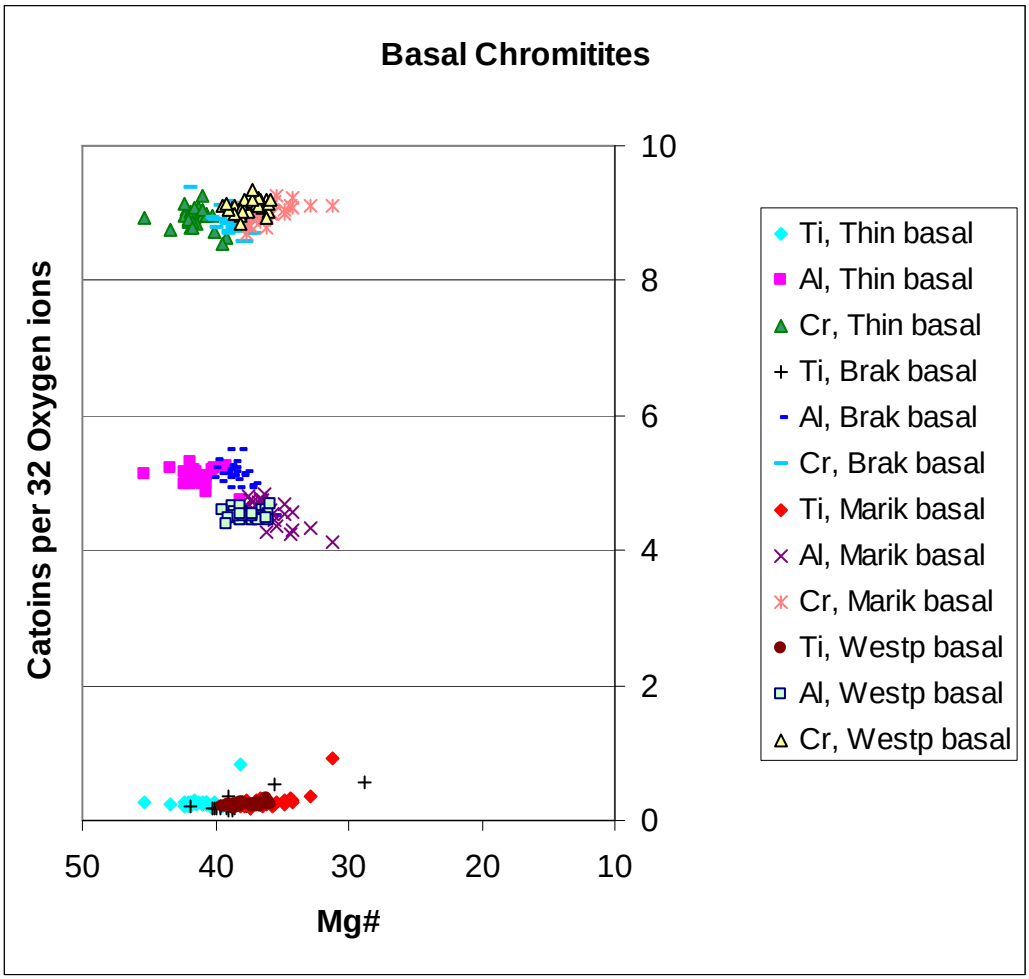

Fig. 6.7 Cation compositions of basal chromitite layers in the Merensky Unit.

Figure 6.8 shows cation compositions for the intermediate and upper chromitite layers of the Brakspruit and Marikana reef types respectively. Different populations of cation compositions are identifiable here, although some overlap exists. All chromitite layers in Fig. 6.8 show comparable Cr proportions, with the different Mg#. All the four (intermediate and upper) chromitite layers show decreasing Al trends with decreasing Mg#. The upper and intermediate layers in the Brakspruit and Marikana reef types show high Al cations of 4.5 to 5.8 and 4.2 to 5 respectively. The

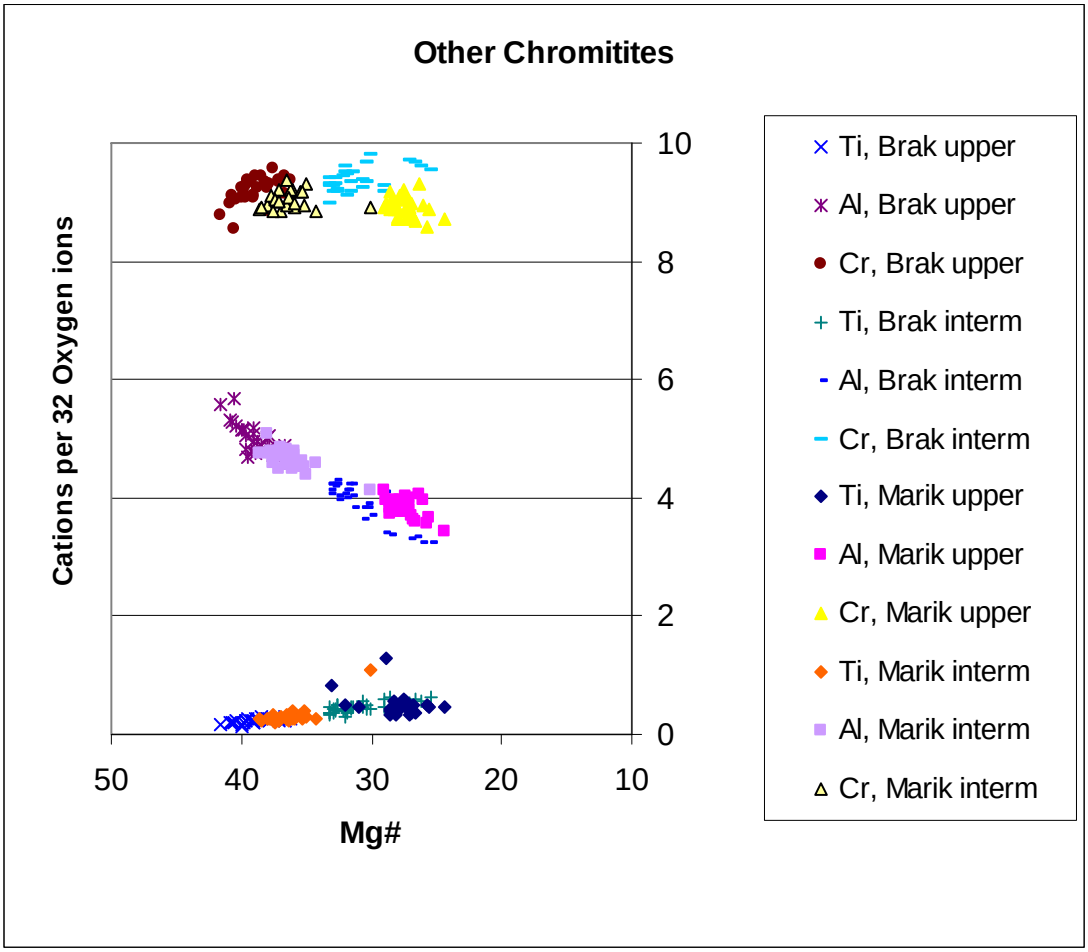

Fig. 6.8 Cation compositions of intermediate and upper chromitite layers in the Brakspruit and Marikana reef types.

intermediate and upper layers in the Brakspruit and Marikana reef types show Al cations abundances ranging from approximately 3 to 4.2. Overlap exists between the populations of the upper layer in the Brakspruit reef type and the intermediate layer in the Marikana reef type. Overlap also exists between the intermediate layer in the Brakspruit reef type and the upper layer in the Marikana reef type. All the four layers in these two reef types have similar Ti cation compositions (0.1 to 0.7).

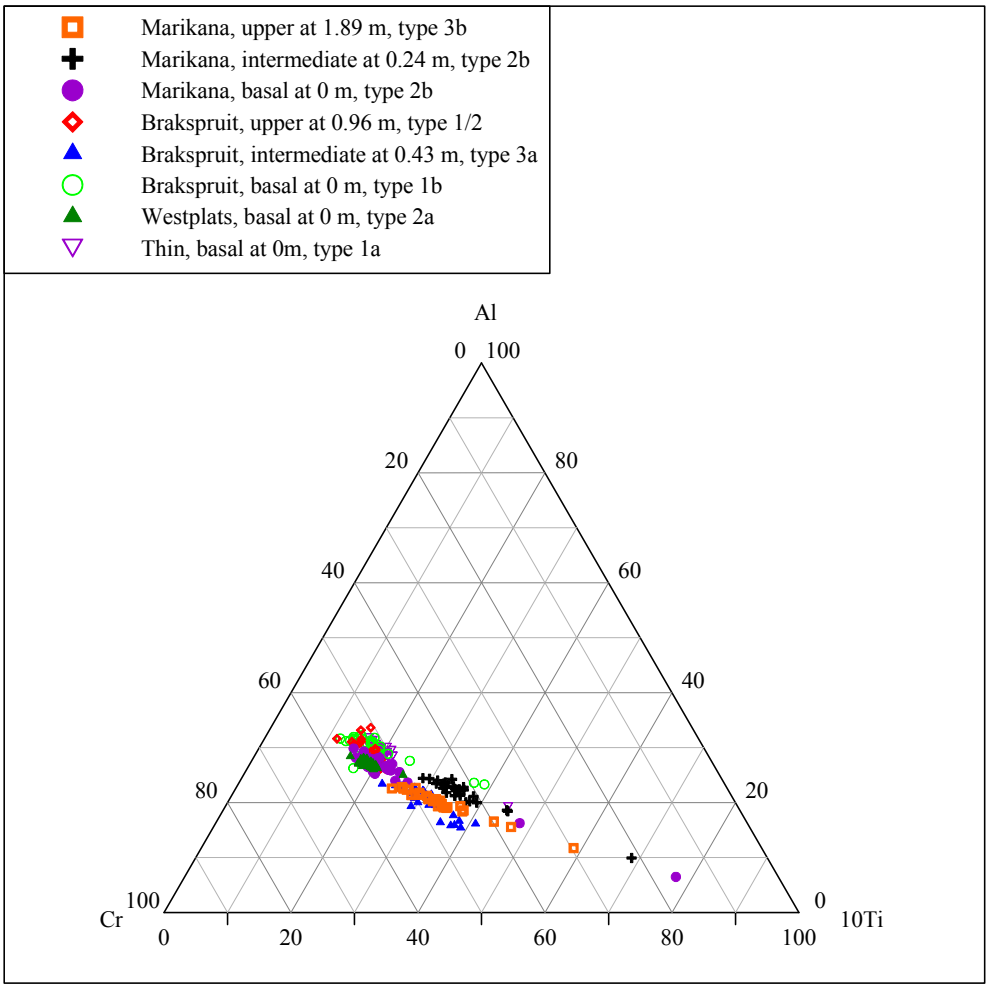

Fig. 6.9 Al-Cr-10Ti diagram of chromites in the Merensky Unit. Types of chromites are also shown in the legend.

Figure 6.9 is a triangular data plot that represents all the chromitites in the Merensky Unit at Lonplats' Mines. The data of the chromites show a significant Cr-Ti trend and a number of chromites evolved toward the Ti-enriched state. The chromitite layers show a wide range of compositions along this trend. This is especially indicated by the chromites in the Marikana reef type, where a few chromites from the intermediate and basal layers are more evolved.

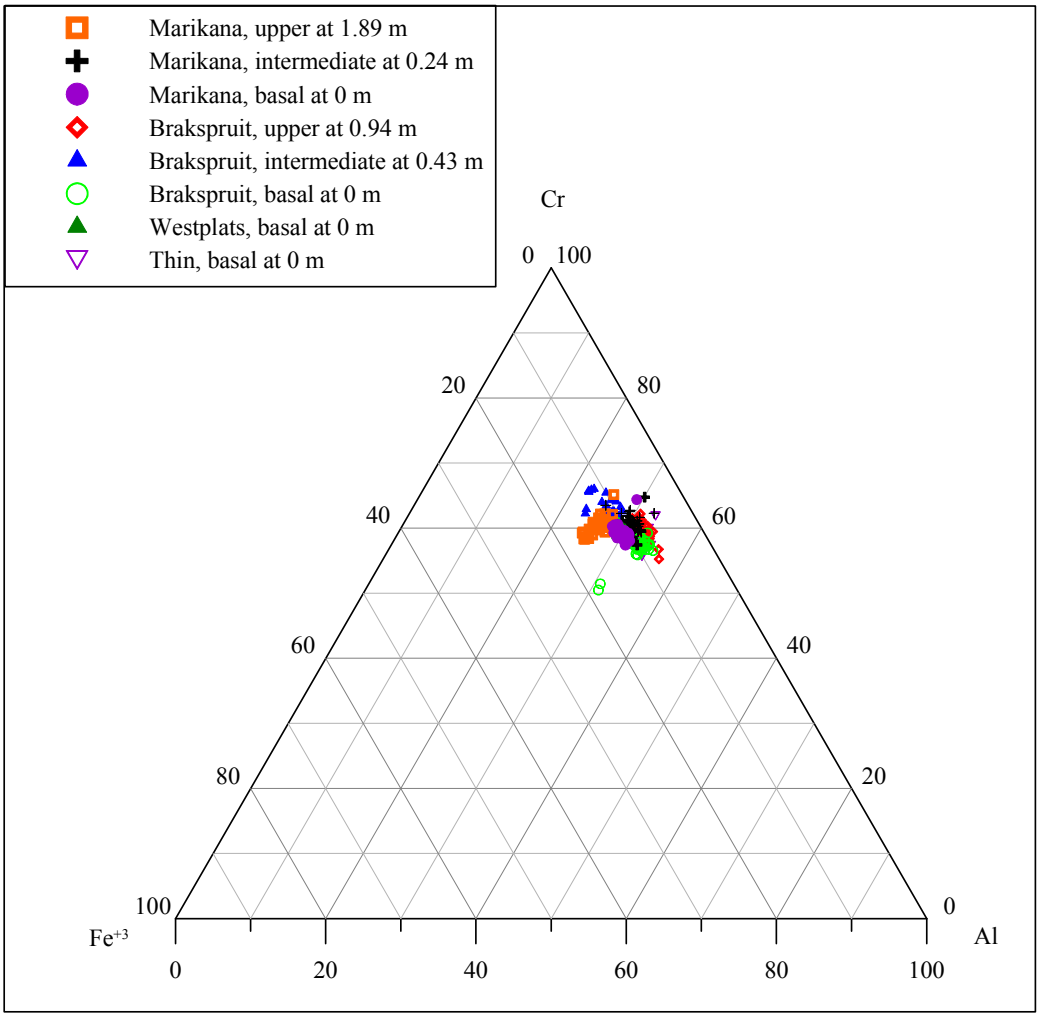

Fig. 6.10 Trivalent cation content in the chromites of the Merensky Unit at Lonplats' Mines.

In terms of trivalent ions, all chromite grains, except a few, are clustered together at relatively low Fe^{+3} contents (Fig. 6.10). Very little variation in terms of Fe+3 is observed in the different chromitite layers.

6.2 Plagioclase compositions

Pure plagioclase mineral separates of about 0.2 g, obtained from anorthosites, norites, and pyroxenites were used for Rb and Sr analyses by mass spectrometry. There have been several studies undertaken across the Merensky interval. However, these studies have been from relatively thin reef facies reviewed by (Kruger, 1994). Hence 26 plagioclase mineral separates were taken from the thick reef type; the Westplats reef type. The samples were cleaned by hand picking of minerals such as mica, in which Rb is compatible. The presence of micas in the plagioclase separate samples could yield unreliable data. Cumulus and intercumulus plagioclase cannot be separated.

6.2.1 Strontium contents

The Hugh Allsopp Laboratory at the University of the Witwatersrand, Johannesburg, the Stable Light Isotope Laboratory at the University of Cape Town (UCT) and the Isotope Geology Laboratory (Institute of Geological Science) at Bern University, Switzerland, were used to test for reliability of data. Because the Hugh Allsopp Laboratory was shut down after the first set of data from 12 samples were collected, another set of plagioclase separates and repeats, are sent to Bern University's Isotope

Geology Laboratory. The results for absolute Sr concentrations of duplicate samples were different from results from the Hugh Allsopp Laboratory and so replicate samples were sent to UCT Stable Light Isotope Laboratory for further analysis for absolute Sr contents only.

Out of the 26 plagioclase mineral samples, 10 samples were replicated at the above mentioned analytical laboratories. Four of these 10 samples that occur at -4.65 m, 1.24 m, 6.11 m, and 12.1 m respectively, were analyzed by all three laboratories and six samples analyzed by a combination of two out of these three laboratories. Table 6.2 represents the absolute Sr concentrations of the plagioclase minerals analysed by these different laboratories. The Sr concentrations from the three laboratories are plotted against height in Fig. 6.12.

The four samples that were analysed by all the three laboratories, listed in Table 6.2 produced Sr contents ranging from 438 to 588 ppm, 487 to 543 ppm, 463 to 609 ppm, and 472 to 708 ppm. Moreover, the remaining six samples analysed by a combination of two out of the three analytical laboratories yielded Sr abundance values of 415 and 530 ppm, 410 and 506 ppm, 424 and 429 ppm, 439 and 453 ppm, 393 and 470 ppm, and 491 and 496 ppm, respectively (Table 6.2). All of the differences between the Sr concentrations are significant. There is no consistent difference in the values or relative proportions between the different laboratories, although the laboratory at Bern University gives generally variably higher concentrations than the other two laboratories. The reason for such variations is not apparent. The weight of sample

analysed at each facility is approximately 0.2 g, presenting about 70 plagioclase grains of about 100 μm, and so grain to grain variation is considered unlikely.

Table 6.2 Absolute Sr concentrations from 10 plagioclase separates analysed at Hugh Allsopp (Lab 1), Isotope Geology Laboratory (Institute of Geological Science), Bern University (Lab 2) and Stable Light Isotope Laboratory, University of Cape Town (Lab 3). Px (pyroxenite), An (anorthosite) and No (norite). The method of calculation of Sr contents is described in the text.

Height in meters	Rock type	Lab 1 Sr ppm	Lab 2 Sr ppm	Lab 3 Sr ppm	Calculated Sr ppm
29.85	No		530	415	415
22.33	No		506	410	410
18.24	Px		428.9	424	425
13.29	An	439.3		453	455
12.1	An	438.3	588	467	445
11.07	Px	393.4		470	220
6.11	Px	487.2	543.4	492	320
3.2	Px	490.5		496	350
1.24	Px	525.6; 551	609	463	445
-4.65	An	658	708	472	410

Because of the major differences between Sr contents from the three laboratories, a fourth method has been devised that determines the approximate Sr concentrations of plagioclase minerals. This method works on the principle that the rocks are composed almost entirely of orthopyroxene with 0 ppm Sr and plagioclase. Figure 6.11 shows a

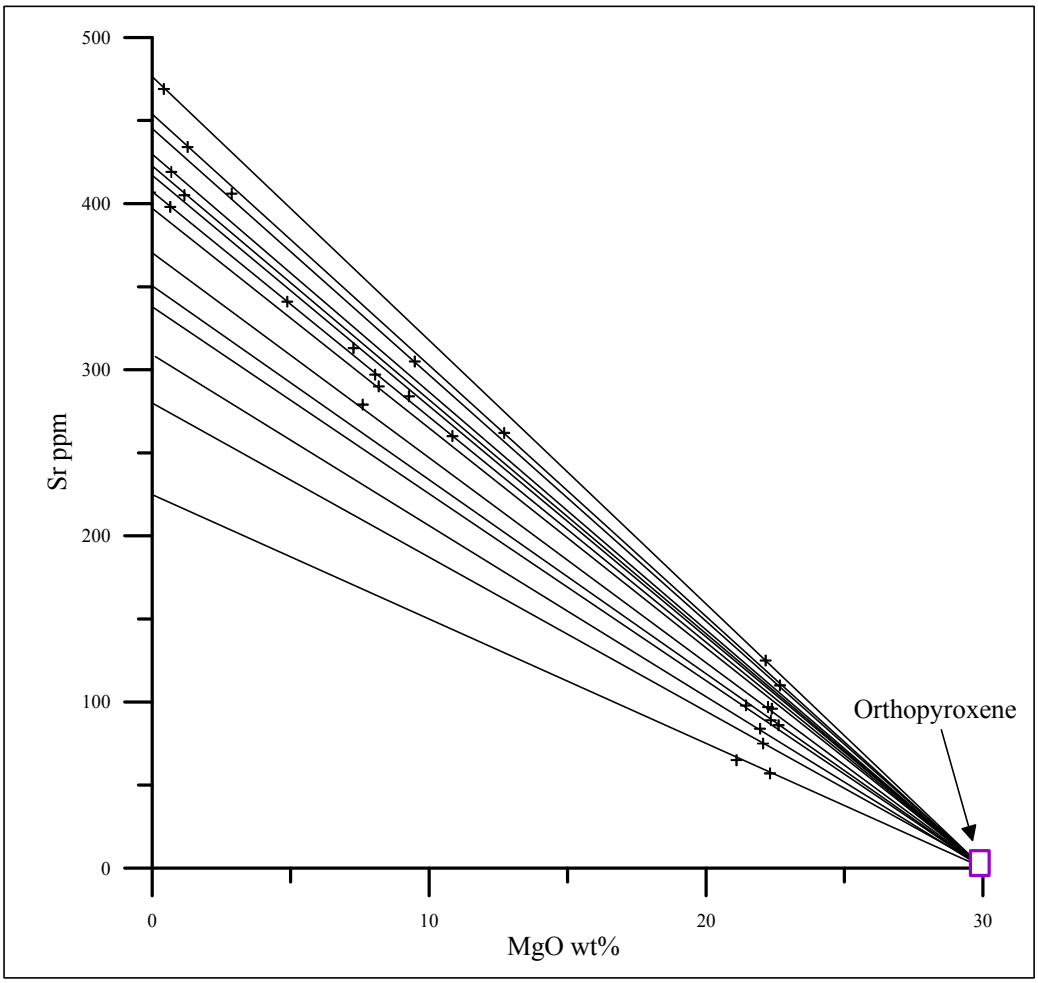

Fig. 6.11. Extrapolated Sr contents in plagioclase from whole-rock analyses. Orthopyroxene composition (30wt% MgO) is also shown.

plot of Sr concentrations versus whole-rock MgO content in wt%. Each whole-rock analysis is extrapolated to 0 wt% MgO from the orthopyroxene composition and the calculated Sr contents are presented in Table 6.2. The calculated Sr contents are mostly comparable with the results obtained from UCT except for the three approximated low values of 220 ppm, 320 ppm and 350 ppm, determined from pyroxenites.

The difference between extrapolated Sr contents and whole-rock Sr contents is greater in pyroxenites (more than 20 wt% MgO) than it is in plagioclase-rich rocks with less than 12 wt% MgO and therefore the error in extrapolated Sr contents in pyroxenites is expected to be greater than the error obtained for calculations for anorthosites and norites.

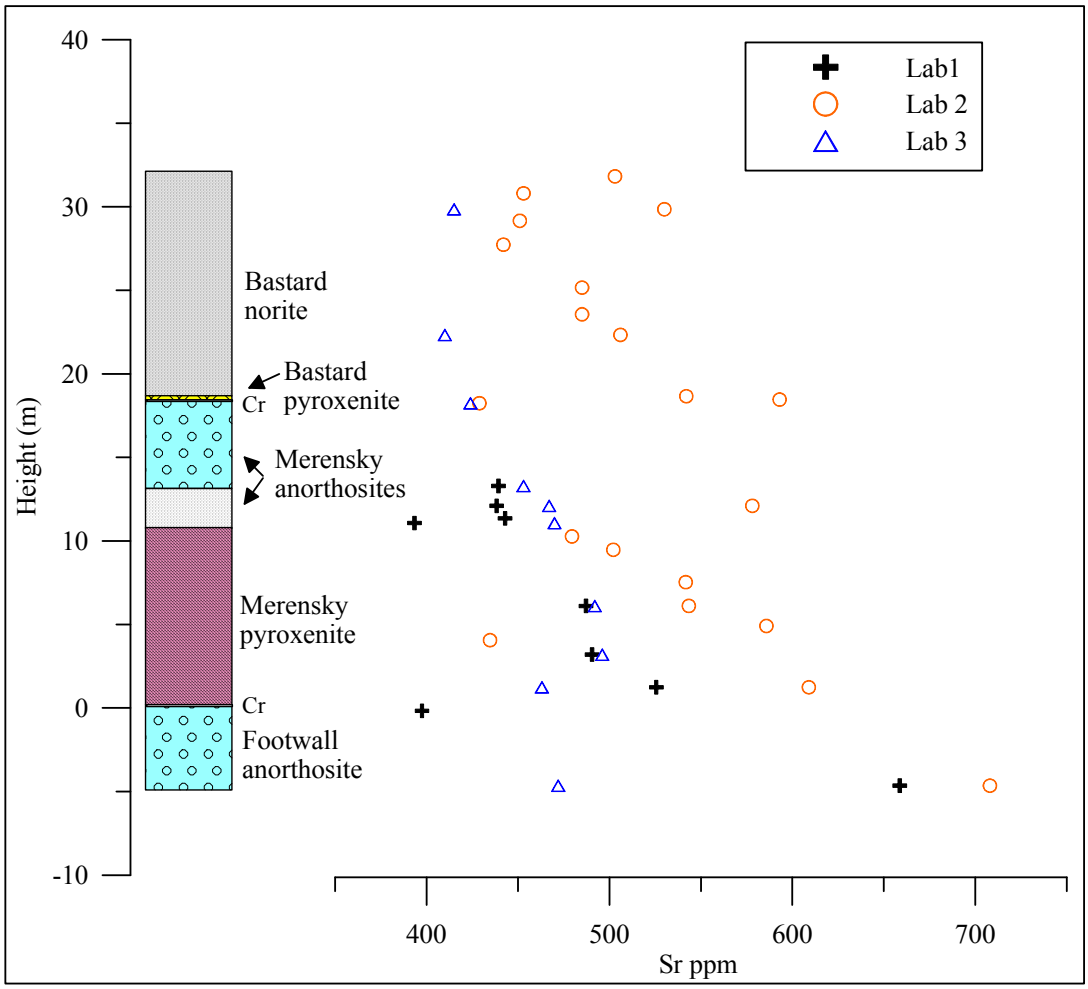

Fig. 6.12 A plot of absolute Sr concentrations from the three laboratories versus height in the Westplats reef type at Eastern Platinum Mine. Hugh Allsopp Laboratory (Lab 1), Isotope Geology Laboratory (Institute of Geological Science), Bern University (Lab 2) and Stable Light Isotope Laboratory, University of Cape Town (Lab 3).

Figure 6.12 illustrates the change of the Sr contents analysed from the three laboratories with height. Although the data from these different laboratories vary from one another, they show similar trends. The graph in Fig. 6.12 shows that absolute strontium abundances in plagioclases generally decrease with increasing height, although it is least pronounced for the data from UCT.

The differences between the results from the three laboratories are extremely large and require further interlaboratory calibration, but that was not possible within the scope of this project. As a result of these problems, no interpretations from these results can be made.

6.2.2 Initial Sr isotope ratios

Strontium isotope data is presented in Tables 6.3 and 6.4. These data are obtained from both the Hugh Allsopp and Isotope Geology (Bern University) Laboratories. Initial strontium isotope ratios ($^{87}Sr/^{86}Sr$) are calculated at 2060 Ma and these ratios are plotted against height (Fig. 6.13). The object of this study is to determine isotopic breaks that occur in magmatic sequences of the Merensky Unit at Lonplats' Mines. The importance of analyzing a thick reef type for strontium isotopes is that the information obtained is much more detailed as opposed to information from a narrow reef type. Profiles produced from such isotopic studies can also be characteristic for specific macro cyclic units.

Table 6.3 Sr isotope data for duplicates obtained from Hugh Allsopp Laboratory and Isotope Geology Laboratory.

Height (m)	$^{87}Sr/^{86}Sr^{\#}$	2 se	Initial Ro	2 sigma	Laboratory
12.10	0.706836	± 43	0.70653	0.00014	W.U.*
12.10	0.706880	± 2	0.70665	0.0002	B.U.$^{+}$
12.10	0.706856	± 2	0.70663	0.0002	B.U.
6.11	0.707258	± 41	0.70679	0.00015	W.U.
6.11	0.706825	± 16	0.70633	0.0002	B.U.
1.24	0.706502	± 38	0.70603	0.00015	W.U.
1.24	0.706273	± 45	0.70689	0.00015	W.U.
-0.17	0.706925	± 76	0.70647	0.00015	W.U.
-0.17	0.706836	± 25	0.70622	0.00015	W.U.
-4.65	0.706729	± 37	0.70648	0.00015	W.U.
-4.65	0.706663	± 2	0.70640	0.0002	B.U.

W.U. * = Hugh Allsopp Laboratory (Wits University), B.U.$^{+}$ = Isotope Geology Laboratory (Bern University), $^{87}Sr/^{86}Sr^{\#}$ is for present time. R_o represents the initial $^{87}Sr/^{86}Sr$ ratios.

Results for duplicate samples used for Sr isotope data are presented in Table 6.3. Some samples have been analysed in duplicate by one laboratory, and some have been analysed by the two laboratories. Error determined for $^{87}Sr/^{86}Sr$ ratios for the present time for each of these duplicated samples varies notably. Errors obtained from the Hugh Allsopp Laboratory are always greater than the errors in the data acquired from Bern University. The present time isotope ratios from the two different

Table 6.4 Initial strontium isotope ratios from the thick reef type; Westplats of the Eastern Platinum Mine. Height in meters is represented in the first column. Datum is set as the basal chromitite layer of the Merensky Unit.

		Height (m)	Rock type	Rb ppm	Sr ppm	$^{87}Rb/^{86}Sr$	$^{87}Sr/^{86}Sr$	±	2 se	Initial Ro @ 2060	±	2 sigma
Hugh	Merensky	13.29	Anorthosite	1.33	439.3	0.0087	0.706937	±	57	0.70668	±	0.00014
Allsopp	Unit	12.10	Anorthosite	1.56	438.3	0.0102	0.706836	±	43	0.70653	±	0.00014
Laboratory,		11.35	Anorthosite	2.79	442.9	0.0182	0.706693	±	42	0.70615	±	0.00015
University		11.07	Pyroxenite	3.35	393.4	0.0259	0.706856	±	58	0.70609	±	0.00015
of the		6.11	Pyroxenite	2.64	487.2	0.0156	0.707258	±	41	0.70679	±	0.00015
Witwatersrand		3.20	Pyroxenite	2.45	490.5	0.0144	0.706406	±	26	0.70598	±	0.00015
		1.24	Pyroxenite	2.88	525.6	0.0158	0.706502	±	38	0.70603	±	0.00015
		1.24	Pyroxenite	2.49	550.9	0.0130	0.706273	±	45	0.70589	±	0.00015
		-0.17	Anorthosite	2.36	444.4	0.0153	0.706925	±	76	0.70647	±	0.00015
		-0.17	Anorthosite	2.86	397.5	0.0208	0.706836	±	25	0.70622	±	0.00015
		-4.65	Anorthosite	1.95	658.7	0.0085	0.706729	±	37	0.70648	±	0.00014
Isotope	Bastard	31.82	Norite	2.24	503.0	0.0129	0.707928	±	28	0.70755	±	0.00002
Geology	Unit	30.80	Norite	2.35	453.0	0.0150	0.707979	±	19	0.70754	±	0.00002
Laboratory,		29.85	Norite	2.24	530.0	0.0122	0.707995	±	29	0.70763	±	0.00002
Bern		29.16	Norite	3.14	451.0	0.0202	0.707829	±	30	0.70723	±	0.00002
University		27.73	Norite	2.29	442.0	0.0150	0.707852	±	38	0.70741	±	0.00002
		25.16	Norite	2.30	485.0	0.0137	0.708007	±	33	0.70760	±	0.00002
		23.56	Norite	2.58	485.0	0.0154	0.707893	±	36	0.70744	±	0.00002

	22.33	Norite	2.17	506.0	0.0124	0.707787	±	16	0.70742	±	0.00002
	18.66	Norite	1.23	542.0	0.0066	0.707283	±	20	0.70709	±	0.00002
	18.46	Pyroxenite	1.39	593.0	0.0068	0.706801	±	21	0.70660	±	0.00002
	18.24	Pyroxenite	1.49	428.9	0.0101	0.707408	±	17	0.70711	±	0.00002
Merensky Unit	12.10	Anorthosite	1.57	588.0	0.0077	0.706880	±	2	0.70665	±	0.00002
	12.10	Anorthosite	1.54	578.1	0.0077	0.706856	±	2	0.70663	±	0.00002
	10.27	Pyroxenite	1.48	479.5	0.0090	0.706593	±	13	0.70633	±	0.00002
	9.47	Pyroxenite	7.09	502.1	0.0409	0.707617	±	29	0.70641	±	0.00002
	7.63	Pyroxenite	5.45	541.7	0.0291	0.707151	±	28	0.70629	±	0.00002
	6.11	Pyroxenite	3.14	543.4	0.0167	0.706825	±	16	0.70633	±	0.00002
	4.91	Pyroxenite	4.03	585.8	0.0199	0.706865	±	22	0.70628	±	0.00002
	4.06	Pyroxenite	22.80	434.7	0.1518	0.710550	±	63	0.70607	±	0.00004
	0.24	Pyroxenite	1.90	609.0	0.0090	0.706542	±	2	0.70628		0.0002
	-4.65	Anorthosite	2.20	708.0	0.0090	0.706663	±	2	0.70640	±	0.00002

laboratories are also slightly variable and the ratios attained from two samples analysed at the Hugh Allsopp laboratory are slightly higher (with one lower value) than those from Bern University (see Table 6.3). Duplicates of samples analyzed at the Hugh Allsopp Laboratory yield different errors for the $^{87}Sr/^{86}Sr$ ratios (present time) but the calculated error on R_o is not significant. R_o (initial $^{87}Sr/^{86}Sr$) values from these two laboratories can be considered within error of each other and these data can be combined and interpreted.

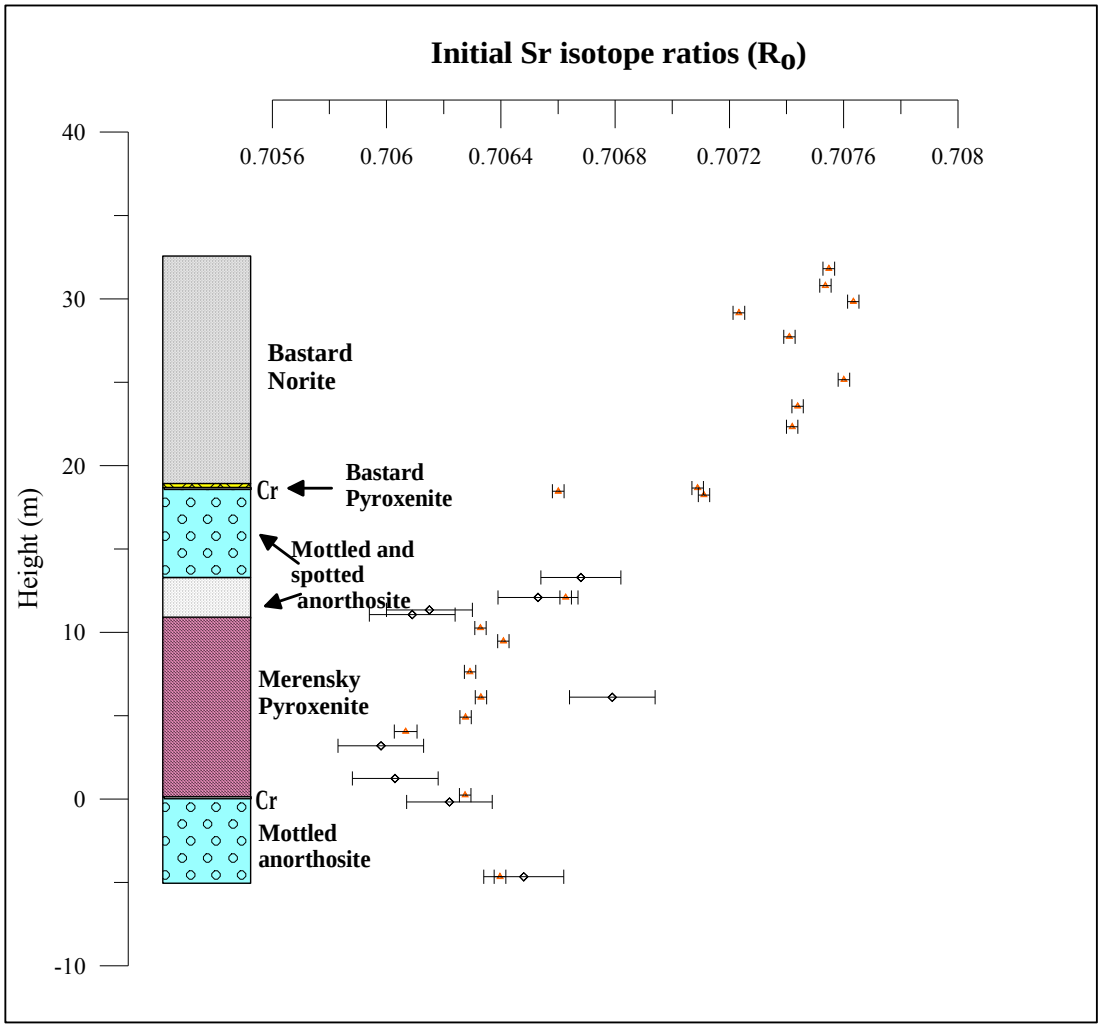

← Fig. 6.13. Initial strontium isotope ratios from the Eastern Platinum Mine are plotted against height. Triangles represent data from Bern University and diamonds are for data from Hugh Allsopp Laboratory. Error bars are indicated for the two sets of data. Height in meters is indicated relative to the basal chromitite layer of the Merensky Unit. A stratigraphic column of the Westplats reef type is also included, showing the Merensky and Bastard Units.

The initial strontium isotope ratio in the two samples of the footwall anorthosite are 0.7064 (Fig 6.13), typical of Critical Zone values. The lower half of the Merensky pyroxenite has slightly lower values than the underlying anorthosite. Such a decrease has not been reported before. The upper half of the Merensky pyroxenite shows a slight increase, but still comparable to Critical Zone values and the underlying anorthosite. One higher value of 0.7068 occurs in the middle of the pyroxenite. The lowest two samples in the spotted anorthosite display a slight decrease with the next two showing a slight increase. These are all within the range of typical Critical Zone values.

A break from 0.7063 to 0.7066 occurs in the Merensky anorthosite, above the Merensky pyroxenite and this is followed by increasing initial $^{87}Sr/^{86}Sr$ ratios in the Bastard Unit. The initial $^{87}Sr/^{86}Sr$ ratios in the Bastard Unit are characteristic of Main Zone values. This unit typically has much more elevated initial $^{87}Sr/^{86}Sr$ ratios that reach a maximum of 0.70763. A notable decrease occurs in one sample in the middle of the Bastard pyroxenite. Ratios increase into the middle of the overlying Bastard norite. A decline above the middle of the norite is typified by ratios decreasing from

0.70760 to 0.70723. Another increase is noted toward the top of the Bastard norite, reaching an elevated ratio of 0.70763.

CHAPTER SEVEN

DISCUSSION

7.1 Introduction

The Merensky Unit studied in detail by Wagner (1929) and Vermaak (1976) is one distinctive cyclic unit of the Rustenburg Layered Suite. Although workers such as Schmidt (1952) and Cousins (1969) have shown that the Merensky Cyclic Unit has remarkable consistency in its mineralogical, chemical and stratigraphic relationships on a regional scale of the Bushveld Complex, the Merensky Unit varies in thickness, mineralization and lithology at Lonplats' Mines. The whole package of the Merensky Unit at Lonplats' Mines ranges in thickness from 7 m to 16 m; a thickness that is less than the thickness that Eales and Reynolds (1986) reported for the Merensky Unit (20 to 25 m) in the north-western section of the Bushveld Complex.

Lateral variations in the Merensky Unit and especially in the Merensky Reef have made it possible to establish a categorization developed by Wager (1929) and extended by Viljoen (1994, 1999) into reef types or facies of normal and potholed reef. One of the major reef facies Viljoen (1999) described is the Rustenburg facies that is in turn composed of four subfacies; the narrow, pegmatitic, highly potholed high-grade reef and the non-pegmatitic wide reef type. The Merensky Unit at Lonplats' Mines is mostly covered by the Rustenburg facies and is represented by

four reef types that are given slightly different names by Lonplats' geologists. The narrow reef is termed the Thin reef type, pegmatitic is celled the Brakspruit reef type and wide non-pegmatitic reefs are labelled the Westplats and Marikana reef types (see Chapter 2). These reef types are evidence of variation in the Merensky Unit.

7.2 Merensky pyroxenite

In many accounts, the Merensky pyroxenite is regarded as synonymous to the Merensky Reef. The Merensky Reef is that portion of the Merensky pyroxenite that is economic with appreciable quantities of PGE (Vermaak 1976). In several places of the Bushveld Complex, the Merensky Reef comprises most of the Merensky pyroxenite especially where the pyroxenite is thin such as in the Rustenburg Platinum Mine. Cousins (1964) described the mafic economic horizon at Rustenburg as a platinum-bearing pegmatitic layer below the porphyritic pyroxenite, where the porphyritic pyroxenite was regarded as the Merensky pyroxenite. At the Western Platinum Mine, Brynard et al. (1976) described the Merensky pyroxenite as a porphyritic melanorite that is platinum-bearing in proximity of the upper chromitite layer. The Merensky pyroxenite (and reef) is usually described as an orthocumulate that is composed of 70-90% euhedral and coarse grains of orthopyroxene and up to 30% of interstitial plagioclase (Lee, 1996). Barnes and Maier (2002b) studied the Merensky pyroxenite at Impala Mine and concluded that it is a "pegmatoidal feldspathic pyroxenite" composed of 70-90% orthopyroxene, and 10-30% interstitial

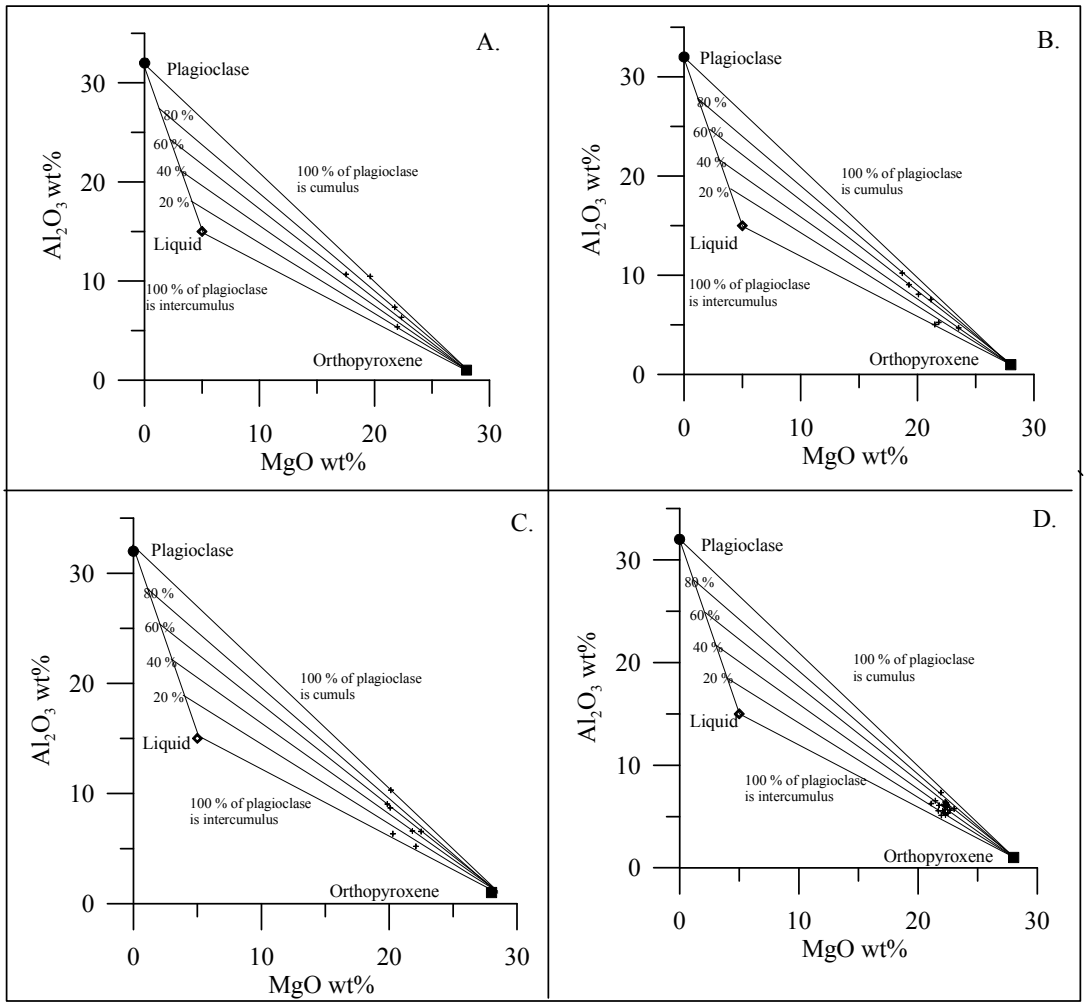

Fig. 7.1. Plots of whole-rock Al_2O_3 versus MgO for samples of the Merensky pyroxenite in a, Thin; b, Braksprui; c, Marikana and d, Westplats reef types. Proportions of cumulus plagioclase are determined in the Merensky pyroxenite. Compositions of plagioclase and orthopyroxene (Boerst, 2001) are also shown. Trapped liquid composition is taken from Li et al. (2001).

plagioclase. However, it has been shown by Seabrook et al. (2005) that the Merensky pyroxenite does not only contain interstitial plagioclase but also cumulus plagioclase. Seabrook et al. (2005) showed that whole-rock analyses of the Merensky pyroxenite rocks do not plot along the orthopyroxene-liquid tie-line, as they would if there was

no cumulus plagioclase. From a diagram similar to Fig. 7.1, Seabrook et al. (2005) showed that it is possible to determine the proportion of cumulus plagioclase in the Merensky pyroxenite and they showed that from 0 to over 80% of the total plagioclase is cumulus.

At Lonplats' Mines, the Merensky pyroxenite contains 70-90% cumulus orthopyroxene and up to 30% of variable proportions of interstitial and cumulus plagioclase. According to Fig. 7.1 shows that 0% to over 80% of plagioclase present in the Merensky pyroxenite is cumulus.

Some recrystallization or annealing can be recognized in the Merensky pyroxenite in the reef types. Where larger grains are present among smaller grains (random size distribution), recrystallization may have occurred, assuming that the larger grains grew by total or partial consumption of adjacent smaller grains (Hunter, 1996). This produced preferential coarsening by secondary growth of cumulus minerals in the selected rocks. 120° triple junctions may have resulted from recrystallization of the grains.

7.3 Major-element chemistry

Orthopyroxene and plagioclase are the important mineral phases that compose the rocks in the Merensky Unit. Whole-rock major element profiles, shown in Chapter 5 depict the distribution of these minerals in the various rock types in the unit. A

combination of accessory minerals such as clinopyroxene, biotite, chromite and apatite are accounted for in rock compositions that plot above the simple mixture lines between orthopyroxene and plagioclase compositions. The major elements; CaO and Al_2O_3 show a strong mutual dependence with MgO for all the reef types (Fig. 5.4 and 5.5). In terms of FeO and TiO_2, MgO-rich samples plot above the line that joins the compositions of plagioclase and orthopyroxene (Fig. 5.1 and 5.2). This displacement in FeO and TiO_2 profiles is a result of the presence of the presence of Fe-Ti oxides (Arndt et al., 2005).

The two trends shown in the K_2O profiles that indicate a negative correlation with MgO and a marked increase of K_2O in the magnesium-rich rocks (Fig. 5.7) are prominent in the Brakspruit, Marikana and Westplats reef types. All samples in the four reef types register K_2O concentrations that are greater than abundances of potassium in both plagioclase and orthopyroxene mineral phases; none of the rocks plot along the simple mixture line joining the minerals compositions. This shows that the reef types are enriched in the K_2O element, especially the pyroxenites.

7.4 Trace-element chemistry

The Merensky pyroxenite is enriched in incompatible trace-elements; Zr, Rb and Y (see figures 7.2 and 7.3), relative to the adjacent rocks unit, including the pegmatite. Wilson et al., (1999) and Arndt et al. (2005) also reported similar observations. Ba is

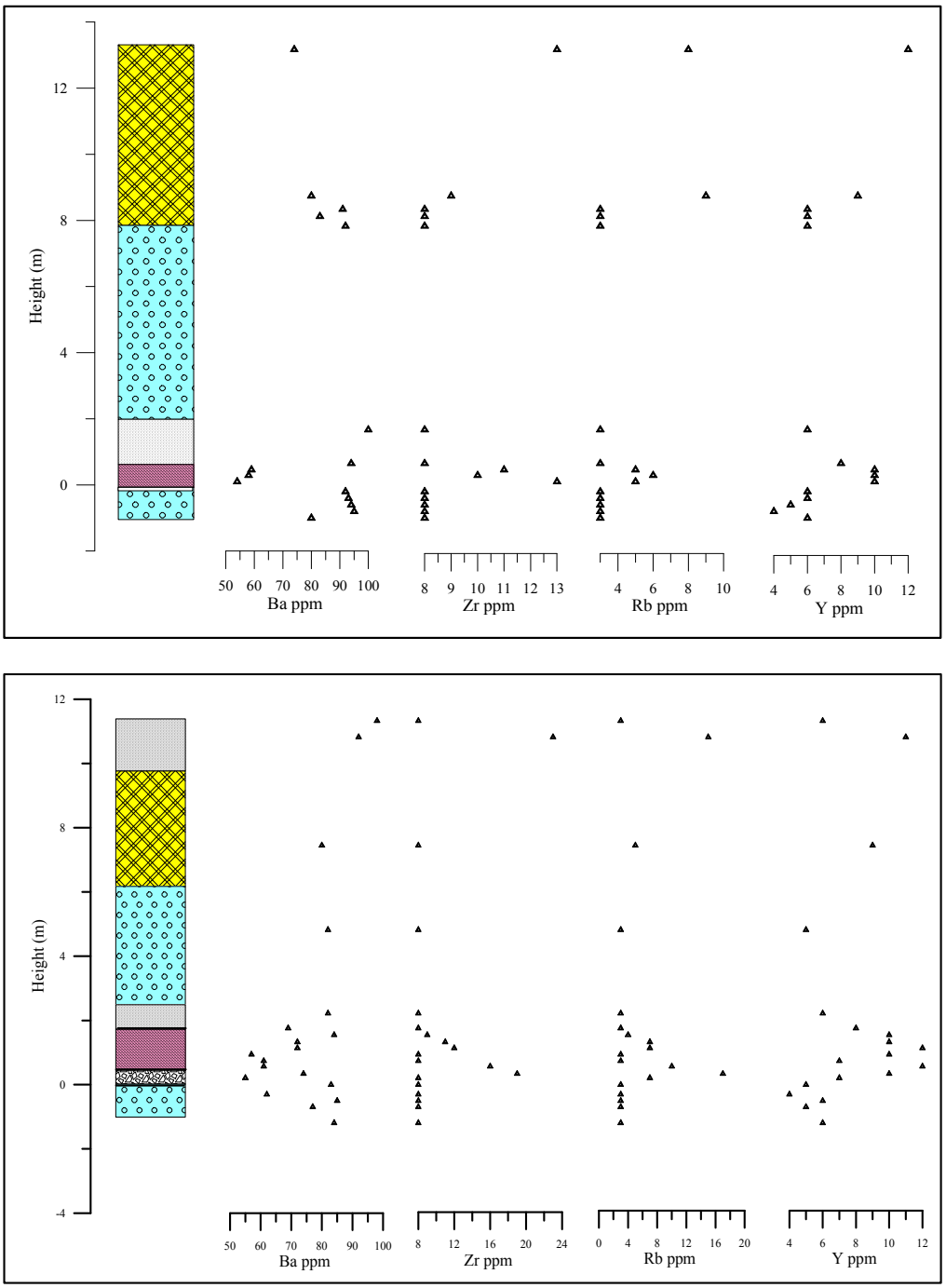

Fig. 7.2 Incompatible trace element data from the Thin (above) and Brakspruit (below) reef types. See Fig. 7.11 for legend for stratigraphy.

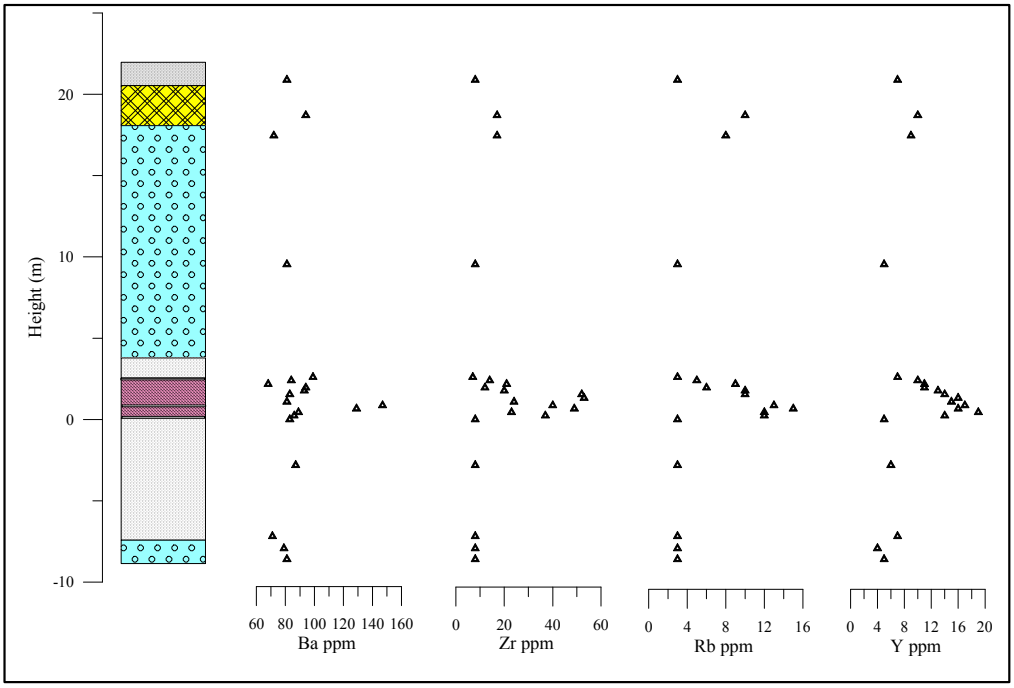

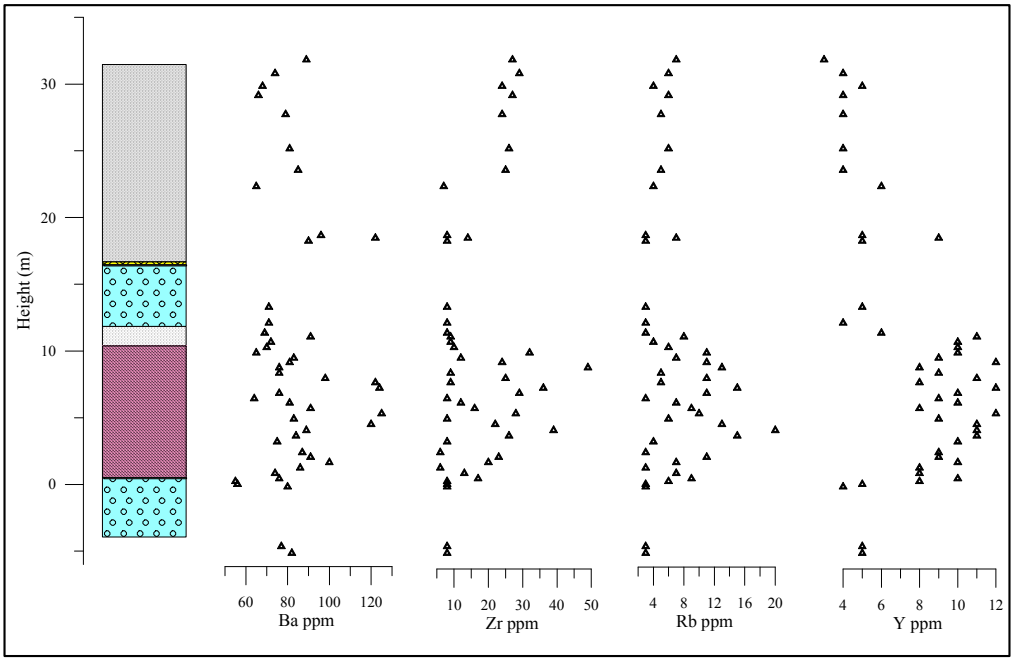

Fig. 7.3. Incompatible trace element data from the Marikana (above) and Westplats (below) reef types. See Fig. 7.11 for legend for stratigraphy.

enriched in the pyroxenite and plagioclase-rich rocks. A plausible explanation of this feature is that a migrating liquid which maintained its ascent until it encountered an anorthositic barrier above the Merensky pyroxenite (Mathez et al., 1997) and was therefore concentrated at the level of the Merensky pyroxenite.

Two trends are demonstrated by these incompatible elements; Y and especially Rb and Zr in the four reef types at Lonplats' Mines (see figures 5.7 to 5.12). There is a wide variation in the concentrations of trace elements in the Merensky Unit. The mafic rocks (excluding the pegmatitic pyroxenite) of Merensky Unit at Lonplats' Mines are relatively high in these incompatibles, a feature which Wilson et al. (1999) and Arndt et al. (2005) also observed for the Rustenburg Platinum Mine. Cawthorn (1996a) showed that these incompatible elements can be concentrated in plagioclase and pyroxene during the crystallization of trapped liquid. It can also be maintained that the reason for enrichment of the above mentioned trace elements therefore resulted from the presence of trapped interstitial melt.

7.5 Trapped interstitial melt in the Merensky pyroxenite

The levels of incompatible trace elements in cumulate successions are not reliable guides to fractionation, as is for fine-grained igneous rocks, because they are controlled by the amount of trapped intercumulus liquid within the adcumulate-mesocumulate-orthocumulate sequence (Henderson, 1975; Cawthorn and McCarthy, 1985). The proportion of the liquid that is trapped during solidification is reflected by

the variation in incompatible trace-element contents of the bulk rocks (Barnes, 1986). Authors such as Cawthorn (1996b), Wilson et al. (1999) and Maier and Barnes (2002) have used variations in concentrations of trace elements to calculate the proportions of trapped liquid. These workers have not only modelled the proportion of the trapped liquid, but have also proposed that the composition of the liquid in the Merensky Reef was uniform. Arndt et al. (2005) argued that isotopic data (e.g. Kruger, 1992) is evidence that the composition of the trapped liquid was rapidly and irregularly changing. They also argued that the liquid that formed the Merensky Reef had a trace-element nature that was different from the liquid that resulted in the adjacent plagioclase-rich rocks, below and above.

Contrasting estimations of trapped liquid contents in the Upper Critical Zone have been proposed by several workers. Wilson et al. (1999) estimated trapped liquid abundances of no more than 10% for the Merensky Reef in the Rustenburg section. Maier and Barnes (2002b) observed a wide range of trapped liquid contents at Impala Mine (3% to 40%) but most rocks contained liquid contents of 5% to 10%. Also for the Rustenburg section, Arndt et al. (2005) estimated liquid contents of no more than 40%. Arndt et al. (2005) also proposed a 9% trapped liquid content for the adjacent noritic rocks.

Trace elements in the Merensky Unit at Lonplats' Mines are also variable in abundances and from these variations the amount of trapped liquid can be estimated. Although possible, it is difficult to estimate precisely the appropriate trapped liquid

abundances. Trapped liquid is modelled using Zr as it is the most incompatible element in this study compared with other trace incompatible elements. The proportion of trapped liquid is modelled by mass balance equation; $C_{wr} = (1-x) \times C_{\min} + (x)C_{liq}$ where C_{wr}, $C_{\min}$ and C_{liq} represent the concentration of the incompatible element in bulk rock, the concentration of incompatible element in crystallizing mineral and concentration of incompatible element in trapped liquid. x is the proportion in trapped liquid.

Zr is incompatible in plagioclase, but fractionates into orthopyroxene to a limited extent and therefore the concentration of Zr in plagioclase is taken as 0 ppm and about 8 ppm in orthopyroxene (Boerst, 2001). For this reason, the cumulus component of pyroxenites, anorthosites and norites are regarded to contain 8 ppm Zr, 0 ppm Zr and about 4 ppm Zr, respectively. Residual liquid concentrations of Zr are taken to be approximately 150 ppm (Cawthorn, 1996b).

Using Zr contents in the equation above, variable proportions of trapped liquid for the different reef types are obtained (Fig. 7.4 and 7.5). The proportions of trapped liquid obtained for the Merensky pyroxenite in the Westplats reef type range from 0% to approximately 28% and the overlying and underlying anorthosite have proportions that average 5%, presupposing that the Zr content is the same for the magma that produced the overlying anorthosite. Noritic rocks in the Westplats reef type contain trapped liquid proportions that range from 14 to 17%. The proportions of trapped

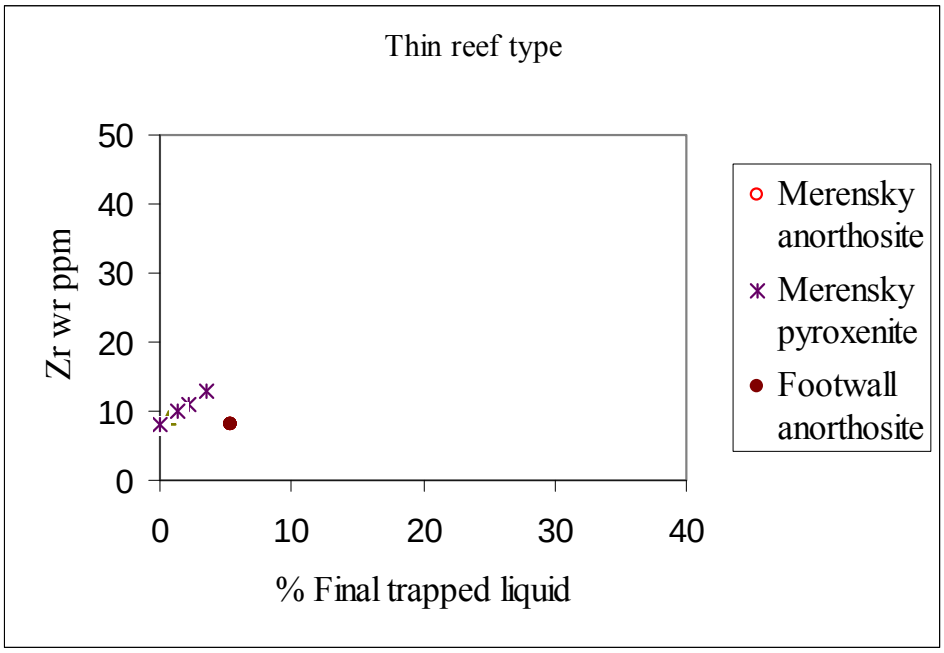

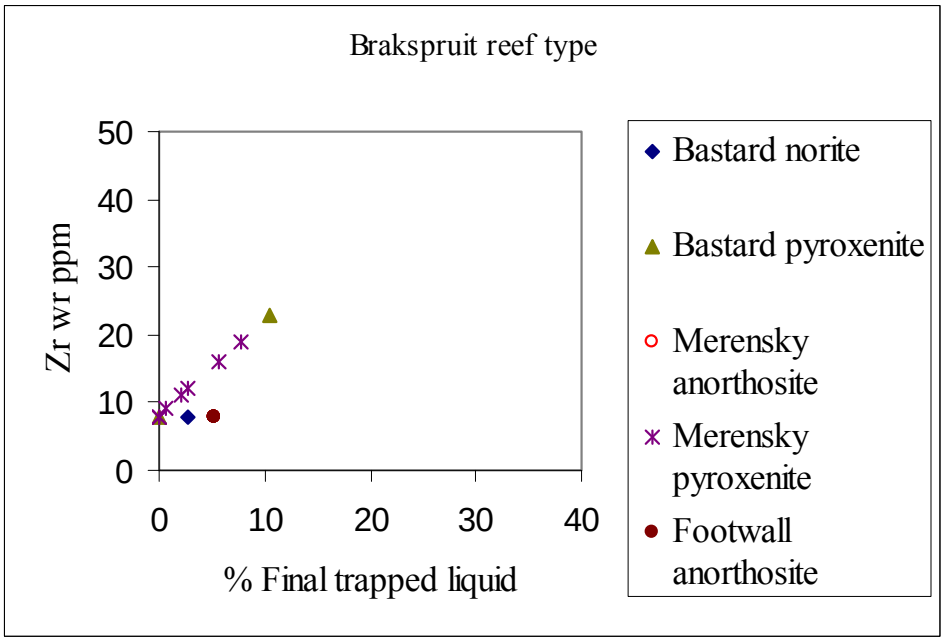

Fig. 7.4 Trapped liquid proportions calculated from Zr for the Thin and Brakspruit reef types. Zr wr represent whole-rock contents in ppm.

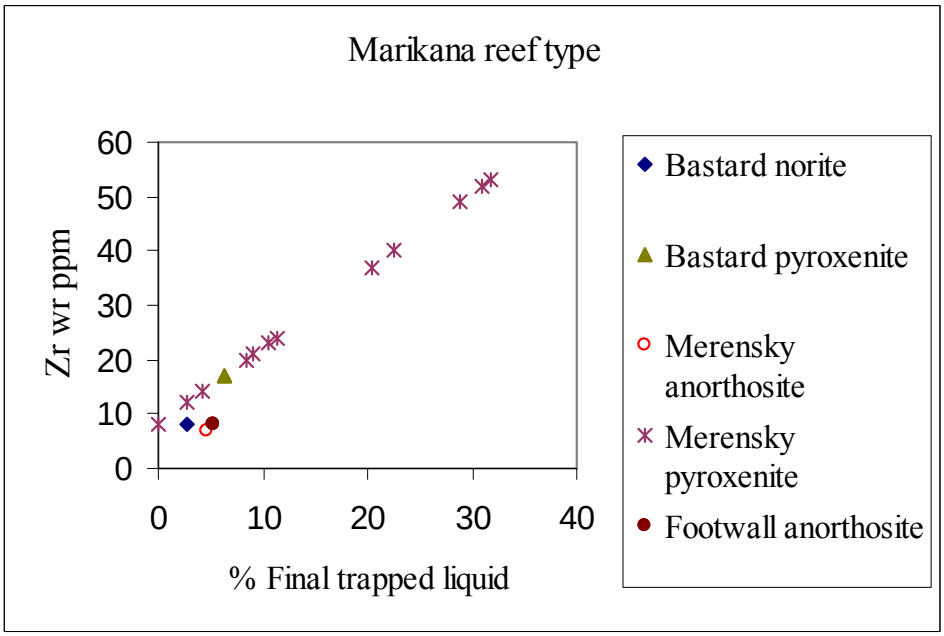

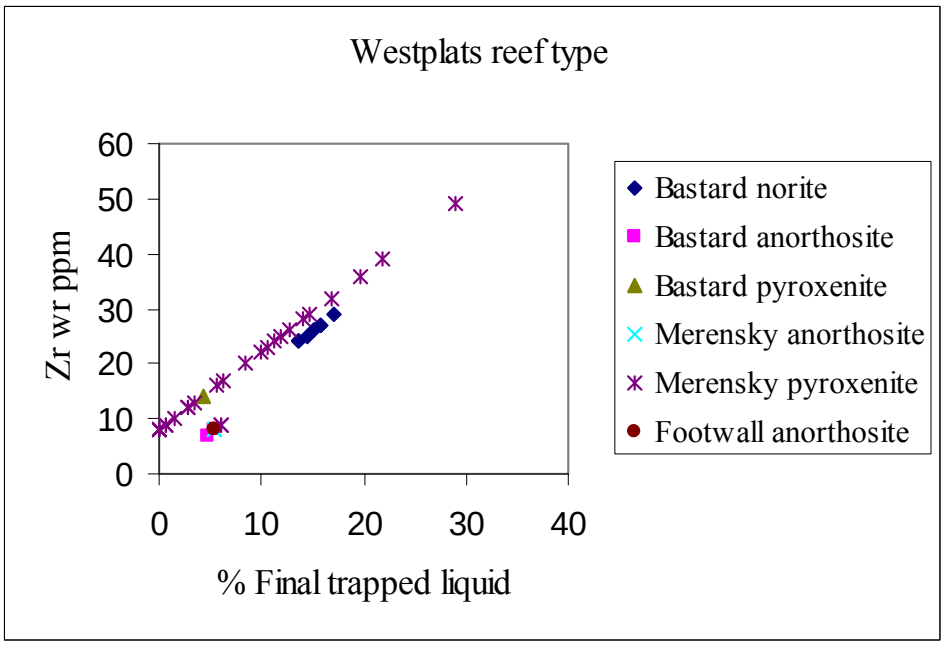

Fig. 7.5 Trapped liquid proportions calculated from Zr for the Marikana and Westplats reef types. Zr wr represent whole-rock contents in ppm.

liquid determined for the Merensky pyroxenite in the Marikana reef type also show a wide range of 0 to 31% and trapped liquid fractions determined for the overlying and underlying anorthosites in this reef type reach a maximum of 5%. The lowest and least variable proportions for trapped liquid in the Merensky pyroxenite are obtained for the Brakspruit and Thin reef types with ranges for 0 to about 8% and a maximum of 4%, respectively.

7.6 Role of trapped melt

Studies performed by several workers such as Wilson (1992), Mathez (1995) and Cawthorn (1996b) have shown that the distribution and abundances of trace elements provides essential information on the role of late fluid phases with moderately and strongly incompatible trace elements. Barnes (1986) suggested that the trapped liquid or as he referred to it; the interstitial melt, reacts with the cumulus phases and thereby alters their compositions or forms completely new phases. Barnes and Campbell (1988) proposed that a high content of interstitial melt was responsible for the formation of the pegmatite associated with the Merensky Reef. Cawthorn and Barry (1992) maintained that the proportion of trapped liquid had no bearing on the formation of the pegmatite as the pegmatite shows a deficiency in incompatible trace elements relative to underlying and overlying rocks. Several studies by workers such as Boerst (2001) and Barnes and Maier (2002a) have shown that the concentrations of incompatible elements in the pegmatitic pyroxenite in the Merensky Unit are less than the amounts in the overlying normal Merensky pyroxenite. Similar observations

are also presented here for Lonplats' Mines (Fig. 7.6). The amount of incompatible trace elements in the pegmatitic pyroxenite that occurs in the Brakspruit reef type at Lonplats' Mines, underlying the Merensky pyroxenite is less than that in the Merensky pyroxenite itself (Fig. 7.6). It therefore follows that the amount of trapped liquid in the Merensky pyroxenite was more than in the underlying pegmatitic pyroxenite, and so these results do not support the ideas that greater proportions of trapped liquid led to the formation of the pegmatitic pyroxenite. It is concluded that

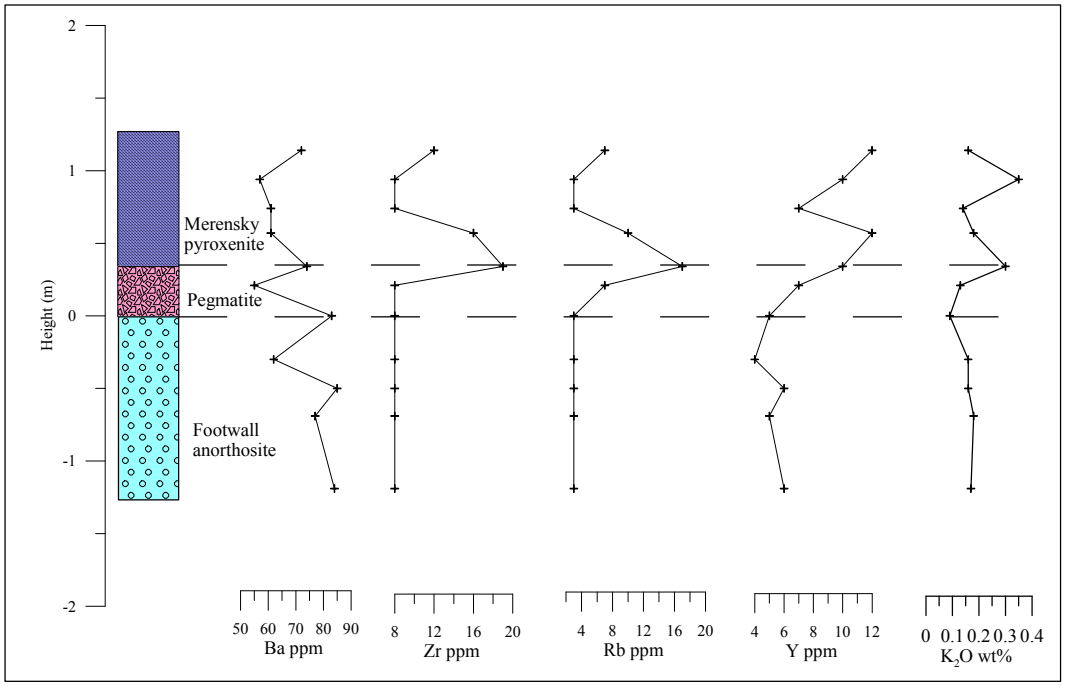

Fig. 7.6. Trace elements in the Merensky pegmatitic pyroxenite in the Brakspruit reef type bounded above and below by the Merensky pyroxenite and the footwall anorthosite respectively.

the formation of the pegmatitic pyroxenite is a result of reconstitution of a pre-existing pyroxenite at the crystal-magma interface (Cawthorn and Barry, 1992;

Viljoen 1999; Viring and Cowell, 1999; Boerst, 2001; Cawthorn and Boerst, in press).

7.7 Ni: Cu: S ratios

The chalcophile nature of Cu and S makes it plausible to assume that all of the Cu and S in whole-rock analyses are concentrated in sulphides. Ni is compatible in sulphide, pyroxene and olivine and thus makes it necessary to compute the amount of Ni concentrated in these phases before estimating its content in sulphides. Olivine is not a common mineral in the sections from the Lonplats' Mines and thus its contribution toward Ni is insignificant. Rocks that plot above the simple extrapolated tie-line between plagioclase and orthopyroxene (Fig. 5.19) are therefore regarded as sulphide-bearing. Pyroxenites at Impala with only pyroxene and plagioclase and with no sulphides have a Ni to MgO ratio of 23 (Cawthorn, 1999a). At Lonplats' Mines, the Ni to MgO ratios differ from those at Impala by small factors. However, each reef type has a particular ratio. For the Thin reef type the Ni/MgO ratio is an average of 27, Brakspruit of 25, Marikana of 28 and Westplats of 26. These ratios are used to calculate the amount of Ni that is in silicates, which by difference from whole-rock content, gives the amount of Ni in the sulphides.

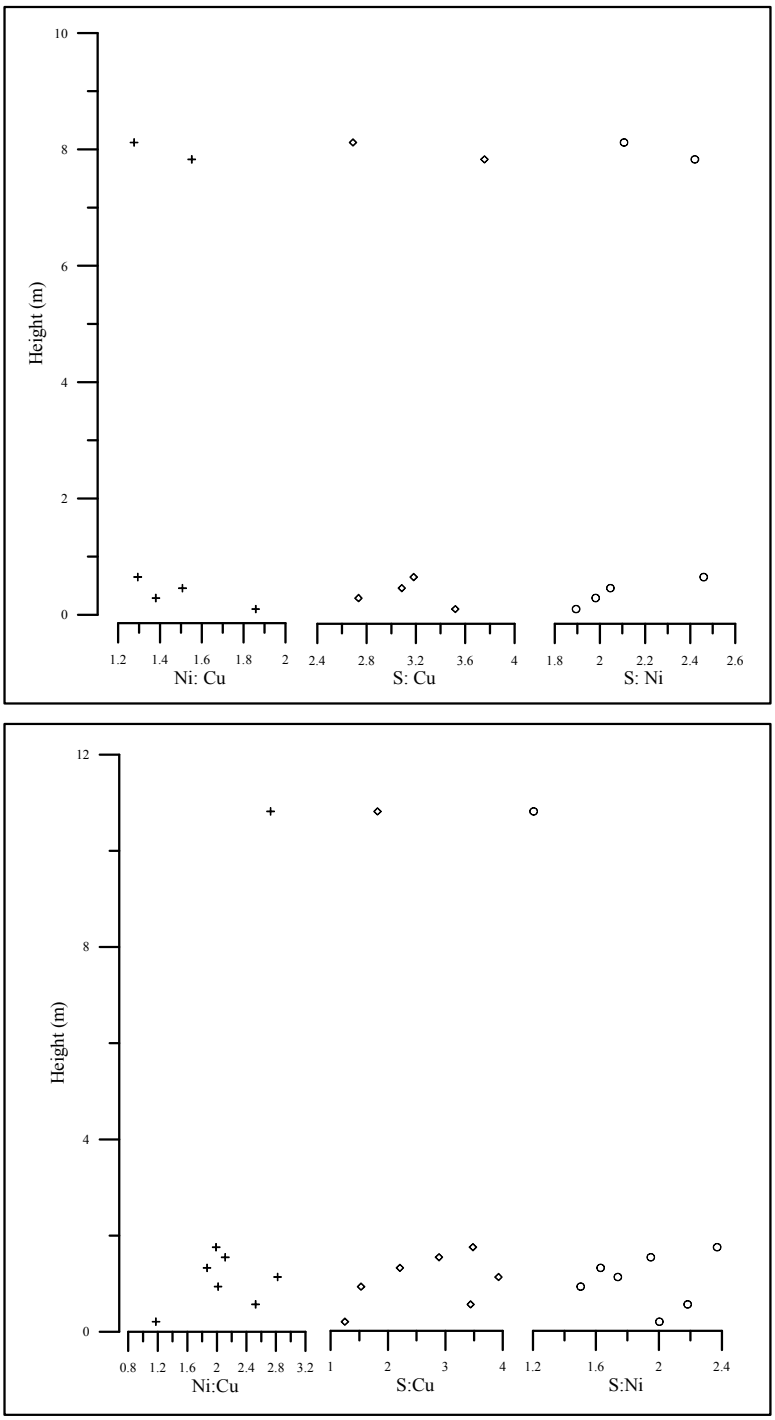

Fig. 7.7 Vertical profiles of Ni: Cu, S: Cu and S: Ni ratios for the Merensky Reef in the Thin (above) and Brakspruit (below) reef types. Only samples with more than 0.1 wt% S are presented here. The base of the Merensky Unit is taken as datum.

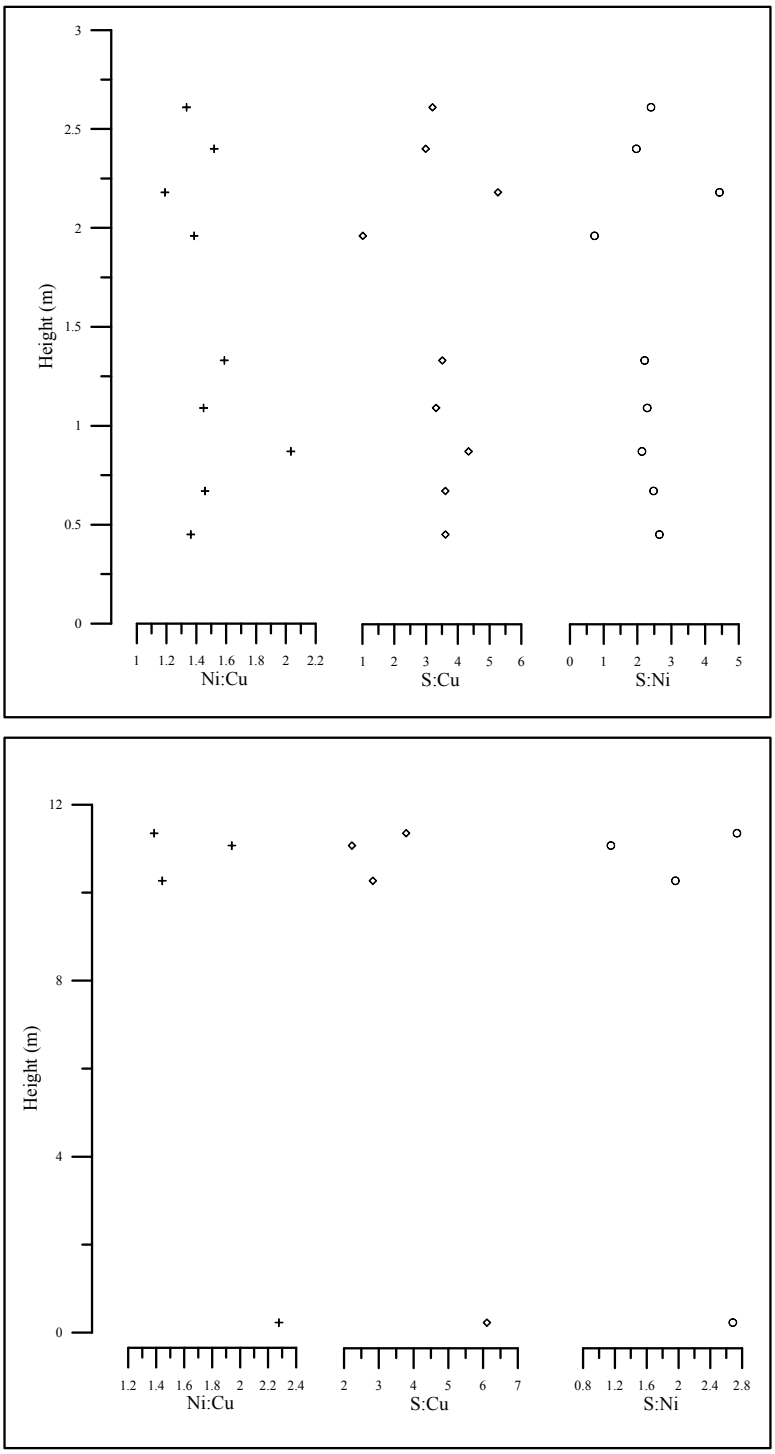

Fig. 7.8 Vertical profiles of Ni: Cu, S: Cu and S: Ni ratios for the Merensky Reef in the Marikana (above) and Westplats (below) reef types. Only samples with more than 0.1 wt% S are presented here. The base of the Merensky Unit is taken as datum.

The amount of Ni (calculated in sulphide), Cu and S present is directly proportional to the quantity in which sulphide minerals occur in rock samples. S, Cu and Ni correlate with one another in the Merensky Unit. The relationship of Ni, Cu and S is represented in Fig. 7.7 and 7.8. This relationship can be translated into ratios. Presented in these figures are the ratios for samples with more than 0.1wt% S, plotted against height. The relationship of Ni: Cu, S: Cu and S: Ni ratios, shows that these ratios are relatively constant. In many cases, an increase in the Ni: Cu ratio is coupled an increase in S: Cu and S: Ni ratios. However, at some levels in the Merensky Reef, an increase in the Ni: Cu ratio is associated with a decrease in the S: Cu and S: Ni ratios (see Fig. 7.7, Thin reef type) and (Fig.7.8, Westplats reef type). Although the inverse proportionality of the already discussed ratios is not common, it may indicate important process that might have taken place resulting in this variation.

The compositions of the sulphides at Lonplats' Mines are different from the compositions of a typical Merensky Reef immiscible sulphide liquid suggested by Naldrett (1981, 1989) and Cawthorn (1999a) (see Fig. 7.9). In Chapter 5 (Fig. 5.29 to Fig. 5.31), Ni: Cu, S: Cu and Ni: Cu ratios from the different reef types are presented. Best fit lines in each graph represent the average ratios for each reef type. Ni: Cu ratios at Lonplats' Mines reach a maximum of 1.8, the largest ratio being evident in the sulphides from Westplats reef type. The S: Ni ratios that are observed for the reef types at Lonplats' Mines reach a maximum of 2: 1. The Brakspruit and the Thin reef types are evident of sulphides that have S: Ni ratios of 1.7: 1 and 1.9: 1 correspondingly. The S: Cu ratios are in the range of 2.2 to 3.6. The Marikana and the

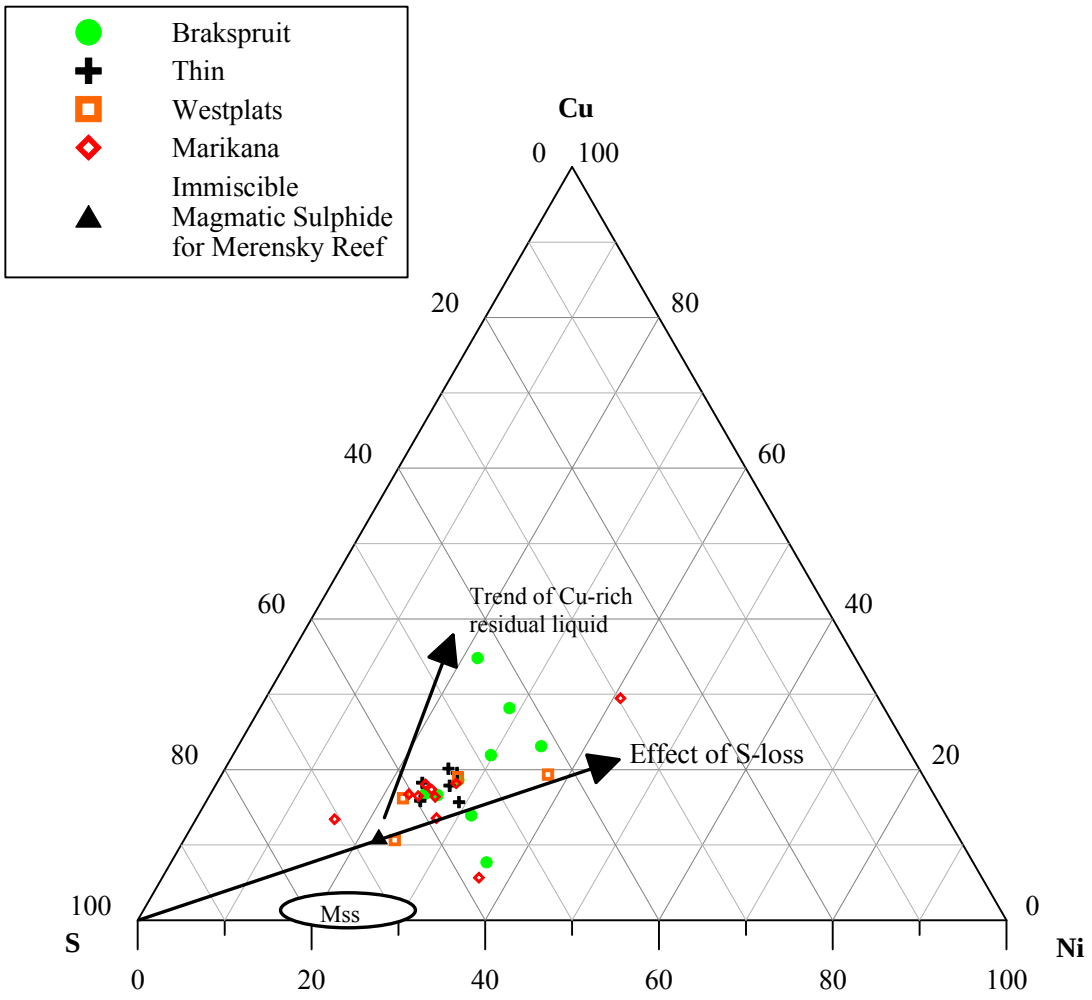

Fig. 7.9 A ternary diagram showing Cu, Ni and S relationships in the sulphide-bearing rocks of the four reef types. Only samples with more than 0.1 wt% S are plotted. Filled triangle represents proposed immiscible magmatic sulphide in the Merensky Reef from Naldrett (1989). Composition of Mss is also shown.

Westplats reef types have the highest and the lowest ratios with values of 3.6 and 2.2, respectively. According to the study at Lonplats' Mines that has been presented here, average Ni: Cu: S ratios in sulphides of the Thin, Brakspruit, Marikana and Westplats are 1.7: 1: 3.2, 1.4: 1: 2.4, 1.7: 1: 3.6 and 1.8: 1: 2.2, respectively. Only slight differences are observed in these ratios from Lonplats' Mines.

Three possible processes are explored here to explain these variations.

1. A possibility to explain the data at Lonplats' Mines is that a Cu-rich residual sulphide liquid would form consequently to fractional crystallization of the first sulphide; supposedly Mss (monosulphide solid-solution which exsolves into pyrrhotite polymorph). The residual liquid would then develop toward the Cu direction and the formed sulphide would have a composition that is S-rich, Cu-deficient and have very little Ni and would therefore plot in the field shown in Fig. 7.9. The data at Lonplats' Mines do not support the possibility of there being Mss that fractionated to produce a Cu-rich residual liquid simply because there are no samples here that are evident of the compositions of Mss, or of the evolving sulphide liquid.

2. The trend of the ratios of sulphides at Lonplats' Mines moves away from the immiscible sulphide liquid with the ratio 2: 1: 6; in the Cu-Ni direction. The data show a range of compositions of the sulphide assemblages and most samples in the Brakspruit reef type are rich in Cu-rich compared to the immiscible magmatic sulphide composition proposed by Naldrett (1989) and Cawthorn (1999a), as well as the samples in the other reef types. This may have been a result of S leaving the sulphide phases and thereby causing it to be S-poor (Barnes and Maier, 2002b) due to the breakdown of pyrrhotite, or addition of Cu and Ni. During this breakdown, the iron would have been distributed into orthopyroxene and magnetite. Intergrowths of magnetite and sulphides shown in Fig. 4.8c support the process of loss of S. However, if there was S-loss or addition of Cu and Ni to the sulphide-silicate magma

at Lonplats' Mines, the trend of the ratios of sulphides at Lonplats' Mines would have been toward the S-poor trend indicated in Fig. 7.9. However, the Ni: Cu: S data at Lonplats' Mines show that there are no samples that could indicate the process of S-loss.

3. The model by Boudreau et al. (1986) would have envisaged that the Cu and the Ni were introduced by the migrating hydrothermal fluids. The hydrothermal fluids in this case are thought to have caused alteration to the original sulphide composition and thereby distribute the Cu and Ni and possibly S. This would explain the Ni: Cu: S data at Lonplats' Mines.

7.8 Chromitite layers

Cr-Spinels in terrestrial rocks show a wide range of compositions due to a range of igneous processes (Barnes and Roeder, 2001). The composition of chromite is sensitive to the environment in which it forms (Irvine, 1965). It particular, the composition of the parent magma is a major contributing factor (Roeder and Reynolds, 1991). Other contributing factors that influence the composition of chromite are the temperature, oxygen fugacity and pressure (Roeder and Reynolds, 1991). The object of the presentation of these facts is not to elaborate more on them as they are beyond the scope of this project, but it is to appreciate their influence.

Accessory chromites are known to be different in chemistry from layered chromites because their chance of reacting with late stage fluids is greater (Eales and Reynolds, 1986). The high proportion of chromite in a layer buffers the amount of change that can occur. It must also be emphasized that the chromite grains that were analyzed from Lonplats' Mines are not inclusions in cumulus silicate minerals and therefore discussions of reactions with different host (Roeder and Campbell, 1985) are not relevant here.

There are no disseminated chromites that were analyzed for this work, only layered chromites were studied. The eight sections of chromitite layers analysed in the Merensky Unit at Lonplats' Mines are varied in their chemistry. The chromitite layers have characteristic Mg# and Cr# and may also have different sets of Ti, Al, Cr, Mg, and Fe cations, although overlaps exist. The differences or similarities in these chromitite layers can be used to correlate them, which is the focus of the study of the chromites in the Merensky Unit at Lonplats' Mines. Each chromitite layer is assigned into a suitable group.

At Lonplats' Mines, several chromite grains have different compositions from the rest of the population (e.g. some chromites in the Marikana chromitite layers are Ti-rich relative to other chromite from other layers in this study). These chromites are part of the semi-massive spinel layers. This shows that the variation in the compositions of the chromite grains is not dependent on whether the chromites are disseminated on the edges of layers or not. The populations of chromite grains analysed for this work

indicate an evolutionary trend of slight Ti-enrichment (Fig. 6.10). The chromite grains with distinctly different compositions are the most evolved. A number of the spinels in the Merensky Unit at Lonplats' Mines are titaniferous chromites.

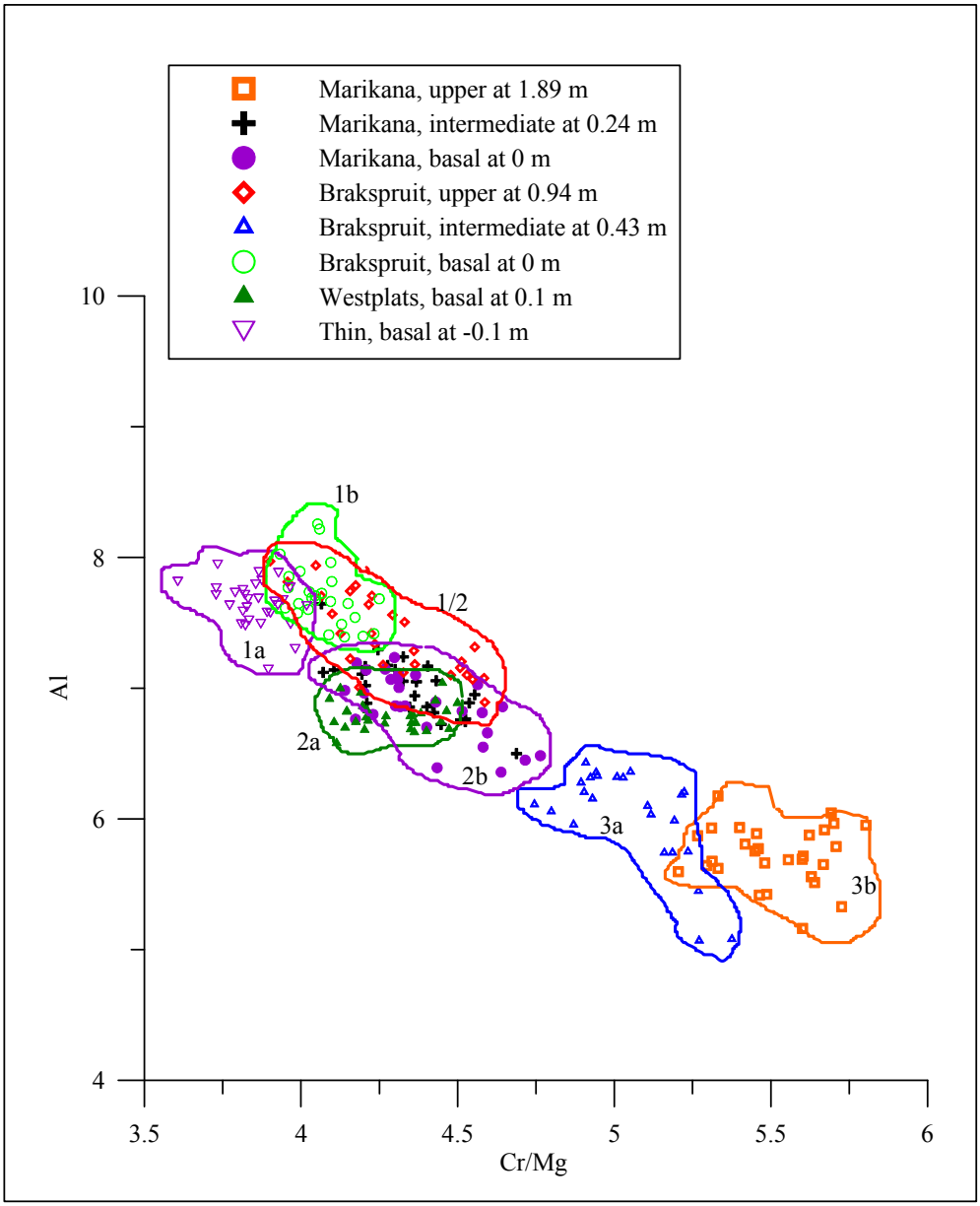

Fig. 7.10 Comparison of Al, Cr and Mg cations for chromitite layers in the different reef types. Groups into which the layers are classified are shown here.

The chromitite layers can be correlated. The groups into which the chromitite layers are classified have subgroups (Fig. 6.6 and Table 5.1). The basal chromitites of the Thin and Brakspruit reef types are classified as type 1a and type 1b respectively. The chromites from these reef types are Al-rich compared to other chromites and types 1a have higher Mg# compared to type 1b (Fig. 6.6). The basal layers in the Westplats and Marikana reef types are type 2a and type 2b chromitites respectively. Hence, the compositions suggest that the basal chromitite should not be considered as a simple homogenous layer. The intermediate layer of the Marikana reef type has chromites that can be classified as type 2b. The intermediate Brakspruit chromites and the upper Marikana chromitites are classified as type 3a and type 3b respectively. The upper chromitite layer in the Brakspruit reef type has affinities of both type 1 and type 2 (see Fig. 7.10).

Figure 7.11 illustrates possible correlations between the chromitite layers in the Merensky Unit at Lonplats' Mines. The relationship of the basal chromitite layers of type 1 (Thin and Brakspruit reef types) and type 2 (Marikana and Westplats reef types) is not necessarily clear. The upper chromitite layers of the Brakspruit and Marikana reef types are clearly different. According to the data presented, the upper Brakspruit chromitite layer is shown to have similarities with all basal chromite layers in the four reef types and also similar to the intermediate chromitite layer of the Marikana reef type. The intermediate layer in the Brakspruit reef type is similar in chemistry to the upper chromitite layer in the Marikana reef type. These observations

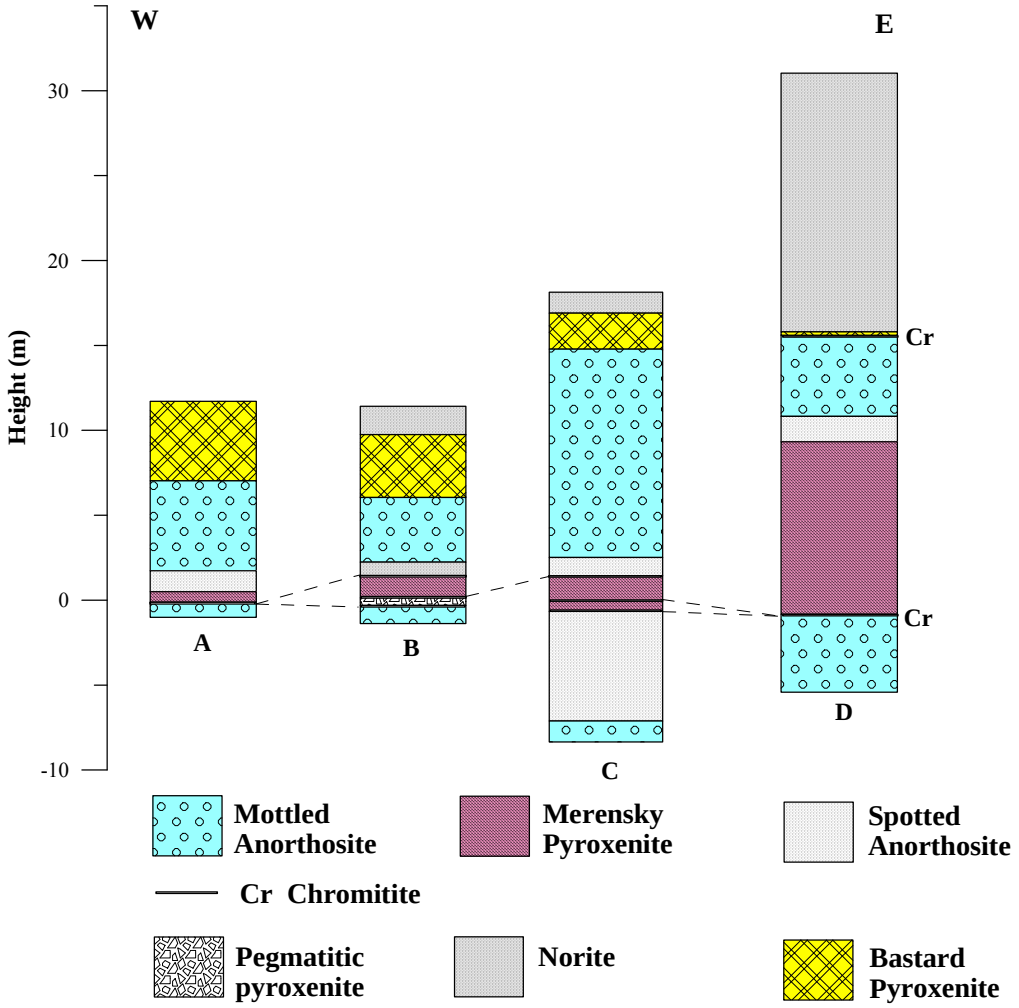

Fig. 7.11. Possible relations between chromitite layers in the Merensky Unit at Lonplats' Mines in the Thin (A), Brakspruit (B), Marikana (C) and Westplats (D) reef types.

show that chromitite layers cannot be correlated simply based on stratigraphic position. Two different sequences of events may be considered to explain these observations.

1. Chromite groups of similar compositions may perhaps plausibly be formed from similar liquids. In instances where the chromitite layers are not correlatable, resorption and erosion by a hot magma (Irvine et al., 1983) and by superheated liquids (Eales et al., 1988) may have occurred. The sequence of deposition of the chromitite layers may have occurred in the fashion explained below (Fig. 7.11 and 7.12). One possibility is that after the accumulation of the mottled and spotted anorthositic footwall the first chromitite layer was precipitated, possibly by way of a pressure change in the chamber (Cawthorn, 2005b), and is preserved as the basal chromitite layer in the Marikana and Westplats reef type. The spotted anorthosite and the first chromitite layer may have been eroded from the Thin and Brakspruit reef types. A second chromitite layer was deposited on the anorthosite at Brakspruit and Thin reef types, but on the Merensky pyroxenite at the Marikana and Westplats reef types. The second layer may have been subsequently eroded in the Westplats reef type. The compositions of the intermediate and basal chromitite layers in the Marikana reef type are the similar and this, so since they cannot be correlated, it is assumed that similar compositions can be produced by successive magmas (Fig. 6.6 and 7.12C). The Merensky pyroxenite continued to be deposited after the second chromitite deposition. After a portion of the Merensky pyroxenite had accumulated, a third chromitite layer was precipitated. This layer is typified by the intermediate and upper chromitite layer of the Brakspruit and Marikana reef types respectively. The second and third chromitite layers are absent in the Thin and Westplats reef types possibly due to magmatic erosion. After this episode of erosion, more of the Merensky pyroxenite was accumulated hence the presence of the pyroxenite above

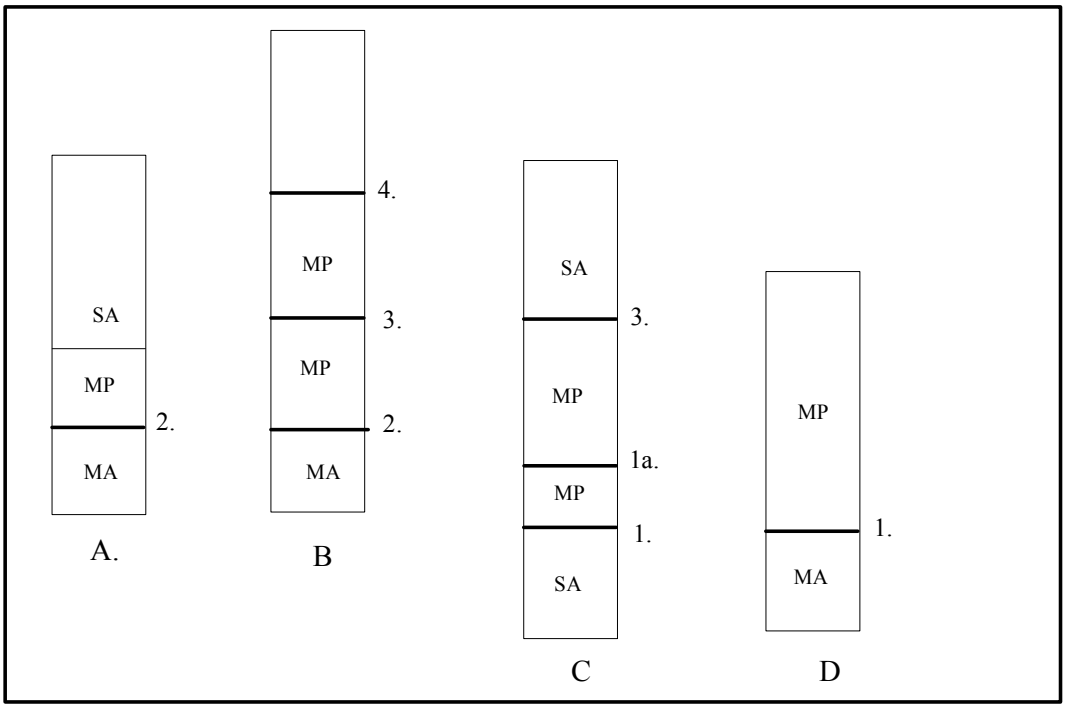

Fig. 7.12 Sequence of chromitite deposition in the four reef types. Thin (A), Brakspruit (B), Marikana (C) and Westplats (D) reef types are represented. The diagram is not to scale. Lithologies are also shown; Spotted anorthosite (SA), mottled anorthosite (MA), and Merensky pyroxenite (MP).

the basal chromitites in these two reef types. A fourth and most probably final chromite deposition event in the Merensky Unit at Lonplats' Mines, that is marked by the upper chromitite layer in the Brakspruit reef type occurs. This fourth layer is not evident in the other three reef types and its absence can again be explained by the erosional periods that may have occurred.

2. The previous possibility discussed above assumed that the chromitite layers form everywhere and then were eroded, leaving the current sections of the chromitite

layers. Another possibility for the discontinuity of the chromitite layers in the Merensky Unit may be that the layers do not originally form continuously. The chromitite layers in the different reef types may have formed in separate depressions that were separated by the Spruitfontein inlier. This inlier had a profound effect on the continuity and distribution of the rocks of the Rustenburg Layered Suite (Clarke et al., 2000). There might have been compartmentalization of the chamber such that the sub-chambers lie to the west and east of the Spruitfontein inlier, as Hatton and von Gruenewaldt (1985) and Davey (1992) proposed. It may have followed that the sub-chambers were subjected to different times of chromite precipitation or different compositions of chromite forming simultaneously, hence the different levels and compositions of the chromitite layers in the four reef types in the Merensky Unit.

7.9 Initial $^{87}Sr/^{86}Sr$ ratios

Pure plagioclase separates have been used to determine Sr contents and Sr isotope initial ratios (initial $^{87}Sr/^{86}Sr$). Profiles produced from these ratios are used to locate levels of new magma influxes in magmatic sequences (Kruger and Marsh, 1982). In their study, Kruger and Marsh (1985) suggested that the Merensky pyroxenite and its corresponding underlying pegmatitic pyroxenite contain interstitial plagioclase with higher Sr contents relative to cumulus plagioclase in the Merensky anorthosites. Bearing in mind the major problems in the analyses obtained from the three different laboratories, it is not possible to discuss with confidence the Sr concentrations in samples from Lonplats' Mines.

Initial $^{87}Sr/^{86}Sr$ ratios of the layered mafic Bushveld Complex are variable with highly radiogenic signatures of up to 0.709 in the Main Zone (Hamilton, 1977; Kruger and Marsh, 1982; Sharpe, 1985). Several Sr isotope vertical profiles for various sections from the footwall anorthosite through to the Bastard Unit also demonstrate this variation. Vertically, the initial $^{87}Sr/^{86}Sr$ ratios at the Union Mine increase and reach a maximum at the top of the Merensky Unit (Eales et al., 1986). Initial $^{87}Sr/^{86}Sr$ ratios increase in an oscillatory manner in the Merensky Unit at the Rustenburg Platinum Mine (Kruger and Marsh, 1982). Lee and Butcher (1990) also observed a rapid increase in the initial $^{87}Sr/^{86}Sr$ ratios from the Merensky pyroxenite to the top of the Merensky Unit at the Atok Mine in the Eastern Bushveld Complex. Amandelbult Mine is also characteristic of initial $^{87}Sr/^{86}Sr$ ratios with a marked raise at the base of the Merensky Unit (Kruger, 1992). A marked increase in initial $^{87}Sr/^{86}Sr$ ratios is also observed in the normal Merensky sequence at the Brakspruit reef type of Western Platinum Mine (Carr et al., 1999). Vertical isotopic profiles of the above-mentioned mines are shown in Figure 7.14. All the above-mentioned sections in the Bushveld Complex show an overall upward trending increase of the initial $^{87}Sr/^{86}Sr$ ratios. Seabrook et al. (2005) have shown that this trend is also followed at the Richmond farm, eastern Bushveld Complex but the increase begins higher up in the Merensky Unit.

A prominent facet of the different zones of the Bushveld Complex is their characteristic variation in the initial $^{87}Sr/^{86}Sr$ ratios (Hamilton, 1977). Several workers such and Hamilton (1977), Kruger and Marsh (1985) as well as Kruger

(1992, 1994) have attributed this fact to repeated emplacements of magma most notably in the Merensky Unit. It should be borne in mind that Kruger (1992, 1994) conducted isotope studies at the Rustenburg Platinum Mine where the Merensky Reef occupies most of the thin Merensky pyroxenite which is situated at the base of the Merensky Unit, and therefore at this locality, the Merensky Reef marks the base of the Merensky Unit. This is not observed at Lonplats' Eastern Platinum Mine; the Merensky Reef is not located at the base of the Merensky Unit.

A vertical profile of initial $^{87}Sr/^{86}Sr$ ratios produced for the Westplats reef type (thick reef type) at the Eastern Platinum Mine (Fig. 6.13), where the existence of an 11-m thick Merensky pyroxenite allows for detailed study, shows a marked oscillatory increase in initial $^{87}Sr/^{86}Sr$ ratios, with increasing height. There are at least six isotopic shifts in the Eastern Platinum Mine isotopic profile. Three minor (one at the base; 0.7064 to 0.7062 of the unit and two; 0.706 to 0.70679 and 0.706 to 0.7064, within the Merensky pyroxenite) isotopic shifts in the Merensky Unit indicate that there were small influxes of magma and that these inputs of magma were influxes of Critical Zone magma. An isotopic break from 0.7063 to7066 in the Merensky Unit that is located 2 m above the Merensky pyroxenite is evidence of an influx of magma with Merensky initial $^{87}Sr/^{86}Sr$ signature (see Fig. 7.13). Two abrupt isotopic shifts also occur in the Bastard Unit (0.7071 to 0.7066 and 0.7072 to 0.7076); at the second sample above the base of the Bastard pyroxenite and within its overlying norite. These two shifts show that magma influxes had different signatures. The shift with lower initial $^{87}Sr/^{86}Sr$ ratios indicates Critical Zone influx and the shift with higher

initial $^{87}Sr/^{86}Sr$ ratios in the Bastard pyroxenite show Main Zone isotopic signatures. The chromitite layers at the base of the Merensky and Bastard are coincident with isotopic breaks and therefore also associated with magma influxes. However, the other isotopic breaks in the Merensky Unit are not associated with chromitites.

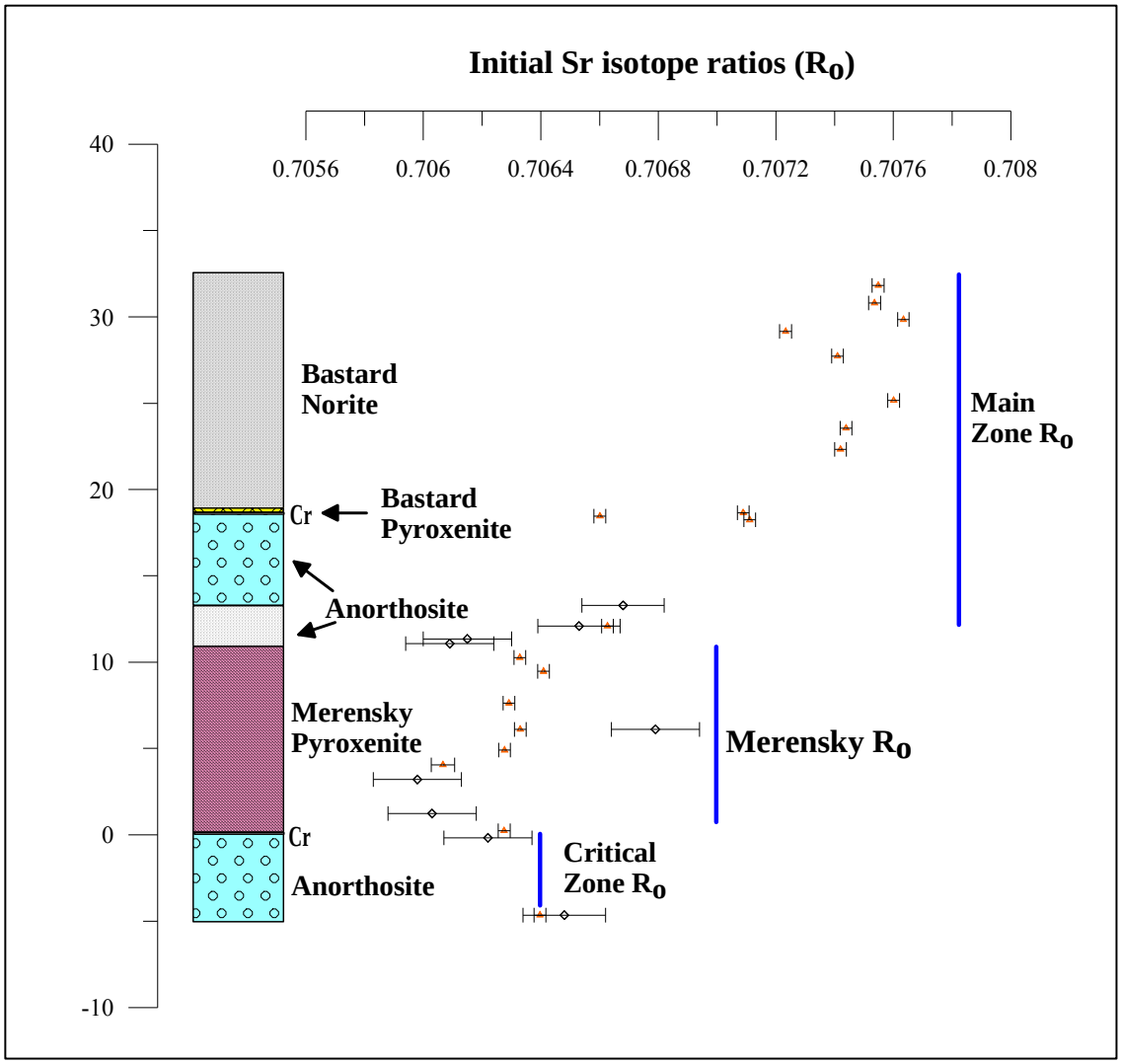

Fig. 7.13 Sr-isotopic data from the Eastern Platinum Mine. Vertical solid lines represent the isotopic ratios produced by Kruger and Marsh (1982).

The relatively consistent isotopic break at the level of the Merensky Reef elsewhere in the Bushveld Complex has been used to suggest that new magma influx (e.g. Kruger, 1994) and mixing (Campbell et al. 1983) occurred at this level and that this had a bearing to the mineralization in the complex. The most prominent isotopic shift occurs directly above the Merensky Reef at the Eastern Platinum Mine and not specifically at the Merensky Reef level. It is probable that magma addition occurred at the level above the Merensky Reef and at other levels where isotopic shifts were observed but their relationship to PGE mineralization is not clear.

Fig. 7.14 A summary of initial $^{87}Sr/^{86}Sr$ profiles through the Merensky Unit from the Western Platinum Mine and other PGE mining centres around the Bushveld Complex (after Eales et al., 1986; Kruger and Marsh, 1982; Lee and Butcher, 1990; Kruger, 1992; Carr et al., 1999).

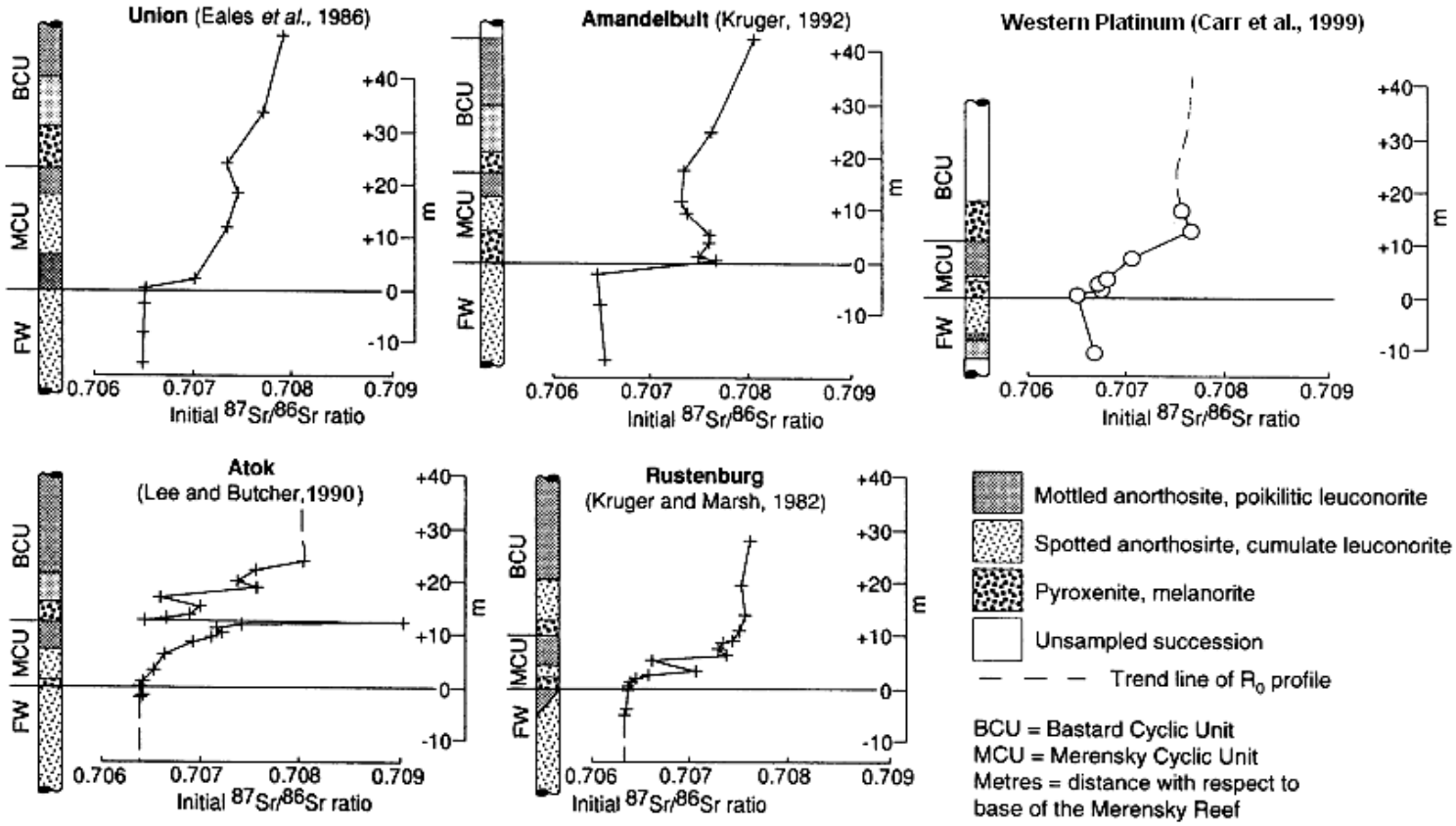

7.10 Sulphide mineralization

The sulphur concentrations in the Critical Zone rocks are as low as 0.01% (Maier and Barnes, 1999). It is only in the Merensky Reef where sulphur values reach 1% (Lee, 1996). Wilson et al. (1999) have reported maximum sulphur contents of 2 % in the Rustenburg section. At Lonplats' Mines, sulphur abundances in the Merensky Reef average 0.3 % and can reach a maximum of 0.8%. Nonetheless, these values indicate the amount of sulphide minerals there is in the rocks of the Critical Zone and also show how low the Bushveld Complex is in terms of sulphur contents. Sulphur contents have been used as a guide to indicate the levels of saturation of the sulphide liquid in a silicate magma and whether saturation was maintained or not. Early theories (e.g. Naldrett and von Gruenewaldt, 1989) about sulphide saturation maintained that sulphide liquid continued to separate at saturation. In contrast, the low sulphur contents are not consistent with the continued sulphide saturation (Cawthorn, 2005a).

Theories regarding the formation of an immiscible sulphide liquid have been a major focus of research in the Bushveld Complex. The early sulphide genesis models that have been in the scientific literature for a length of time were introduced by workers such as Campbell et al. (1983). Campbell et al. (1983) and Naldrett and von Gruenewaldt (1989) postulated that the effect of magma mixing is pre-requisite to the production of immiscible sulphide liquid. Naldrett and von Gruenewaldt (1989), Naldrett (1989), Li et al. (2001a) and Barnes and Maier (2002a, b) maintained that the

liquid sulphide immiscibility is a consequence of mixing between differentiated residual magma and replenishing parental magma.

The term R-factor has been used to define silicate magma to sulphide ratios. High R-factors cause sulphide globules that resulted from mixing, carried in suspension (Campbell et al., 1983) to be richly concentrated in PGE. The opposite applies for low R-factors (Campbell and Naldrett, 1979). The Merensky Reef was considered as a high R-factor economic horizon and therefore needed an enormous amount of silicate magma in relation to the volume of the sulphide liquid. The Bushveld Complex is quite a large deposit by volume but is it not possible to make an estimation of how much silicate magma existed or even how much sulphide liquid there was in the Bushveld chamber (Cawthorn, 1999a). Cawthorn (1999a) showed that for a 3 cm sulphide concentration in 1 m thick Merensky Reef needing an R-factor of 10^6, there should have been 30 km of sulphide-saturated magma. The present capacity of the Bushveld Complex does not support the existence of 30 km of sulphide-saturated magma. This shows that the use of R-factors in genetic models of immiscible sulphide liquids is questionable and therefore challenges the magma mixing genetic models.

Cawthorn (2002) demonstrated that mixing between the two magmas in the model discussed above does not produce sulphide liquid immiscibility. Further work by Seabrook et al. (2005) established, by way of using data of Cr/MgO ratios and Sr isotope data, that the Main Zone and Critical Zone magmas did not mix. Seabrook et

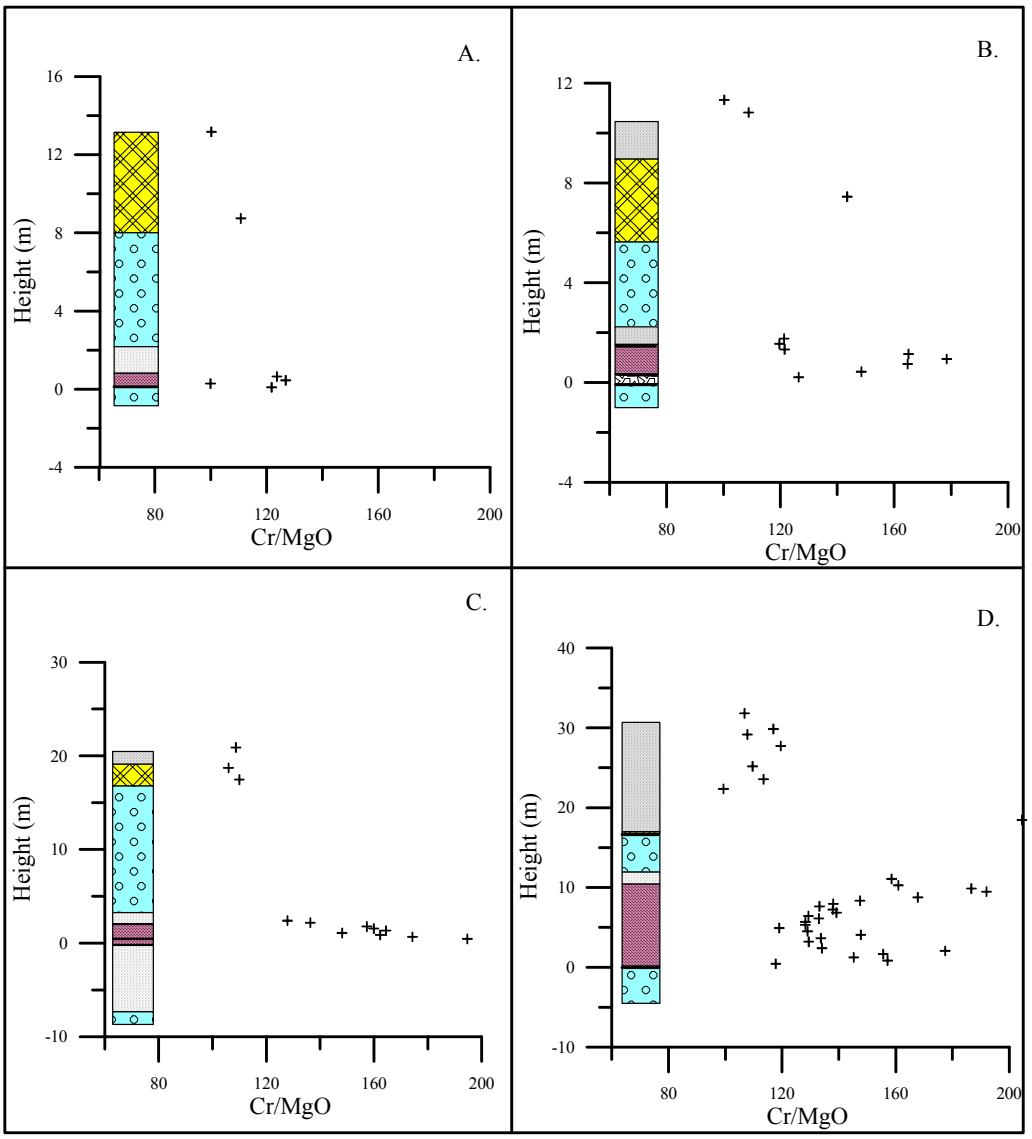

Fig. 7.15. Cr/MgO ratios for a, Thin; b, Brakspruit; c, Marikana and d, Westplats reef types plotted against height in metres. Samples with abundant cumulus chromite and with no cumulus orthopyroxene are not included here. Stratigraphic profiles for the reef types are also presented with the base of the Merensky Unit regarded as datum. Refer to Fig. 7.11 for legend for stratigraphic profiles.

al. (2005) showed, by presenting Cr/MgO values, that there are orthopyroxenes with Critical Zone affinities (80 ≤ Cr/MgO ≤ 120) associated with plagioclase having initial $^{87}Sr/^{86}Sr$ ratios greater than 0.707, with Main Zone affinities in the Merensky

and Bastard Units (geochemical disequilibrium). Seabrook et al. (2005) defined the base of the Main Zone at the top of the Bastard Unit and showed that the Cr/MgO ratios from Main Zone rocks are in the range of 40 to 60.

The whole-rock Cr/MgO data presented in this study do not include results from samples with significant cumulus chromite so that the variations in Cr/MgO do not depend on modal proportion. Rocks with no cumulus orthopyroxene are also excluded. At Lonplats' Mines, the Cr/MgO data presented for the four reef types (Fig. 7.15) show a decreasing trend from the base of the Merensky Unit through to the Bastard Unit. Cr/MgO values in the Merensky Unit generally range from 80 to 200. Cr/MgO ratios presented for the lower part of the Bastard Unit average 120. Cr/MgO data presented here show that there are Critical Zone orthopyroxene in the Bastard Unit. However, the presence of Main Zone orthopyroxene in the Merensky Unit is not obvious. Nonetheless, it can be concluded that the Main Zone and Critical Zone magma did not mix (Seabrook et al., 2005).

Sr isotope data from this study and the study by Seabrook et al. (2005) do not support the simple magma mixing model whereby the highly radiogenic Main Zone magma mixes with the Critical Zone magma at the level of the Merensky Reef. The isotopic profile that was produced for the thick reef type at Eastern Platinum Mine showed that isotopic breaks exist below and above but not at the level of the Merensky Reef and therefore magma mixing could not have occurred at this level.

Irvine (1975) and Maier et al. (2000) as well as Li et al. (2001b) proposed that sulphide immiscibility can be a result of crustal contamination. This is true for the Platreef (Buchanan and Nolan, 1986), as indicated by its isotopic signatures, but not necessarily true for other parts of the Bushveld Complex. Li et al. (2001b) argued that contamination of basaltic magma with siliceous magma can cause sulphide super-saturation whether there is sulphur in the contaminant or not. They argued that the contamination results in a decrease in FeO concentrations and temperature in the hybrid magma and thereby cause decreased sulphur solubility (Irvine, 1975). Whole-rock K_2O:TiO_2 ratios can be used to identify whether there has been a crustal component involved in the crystallization of magmatic rocks. K_2O and TiO_2 data exist for Lonplats' Mines, and the ratios of these elements can be computed. However, K_2O and TiO_2 are present in small quantities in the rocks at Lonplats' Mines and therefore the uncertainty in these small concentrations is huge and calculating K_2O:TiO_2 ratios involves even larger uncertainties. For this reason, K_2O:TiO_2 ratios cannot be discussed for interpretations regarding crustal contamination.

Another method of ascertaining the process of contamination is by using initial $^{87}Sr/^{86}Sr$ ratios. Kruger (1982, 1994) proposed that high initial $^{87}Sr/^{86}Sr$ ratios may indicate in situ contamination of resident magma by its wall rocks. He argued that the start of the accumulation of the Merensky Unit was marked by contamination of more radiogenic partial melts generated in the roof and wall rocks of the Bushveld intrusion. Kruger (1982) also envisaged that further increase of initial $^{87}Sr/^{86}Sr$ ratios

could reflect progressive contamination. At Lonplats' Mines, initial $^{87}Sr/^{86}Sr$ ratios from the footwall anorthosite through to the Merensky Reef reach a maximum of 0.7064 and are Critical Zone values which are not considered high. Elevated initial $^{87}Sr/^{86}Sr$ ratios are only evident above the Merensky Reef; from the Merensky anorthosite to the Bastard norite (Fig. 6.13) and these ratios are considered to be a result of a more radiogenic and isotopically distinct influx of magma (Kruger, 1992) and not as a result of wall rock contamination. The Sr isotopic ratios at Lonplats' Mines do not support the process of contamination and also show that sulphide immiscibility could not have occurred as a consequence of contamination.

Boudreau et al. (1986) proposed that another way of achieving sulphide liquid immiscibility was by percolation of Cl-rich fluids enriched in S, Cu and PGE through a crystal pile, exsolved from a solidifying cumulate sequence. Boudreau and Meurer (1999) suggested that the chlorine-rich interstitial fluids reached the crystal-magma interface and re-dissolved to produce an immiscible sulphide liquid that is rich in PGE, which were deposited at a chemical front. The residual interstitial magma was thought to have been able to migrate in the upward direction (Mathez et al., 1997). In this respect, the hydrothermal model has to take into account that the upward-percolating chlorine-rich fluids have to be transported over considerable distances to reach a chemical front at the level of the Merensky Reef. The distances between the footwall cumulates and the Merensky Reef differ for different sections in the Bushveld Complex. It is logical to assume that the grade of mineralization would vary for different path lengths of migrating fluids. Regardless of this, the grade of

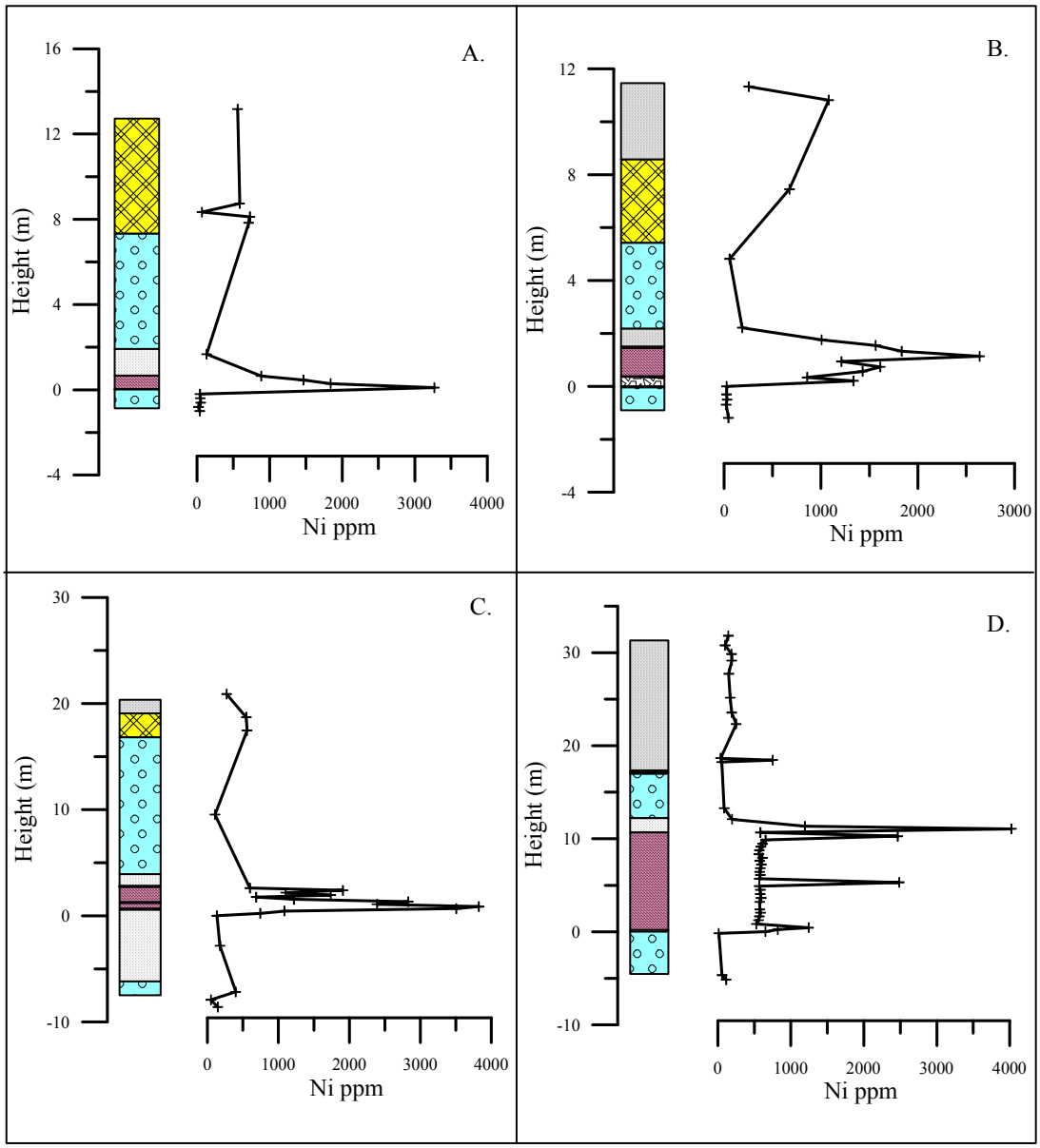

Fig. 7.16 Ni contents in the Thin (A), Brakspruit (B), Marikana (C) and Westplats (D) reef types with varying height in meters.

mineralization in the Merensky Reef at various mines is not different (Vermaak, 1995). The hydrothermal model is not accounted for by this observation made by Vermaak (1995).

The hydrothermal model has not also accounted for the absence of immobile Ni in the footwall cumulates. As the model anticipated that sulphides were re-dissolved in a migrating medium (Boudreau and Meurer, 1999), Cu and PGE would have been more soluble than Ni. Ni would have remained in the footwall cumulates (Cawthorn, 1999a). The Ni contents of the footwall, elsewhere in the Bushveld Complex, even at Lonplats' Mines do not support any enrichment of Ni (Fig. 7.16). By this, it can be demonstrated that no sulphide existed and the process of re-dissolution in the footwall cumulates did not occur (Cawthorn, 1999a).

Sulphur saturation or solubility depends on the composition of the magma, temperature and pressure (Haughton et al., 1974; Wendlandt, 1982; Mavrogenes and O'Neill, 1999; O'Neill and Mavrogenes, 2002). These workers have shown that the solubility of sulphur in a mafic magma increases with increasing TiO_2 and FeO contents of a silicate melt and proved to have an inverse proportion with respect to pressure. Haughton et al. (1974) postulated that sulphide immiscibility can be a result of a decrease in the FeO contents and this drop can be accounted for by the crystallization of chromite. However, the validity of this hypothesis is questionable. The upper chromitite layer in the Westplats reef type, where sulphide mineralization occurs, is poorly developed. Hence, chromite precipitation cannot significantly reduce FeO in a magma. Chromite contains about 45% Cr_2O_3 and 30 % FeO and the

magma has 500 ppm Cr. The precipitation of chromite will only deplete the magma by a very small amount of Cr and FeO. Haughton et al's (1974) theory of decreasing the FeO content by precipitation of chromite in order to cause sulphide immiscibility therefore is considered implausible.

7.11 Proposed Model

All models that were discussed previously here do not adequately explain features of the sulphide mineralization and its genesis in the Merensky Reef and so an alternative model is necessary.

The following model does not negate the addition of magma into the Bushveld chamber but proposes that the effect of the addition of magma into the chamber was largely physical rather than chemical. The effect of the added magma is to increase pressure in the resident magma that just began to crystallize plagioclase and orthopyroxene (Fig. 7.17). The floor of the chamber is inclined allowing for the geometry of the chamber to resemble a wide cone. The Rustenburg Platinum Mine is relatively close to the feeder of the chamber and the Eastern Platinum Mine is distal to the feeder of the magma chamber. Sr-isotopic data show that the Critical Zone magma was introduced to the chamber intermittently to form the Merensky pyroxenite. The Critical Zone resident magma is sulphur-bearing but has not reached saturation.

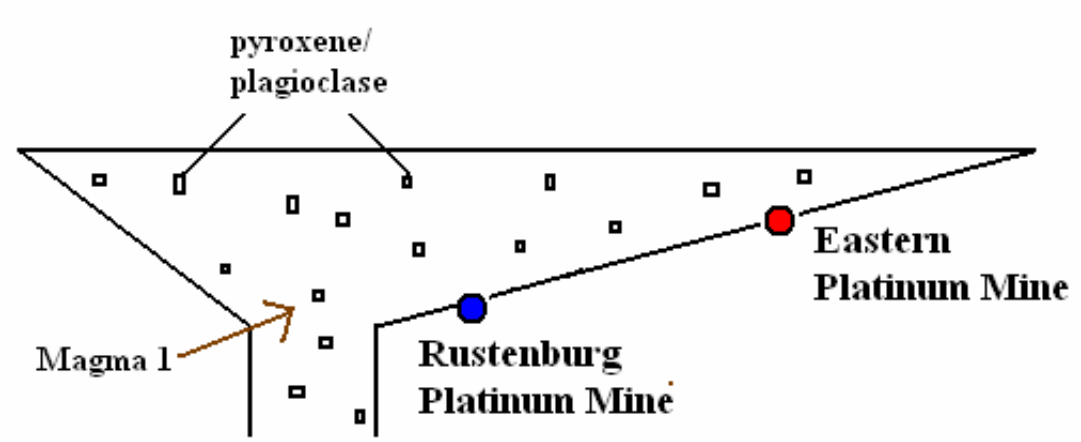

Fig. 7.17 Bushveld chamber with resident magma 1 representing the Critical Zone magma. Note that the Eastern Platinum Mine is distal to the feeder of the chamber and that the Rustenburg Platinum Mine is proximal to the feeder.

A major influx of Main Zone magma is introduced into the Bushveld chamber (Kruger, 2005) that contains the sulphur-bearing Critical Zone magma (Fig. 7.18) but did not initially reach the Eastern Platinum Mine. However, this influx was sufficient to subject the resident Critical Zone magma to a pressure increase and the effect was wide spread. The Rooiberg felsites prevent the dense magma from escaping and the pressure is increased (Cameron, 1982). The new Main Zone magma influx, with high isotopic ratio is different in composition to the resident magma and ultimately crystallizes into the plagioclase-rich rocks that overlie the Merensky pyroxenite. Due to the pressure increase, the solubility of sulphur in the resident Critical Zone magma decreases (Fig. 7.19) (Mavrogenes and O'Neill, 1999) and subsequently forms and separates sulphide globules enhanced in PGE (Campbell et al., 1983; Hamlyn and Keays, 1986) that are essentially concentrated in the resident magma. Because of

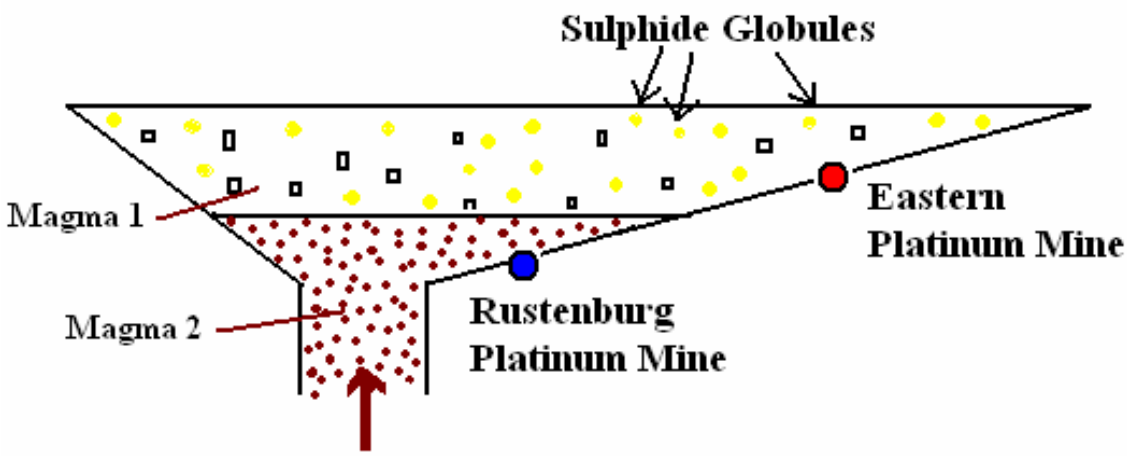

Fig. 7.18. Bushveld chamber during the addition of dense magma 2 and the formation of immiscible sulphide globules.

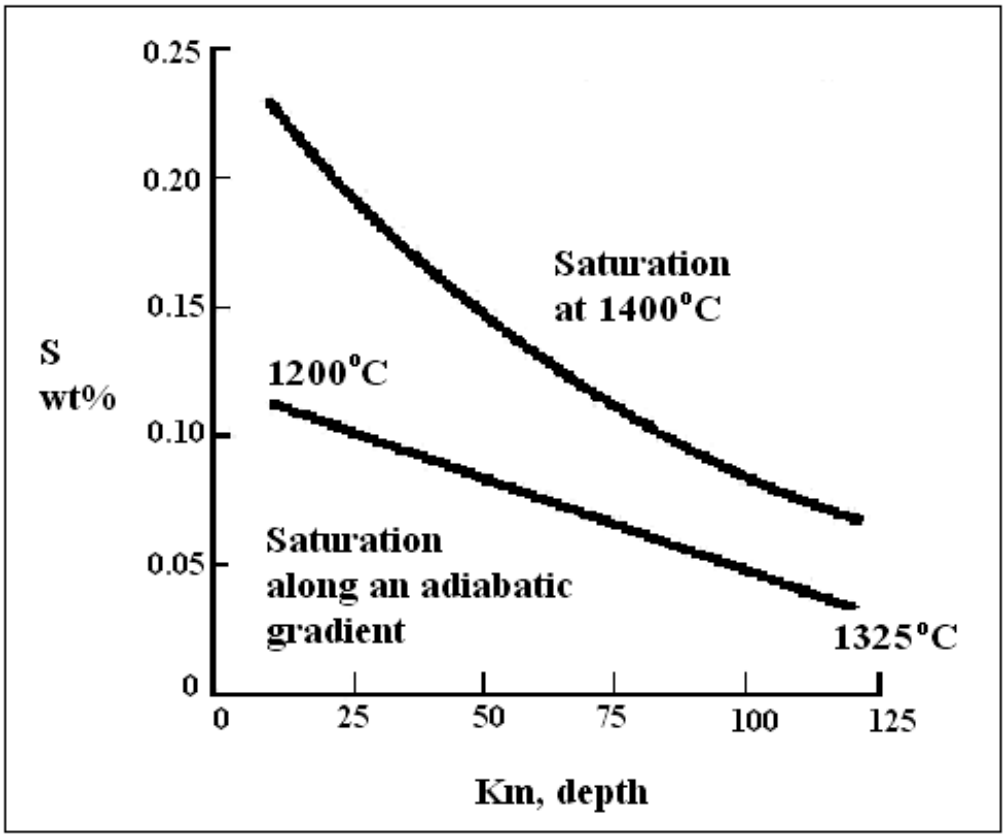

Fig. 7.19. The effect of pressure on the solubility of sulphur in a mafic magma (after Mavrogenes and O'Neill, 1999).

gravity settling, the dense sulphides globules sink (Brynard et al., 1976; Eales and Cawthorn, 1996) to the level of the present Merensky Reef. The poorly developed chromitite layer at the top of the Merensky pyroxenite at Eastern Platinum Mine may be associated with addition of magma (Kinnaird et al., 2002) and pressure increase in the Bushveld chamber (Cawthorn, 2005b). Magma influxes may indicate that the magma chamber was subjected to expansion (Kruger, 2005).

After sulphide immiscibility is achieved, de-pressurization and venting in the chamber because of the unstable roof of the magma chamber occurs (Cawthorn, 2005b). During the stages of venting and de-pressurization, the solubility of sulphur

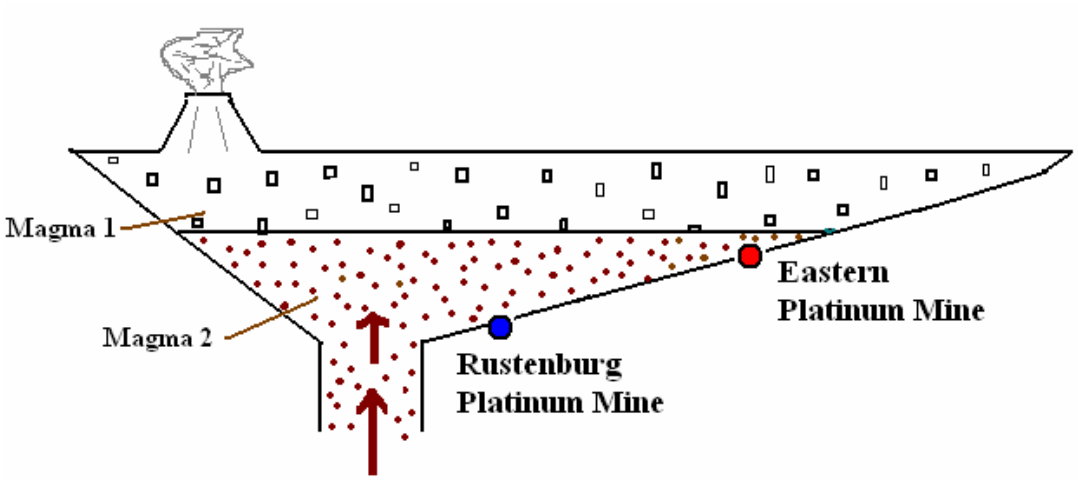

Fig. 7.20 Bushveld chamber during depressurization; after sulphide immiscibility has occurred.

increased and the precipitation of sulphide globules is halted until the next event of pressurization in the magma chamber. Following these events, more of Main Zone magma was added into the chamber and spread beyond the Eastern Platinum Mine (Fig. 7.20). This addition is recorded by an isotopic shift that occurs at the base of Bastard pyroxenite at Lonplats' Mines.

CHAPTER 8

CONCLUSIONS

The Merensky Unit varies across the strike length of Lonplats' Mines and this is evident in the four reef facies; Thin, Brakspruit, Marikana and Westplats reef types. The thickness of the Merensky pyroxenite varies from 0.7 m to just over 11 m. The Merensky pyroxenite is composed of 70 to 90% cumulus orthopyroxene and up to 30% of variable proportions of intercumulus and cumulus plagioclase. 0 to 80% of this plagioclase is cumulus. The Merensky Unit, especially the Merensky pyroxenite, is enriched in incompatible trace-elements and this can be attributed to the presence of trapped liquid. The Merensky Unit in the different reef types shows different proportions of trapped liquid, the Westplats and Marikana reef types show the most amount of trapped liquid reaching maxima of 28% and 30% respectively. Trapped liquid proportions in the Thin and Brakspruit reef types vary from 0 to 4% and 0 to 8% respectively. The overlying and underlying anorthosites in all the reef types have trapped liquid proportions that average 5%.

A maximum of three chromitite layers can develop in the reef types, specifically the Brakspruit and Marikana reef types. The chromitite layers, which may have formed by way of pressure changes due to magma additions in the Bushveld chamber, are confined to the Merensky pyroxenite. Some of the chromitite layers can be correlated based not only on their stratigraphic positions, but also based on their chemistry.

However, some cannot be correlated based on their compositions. The chromitite layers that cannot be correlated may have experienced erosion by hot magmatic fluids or may have been originally discontinuous. The discontinuity may have been due to the presence of the Spruitfontein inlier that acted as a barrier separating the depressions in which the chromitite layers formed. It followed that the processes of chromite precipitation occurred at different times in sub chambers with different magma compositions, also yielding different compositions of the chromitite layers.

Ni (calculated in sulphide): Cu: S ratios from the Merensky Reef at Lonplats' Mines are different to the Ni: Cu: S ratios determined by Naldrett (1981, 1989) and Cawthorn (1999a) for the magmatic immiscible sulphide liquid in Merensky Reef. The sulphides at Lonplats' Mines are more Cu- and Ni- rich compared to those in the Merensky Reef studied by Naldrett (1981, 1989) and Cawthorn (1999a). The Cu and Ni may have been transported by hydrothermal fluids to the Merensky Reef at Lonplats' Mines. S-loss may also have been due to hydrothermal activity in the reef.

The initial $^{87}Sr/^{86}Sr$ ratios from the Eastern Platinum Mine (Lonplats' Mine) show that several isotopic breaks exist in the Merensky Unit. At least three breaks occur from the footwall anorthosite to the Merensky Reef and these can be identified as indicating additions of Critical Zone magma. At a level 2 m above the Merensky Reef, an isotopic shift occurs in the anorthosite and the initial $^{87}Sr/^{86}Sr$ ratios increase from 0.7063 to 0.7066 and finally to 0.7071 in the anorthosite below the Bastard pyroxenite. This isotopic break indicates that magma with Main Zone signature was

added above the Merensky pyroxenite. Other isotopic shifts occur in the Bastard pyroxenite and also in the middle of the Bastard norite. The isotopic break that occurs in the middle of the Bastard pyroxenite decreases from 0.7071 to 0.7066 and that in the middle of the Bastard norite increases from 0.7072 to 0.7076. These two shifts indicate that both Critical Zone and Main Zone magma were involved in the formation of the Bastard Unit.

Based on this isotopic constraint, conventional models of sulphide genesis are questioned and this necessitates the use of an alternative model. This model uses the principle that sulphide liquid immiscibility can be achieved by a pressure increase in a magma chamber. At Lonplats' Mines, there is no evidence of magma mixing to produce the sulphide mineralization in the reef. The sulphide mineralization at Lonplats' Mines may have been a consequence of increased pressure in the Bushveld chamber that was caused by the addition of Main Zone magma above the Merensky pyroxenite and this is recorded as an isotopic break 2 m above the pyroxenite. In this model, the Eastern Platinum Mine is distal to the feeder of a wide conical chamber with inclined floors representing that of the Bushveld Complex. Due to the geometry of the chamber, the added Main Zone magma only reaches the Eastern Platinum Mine after the Merensky pyroxenite and reef have formed.

References

Arndt, N., Jenner, G., Ohnenstetter, M., Deloule, E. and Wilson, A.H. (2005) Trace elements in the Merensky Reef and adjacent norites, Bushveld Complex, South Africa, Mineralium Deposita, **40**, 550-575

Barnes, S.J. (1986) The effect of trapped liquid crystallization on cumulus mineral compositions in layered intrusions, Contributions to Mineralogy and Petrology, **93**, 524-531

Barnes, S.J. (1993) Partitioning of the platinum-group elements and gold between silicate and sulphide magmas in Munni Munni Complex, Western Australia. Geochemica et Cosmochimica Acta, **57**, 1277-1290

Barnes, S.J and Campbell, I.H. (1988) Role of late magmatic fluids in the Merensky-type platinum deposits: a discussion, Geology, **16**, 488-491

Barnes, S.J. and Roeder, P.L. (2001) The range pf spinel compositions in the terrestrial mafic and ultramafic rocks, Journal of Petrology, **42**, 2279-2302

Barnes, S-J. and Maier, W.D. (2002a) Platinum –group elements and microstructures of normal Merensky Reef from Impala Platinum Mines, Bushveld Complex, Journal of Petrology, **43**, 103-128

Barnes, S-J and Maier, W.D. (2002b) Platinum-group element distributions in the Rustenburg Layered Suite of the Bushveld Complex, South Africa In: Cabri, L.J. (ed), The geology, geochemistry, mineralogy and mineral beneficiation of platinum-group elements, Canadian Institute of Mining, Metallurgy and Petroleum, Special Volume, **54**, 553-580

Boerst, K.D. Geochemistry of the Merensky Reef on Impala Platinum Mine, western Bushveld Complex, MSc Thesis, University of the Witwatersrand, 2001

Boudreau, A.E, and Meurer, W.P. (1999) Chromatographic separation of the platinum-group elements, gold, base metals and sulphur during degassing of a compacting and solidifying igneous crystal pile. Contributions to Mineralogy and Petrology, **134**, 174-185

Boudreau, A.E., Mathez, E.A. and McCallum, I.S. (1986) Halogen geochemistry of the Stillwater and Bushveld Complexes: Evidence for transport of the platinum–group elements by Cl-rich fluids. Journal of Petrology, **27**, 967-986

Brynard, H.J., de Villiers, J.P.R. and Viljoen, E.A. (1976) A mineralogical investigation of the Merensky Reef at the Western Platinum Mine, near Marikana, South Africa. Economic Geology, **71**, 1299-1307

Cameron, E.N. (1982) The upper Critical Zone of the eastern Bushveld Complex – Precursor of the Merensky Reef. Economic Geology, **77**, 1307-13

Campbell, I.H. and Naldrett, A.J. (1979) The influence of silicates: sulphide ratios on the geochemistry of magmatic sulphides. Economic Geology, **74**, 1503-1505

Campbell, I.H., Naldrett, A.J. and Barnes, S.J. (1983) A model for the origin of the platinum-rich sulphide horizons in the Bushveld and Stillwater Complexes. Journal of Petrology, **24**, 133-165

Carr, H.W. The petrogenesis of the Merensky Reef potholes at the Western Platinum Mine, Bushveld Complex, South Africa, PhD Thesis, University of the Witwatersrand, 1995

Carr, H.W., Kruger, F.J., Groves, D.I. and Cawthorn, R.G. (1999) The petrogenesis of the Merensky Reef potholes at the Western Platinum Mine, Bushveld Complex: Sr-isotopic evidence for synmagmatic deformation, Mineralium Deposita, **34**, 335-347

Cawthorn, R.G. (1996a) Models for incompatible trace-element abundances in cumulus minerals and their application to plagioclase and pyroxene in the Bushveld Complex, Contributions to Mineralogy and Petrology, **123**, 109-115

Cawthorn, R.G. (1996b) Re-evaluation of magma compositions and processes in the uppermost Critical Zone of the Bushveld Complex, Mineralogical Magazine, **60**, 131-148

Cawthorn, R.G. (1999a) Platinum-group element mineralization in the Bushveld Complex – a critical reassessment of geochemical models. South African Journal of Geology, **102**, 268-281

Cawthorn, R.G. (1999b) The platinum and palladium resources of the Bushveld Complex. South African journal of Science, **95**, 481-489

Cawthorn, R.G. (2002) The role of magma mixing in the genesis of PGE mineralization in the Bushveld Complex: Thermodynamic calculations and new interpretation – A discussion. Economic Geology, **97**, 663-667

Cawthorn, R.G. (2005a) Contrasting sulphide contents of the Bushveld and Sudbury Igneous Complexes, Mineralium Deposita, **40**, 1-12

Cawthorn, R.G. (2005b) Pressure fluctuations in the formation of the PGE-rich Merensky and chromitite reefs, Bushveld Complex, Mineralium Deposita, **40,** 231-235

Cawthorn, R.G. and McCarthy, T.S. (1985) Incompatible trace-element behaviour in the Bushveld Complex, Economic Geology, **80**, 1016-1026

Cawthorn, R.G, and Barry, S.D, (1992) The role of intercumulus residua in the formation of pegmatoid associated with UG2 chromitite, Bushveld Complex, Australian Journal of Earth Science, 39, 263-276

Cawthorn, R.G. and Walraven, F. (1998) Emplacement and crystallization time of the Bushveld Complex. Journal of Petrology, **39(9)**, 1669-1687

Cawthorn, R.G. Cooper G.R.J. and Webb, S.J. (1998) Connectivity between the western and eastern limbs of the Bushveld Complex. South African Journal of Geology, **101**, 291-298

Cawthorn, R.G. and Boerst, K. Origin of the pegmatitic pyroxenite in the Merensky Unit, Bushveld Complex, South Africa, In Press.

Clarke, B.M., Ulken, R. and Watkeys, M.K. (2000) Intrusion mechanism of the southwestern Rustenburg Layered Suite as deduced from the Spruitfontein inlier, South African Journal of Geology, **103**, 120-127

Cousins, C.A. (1964) The platinum deposits of the Merensky Reef, In*:* Haughton, S.H. (ed), The geology of some ore deposits of southern Africa: Johannesburg, Geological Society of South Africa, **2**, 225-237

Cousins, C.A. (1969) The Merensky Reef of the Bushveld Igneous Complex, Economic Geology Monography, **4**, 239-251

Davey, R.S. (1992) Lateral variations within the upper Critical Zone of the Bushveld Complex on the farm Rooikoppies 297 JG, Marikana, South Africa. South African Journal of Geology, **95**, 141-150

Eales, H.V., Marsh, J.S., Mitchell, A.A., De Klerk, W.J., Kruger, F.J. and Field, M. (1986) Some geochemical constraints upon models for the crystallization of the Upper Critical Zone-Main Zone interval , northwestern Bushveld Complex, Mineralogical Magazine, **50**, 567-582

Eales, H.V., Field, M., De Klerk, W.J. and Scoon, R.N. (1988) Regional trends of chemical variation and thermal erosion in the Upper Critical Zone, western Bushveld Complex, Mineralogical Magazine, **52**, 63-79

Eales, H.V. and Reynolds I.M. (1986) Cryptic variations within chromitites of the Upper Critical Zone, Northwestern Bushveld Complex, Economic Geology, **81**, 1056-1066

Eales, H.V. and Cawthorn, R.G, (1996) The Bushveld Complex In: Cawthorn, R.G. (ed) Layered Intrusions: 15 Developments in Petrology. Elsevier Science, The Netherlands, 181-230

Eriksson, P.G., Hattingh, P.J. and Altermann, W. (1995) An overview of the geology of the Transvaal Sequence and Bushveld Complex. Mineralium Deposita, **30**, 98-111

Hamilton, J. (1977) Strontium isotope and trace element studies of the Great Dyke and Bushveld mafic phase and their relation to the to early Proterozoic magma genesis in Southern Africa. Journal of Petrology, **18**, 24-52

Hamlyn, P.R. and Keays R.R. (1986) Sulphur saturation and second-stage melts: application to the Bushveld platinum metal deposits, Economic Geology, **81,** 1431-1445

Hatton, C.J. and Schweitzer, J.K. (1995) Evidence for synchronous extrusive and intrusive Bushveld magmatism. Journal of African Earth Science, **21**, 579-594

Hatton, C.J. and von Gruenewaldt, G. (1985) The geological setting and petrogenesis of the Bushveld chromitite layers, Research Reports on the Bushveld Complex, University of Pretoria, **57**, 1-48

Haughton, D.R., Roeder, P.L, and Skinner, B.J. (1974) The solubility of sulphur in magmas, Economic Geology, **69**, 451-462

Henderson, P. (1975) Geochemical indicator of the efficiency of fractionation of the Skaergaard intrusion, east Greenland. Mineralogical Magazine, **40**, 285-291

Hiemstra, S.A. (1985) The distribution of some platinum-group elements in the UG2 chromitite layer of the Bushveld Complex. Economic Geology, **80**, 944-957

Hunter, R.H. (1996), Texture development in cumulate rocks, In: Cawthorn R.G. (ed) Layered Intrusions: 15 Developments in Petrology. Elsevier Science, The Netherlands, 77-101

Irvine, T.N. (1965) Chromian spinel as a petrogenetic indicator Part I. Theory. Canadian Journal of Earth Science, **2**, 648-672

Irvine, T.N. (1975) Crystallization sequences in the Muskox intrusion and other layered intrusions-II. Origin of chromitite layers and similar deposits of other magmatic ores, Geochemica Cosmochimica et Acta, **39**, 991-1020

Irvine, T.N. (1977) Origin of chromitite layers in the Muskox intrusion and other stratiform intrusions; a new interpretation. Geology, **5**, 273-277

Irvine, T.N., Keith, D.W. and Todd, S.G. (1983) The J-M platinum-palladium reef of the Stillwater Complex, Montana: II origin of double diffusive convective magma mixing and implications for the Bushveld Complex. Economic Geology, **78**, 1278-1334

Jackson, E.D. (1961) Primary textures and mineral associations in the ultramafic zone of the Stillwater Complex, Montana. United States Geological Survey, Professional Papers, **358**, pp106

Kinnaird, J.A., Kruger, F.J., Nex, P.A.M. and Cawthorn, R.G. (2002) Chromitite formation – a key to understanding processes of platinum enrichment, Transactions of the Institute of Mining and Metallurgy, **111**, B23 – B25

Kruger, F.J. (1992), The origin of the Merensky cyclic unit: Sr-isotopic and mineralogical evidence for an alternative orthomagmatic model, Australian Journal of Earth Science, **39**, 255-261

Kruger, F.J. (1994) The Sr-isotopic stratigraphy of the western Bushveld Complex. South African Journal of Geology, **97**, 393-398

Kruger, F.J. (2005) Filling the Bushveld complex magma chamber: lateral expansion, roof and floor interaction, magmatic unconformities and formation of giant chromitite, PGE and Ti-V magnetite deposits, Mineralium Deposita, **40**, 451-472

Kruger, F.J. and Marsh JS (1982) The significance of $^{87}Sr/^{86}Sr$ ratios in the Merensky cyclic unit of the Bushveld Complex. Nature, **298,** 53-55

Kruger, F.J. and Marsh, J.S. (1985) The mineralogy, petrology and origin of the Merensky Cyclic Unit in the Western Bushveld Complex. Economic Geology, **80,** 958-974

Lauder, W.R. (1970) The Origin of the Merensky Reef. Nature, **227**, 365-366

Lee, C.A. (1996) A review of mineralization in the Bushveld Complex and some other layered intrusions In: Cawthorn R.G. (ed) *Layered Intrusions: 15 Developments in Petrology.,* Elsevier Science, The Netherlands, 103-145

Lee, C.A. and Butcher, A.R. (1990) Cyclicity in the Sr isotope stratigraphy through the Merensky and Bastard Reef Units, Atok Section, Eastern Bushveld Complex, Economic Geology, **85**, 877-883

Li, C., Maier W.D. and de Waal, S.A. (2001a) The role of magma mixing in the genesis of PGE mineralization in the Bushveld Complex: thermodynamic calculations and new interpretations Economic Geology, **96**, 653-662

Li, C., Maier, W.D. and de Waal, S.A. (2001b) Magmatic Ni-Cu versus PGE deposits: Contrasting genetic controls and exploration implications, South African Journal of Geology, **104**, 309-318

Maier, W.D. and Barnes, S-J (1999) Platinum-group elements in the silicate rocks of the Lower, Critical and Main Zones of the Union Section, western Bushveld Complex, Journal of petrology, **40**, 1647-1671

Maier, W.D., Arndt, N.T. and Curl, E.A. (2000) Progressive crustal contamination of the Bushveld complex: evidence from Nd isotopic analyses of the cumulate rocks, Contributions to Mineralogy and Petrology, **140**, 316-327

Mathez, E.A. (1995) Magmatic metasomatism and formation of the Merensky Reef, Bushveld Complex, Contributions to Petrology and Mineralogy, **140**, 328-343

Mathez, E.A. Hunter, R.H. and Kinzler R. (1997) Petrologic evolution of partially molten cumulate: the Atok section of the Bushveld Complex, Contributions to mineralogy and Petrology, **129**, 20-34

Mavrogenes, J.A and O'Neill, H. St. C. (1999) The relative effects ofpressure, temperature and oxygen fugacity on the solubility of sulphide in mafic magmas, Geochemica et Cosmochimica Acta, **63**, 1173-1180

Merkle, R.K.W. (1992) Platinum-group minerals in the middle group of chromitite layers at Marikana, western Bushveld Complex: indications for collection mechanisms and post-magmatic modifications. Canadian Journal of Earth Science, **29**, 209-221

Myson, B.O. and Popp, R.K. (1980) solubility of sulphur in $CaMgSi_2O_6$ and $NaAlSi_3O_6$ melts at high pressure and temperature with controlled fO_2 and fS_2. American Journal of Science, **280**, 78-92

Naldrett, A.J., Gasparrini, E.C., Barnes, S.J, Von Gruenewaldt, G. and Sharpe, M.R. (1986) The Upper Critical Zone of the Bushveld Complex and the origin of the Merensky-type ores, Economic Geology, **81**, 1105-1117

Naldrett, A.J. (1989) Stratiform PGE deposits in layered intrusions. Reviews in Economic Geology, **4**, 135-166

Naldrett, A.J. and Von Gruenewaldt, G. (1989) Association of platinum-group elements with chromitite in the layered intrusions and ophiolite complexes. Economic Geology, **84**, 180-187

Nicholson, D.M. and Mathez, E.A. (1991) Petrogenesis of the Merensky Reef in the Rustenburg section of the Bushveld Complex, Contributions to Mineralogy and Petrology, **107**, 293-309

O'Neill, H. St. C. and Mavrogenes, J.A. (2002) The sulphide capacity and the sulphur content at sulphide saturation of silicate melts at 1400 ºC and 1bar, Journal of Petrology, **43**, 1049-1087

Ripley, E.M. and Alawi, J.A. (1988) Petrogenesis of politic xenoliths at the Babitt Cu-Ni deposit, Duluth Complex, Minnesota, USA, Lithos, **21**, 143-159

Roeder, P.L. and Reynolds, I. (1991) The crystallization of chromite and chromium solubility in basaltic melts, Journal of Petrology, **32**, 909-934

Schimdt, E.R. (1952) The structure and compositions of the Merensky Reef and associated rocks in the Rustenburg Platinum Mine, Transactions of the Geological Society of South Africa, **55**, 233-279

Schweitzer, J.K., Hatton, C.J. and de Waal, S.A. (1995) Regional lithochemical stratigraphy of the Rooiberg Group, upper Transvaal Supergroup, a proposed new subdivision. South African Journal of Geology, **98**, 245-255

Schwellnus, J.S.I., Hiemstra S.A. and Gasparrini E. (1976) The Merensky Reef at the Atok Platinum Mine and its environs, Economic Geology, **71**, 249-260

Seabrook, C.L., Cawthorn, R.G. and Kruger, F.J. (2005) The Merensky Reef, Bushveld Complex: Mixing of minerals, not magmas. Economic Geology, **100**, 1191-1205

South African Committee for Stratigraphy (SACS), 1980, Stratigraphy of South Africa. Part 1 (Comp. L.E. Kent). Lithostratigraphy of the Republic of South Africa, South West Africa/ Namibia, and the Republics of Bophuthatswana, Transkei, and Venda: Handb. geol. Surv. S. Afr., **8**, pp 690

Tredoux, M., Lindsay, N.M., Davies, G. and McDonald, I. (1995) The fractionation of platinum-group elements in magmatic system with the suggestion of a novel causal mechanism. South African Journal of Geology, **98**, 157-167

Truswell, J.F. (1977) The geological evolution of South Africa. Purnell, Cape Town, pp 218

Vermaak, C.F. (1976) The Merensky Reef: Thoughts on its environment and genesis. Economic Geology, **71**, 1270-1298

Vermaak, C.F. and Hendriks, L.P. (1976) A review of the mineralogy of the Merensky Reef, with specific reference to new data on the precious metal mineralogy. Economic Geology, **71**, 1244-1269

Viljoen, M.J. (1994) A review of the regional variations in facies and grade distribution of the Merensky Reef, western Bushveld Complex, with some mining implications, Proceedings 15th CMMI Congress, South African Institute of Mining and Metallurgy, 183-194

Viljoen, M.J. (1999) The nature and origin of the Merensky Reef of the western Bushveld Complex based on geological facies and geophysical data, South Africna Journal of Geology, **102**, 221-239

Viring, R.G. and Cowell, M.W. (1999) The Merensky Reef on Nartham Platinum Limited, South Africa Journal of Geology, **102**, 192-208

Von Gruenewaldt, G. (1979) A review of some recent concepts of the Bushveld Complex, with a particular reference to sulphide mineralization. The Canadian Mineralogist, **17**, 233-256

Wager, L.R, Brown, G.M. and Wadsworth, W.J. (1960) Types of igneous cumulates, Journal of Petrology, **1**, 73-85

Wager, L.R. and Brown, G.M. (1968) Layered igneous rocks. Oliver and Boyd, Edinburgh

Wagner, P.A. (1929) The platinum deposits and mines of South Africa. Oliver and Boyd, Edinburgh

Walraven, F., Armstrong, R.A. and Kruger, F.J. (1990) A chronostratigraphic framework for the north-central Kaapvaal Craton, the Bushveld Complex and Vredefort Structure. Tectonophysics, **171**, 23-48

Webb, S.J., Cawthorn, R.G., Nguuri, T. and James, D. (2004) Gravity modelling of the Bushveld Complex connectivity supported by Southern African seismic experiment results, South African Journal of Geology, **107**, 207-218

Wendlandt, R.F. (1982) Sulphide saturation of basalt and andesite melts at high at high pressure and temperatures. American Mineralogist, **67**, 885-877

Willemse, J. (1964) A brief outline of the geology of the Bushveld Igneous Complex In: Haughton SH, *The geology of some ore deposits in southern Africa.* Geological Society of South Africa, Johannesburg, 91-138

Willemse, J. (1969) The geology of the Bushveld Complex, the largest repository of magmatic ore deposits in the world In: HDB Wilson (ed) *Magmatic Ore Deposit.,* Economic Geology Monograph 4, 1-22

Wilmore, C.C., Boudreau, A.E. and Kruger, F.J. (2000) Halogen geochemistry of the Bushveld Complex, Republic of South Africa: Implications for chalcophile element distribution in the Lower and Critical Zones, Journal of Petrology, **41**, 1517-1539

Wilson, A.H. (1992) The geology of the Great Dyke, Zimbabwe: crystallization layering and cumulate formation in the P1 pyroxenite of cyclic unit 1 of the Darwendale Subchamber, Journal of Petrology, **33**, 611-663

Wilson, A.H., Lee, C.A. and Brown, R.T. (1999) Geochemistry of the Merensky Reef, Rustenburg Section, Bushveld Complex: controls on the silicate framework and distribution of trace elements, Mineralium Deposita, **34**, 657-672